WIND TOWER TECHNOLOGY: THE IMPACT OF CROSS-SECTION AND TURBINE SELECTION ON THE GENERATED POWER

by

Jonathan Conrad Corbett

A thesis submitted to the faculty of
The University of North Carolina at Charlotte
in partial fulfillment of the requirements
for the Master of Science in
Mechanical Engineering

Charlotte

2019

Approved by:

_____
Dr. Navid Goudarzi

_____
Dr. Praveen Ramaprabhu

_____
Dr. Mesbah Uddin

ABSTRACT

JONATHAN CONRAD CORBETT. Wind Tower Technology: The Impact of Cross-Section and Turbine Selection on the Generated Power (Under the direction of DR. NAVID GOUDARZI, with DR. PRAVEEN RAMAPRABHU as chair of committee)

The performance of wind turbines in the built (urban) environments has been consistently underwhelming. Wind towers, a technology from the Middle East, have a proven history of functioning in the urban environment. Although their normal function is natural ventilation, wind towers might be adapted for power generation. Exploratory work has been completed for conceptualizing and analyzing wind turbines in wind towers using Computational Fluid Dynamics (CFD). Key design parameters are reviewed and discussed, and useful metrics for comparing these turbines are identified. The strengths of the combined technology – both technical and non-technical – are identified and placed into context in industry. In previous research, a wind tower was designed and optimized. In the first part of this work, the tower was analyzed in steady state using ANSYS, applying the SST Transition model. In the second part of this research, after small modifications to improve tower performance for power production, relevant turbine design principles are discussed, and a turbine conforming to those principles is modeled in the flow field derived from the tower analysis. The turbine was modeled using sliding mesh CFD to allow measurement of wake effects and potential disruption of normal tower function, with the added benefit of providing temporal details on turbine power production. The technical performance characteristics of that turbine are measured and discussed. A turbine configuration which generates power was identified and the potential for the technology confirmed. Direction is provided for future design, manufacturing, and optimization of

this tower-turbine system, with emphasis on maintaining the competitive strengths of the technology in industry.

ACKNOWLEDGEMENTS

First and foremost, I want to acknowledge Dr. Goudarzi's technical expertise and indefatigable positive attitude. His adamant insistence that this would all work out turned out to be right.

I need to thank Amin (Mohammadamin Sheikhshahrokhdehkordi) for his assistance helping me get started learning the basics of CFD and how to use ANSYS. It was good to have a friend on the team helping me succeed when I got tripped up, even (and especially) when I thought the problem should be approached from another direction because it helped me refine my argument for each process. His assistance with the analysis of the tower he had originally developed helped speed the research along and understand what methods had been applied previously.

I also want to thank Dr. Jesse A. Fulton for the many hours of practice conversations he had with me as I worked on this project. His expertise with CFD was a big help developing my technical skills quickly.

I must thank Amy and Chris Hunt for their moral support as I worked through my degree. Having a home and not just a place to stay made a big difference to my success.

I also want to thank Judy Gustafson and her associates for their financial support. My success would not have been possible without the funding they provided for my summer internship with Dr. Goudarzi and the time while I completed my thesis.

TABLE OF CONTENTS

LIST OF TABLES

LIST OF FIGURES

LIST OF ABBREVIATIONS AND NOMENCLATURE

α – Angle of attack of an airfoil

β – Angle of attachment of airfoil to turbine

θ – Angle, around a circle or turbine (starting from 0 along the x-axis)

λ – Tip speed ratio

ρ – Density of fluid

τ – Torque

φ – Angle of relative wind from freestream

ψ – Combined angle of attachment and angle around turbine

ω – Angular velocity

A – Area

ANSYS – A software suite used for engineering analysis

ASCD – Anti-short circuit device

c – Chord length of an airfoil

C_D – Drag Coefficient

C_L – Lift Coefficient

C_M – Moment Coefficient

C_P – Power Coefficient

CAD – Computer-Aided Design

CFD – Computational Fluid Dynamics

D – Drag

D_x – Drag acting in the x-direction

D_{xtan} – Component of tangent resultant force from drag acting in the x-direction

D_y – Drag acting in the y-direction

D_{ytan} – Component of the tangent resultant force from drag acting in the y-direction

DES – Detached Eddy Simulation

D-type turbine – A VAWT using lift to generate torque, like a Darrieus turbine

E – Energy of a particle

F – A force

g – Acceleration due to gravity

HAWT – Horizontal Axis Wind Turbine

$\dot{m}$ - mass flow rate (in kg/s)

M_{tot} – Total moment from sum of all tangent forces

MATLAB – A software package for math

NACA – National Advisory Committee for Aeronautics, the precursor to NASA

L – Lift

L_x – Lift acting in the x-direction

L_{xtan} – Component of the tangent force from lift acting in the x-direction

L_y – Lift acting in the y-direction

L_{ytan} – Component of the tangent force from lift acting in the y-direction

Leeward – The side facing away from the wind

LES – Large Eddy Simulation

M – Moment

N – Number of turbine blades

P_0 – Total pressure

P_{wind} – Power in the wind

P_{turb} – Power produced by turbine

p – static pressure

q – dynamic pressure

R – Radius

R_{Local} – The radius as it varies locally along the radius

R_{τ} – The radius at which the torque or moment is applied

r – Radius

S – Solidity (of turbine)

s – Length of the side of a regular polygon

S-type turbine – A VAWT using drag to generate torque, like a Savonius turbine

TSR – Tip Speed Ratio

u_{rel} – Relative wind due to motion of turbine

u_{tot} – Total combined velocity from freestream and relative wind

u_{w} – Freestream wind velocity

VAWT – Vertical Axis Wind Turbine

Windward – The side facing into the wind

CHAPTER 1: INTRODUCTION

Background

There is an increasing need for clean, affordable power production in the world, but the opportunities for producing that power are reduced as resources are developed. As people continue to move to urban areas at an increasing rate [1], their demands for energy grow while the space to generate it diminishes. Currently, 62% of United States power needs are met by burning coal or natural gas in distant power plants [2], but with the changing climate and concern about rising CO_2 levels, that cannot be a long-term solution for all our power needs. Depending on centralized power plants also does not work well for locations in remote areas, like scientific installations or military bases.

Furthermore, when natural disasters happen, populations can be left without power for extended periods of time, as happened in Puerto Rico after hurricane Maria [3]. Diesel generators are an inefficient and expensive solution that require fuel from an outside source, the supply of which could itself be disrupted by that same disaster. Developing "green" technologies that do not depend on burning hydrocarbons promotes energy independence, allowing for off-grid power production in remote areas and making locations that are on-grid more independent and less reliant on centralized power production. With the growing urban population, it is desirable to generate at least some of the power consumed in cities and suburbs on site so that they consume less outside fuel.

While wind power appears to have the potential to meet some of those energy needs, wind turbines which have been built in urban environments have consistently underwhelmed with their performance. While some of this can be attributed to wind

turbines which were constructed for show without consideration for the wind resource, even careful wind projects have underperformed. The wind resource in cities is notoriously difficult to harvest. Because more conventional approaches have failed to adapt to the hostile environment, a novel approach using proven technology may be necessary.

Wind towers are able to reduce some of the energy required to cool buildings and exchange air with the surroundings, thus reducing the need for powered HVAC systems. Almost half the power consumed in the world is consumed in buildings, and up to 60% of that energy consumed is spent on HVAC systems [4], heating and cooling the air inside buildings. In a separate project, another student from the NADGOD research group explored wind tower design to optimize the configuration for a wind tower to provide natural ventilation and reduce the energy consumed for comfort [6].

Wind towers already reduce energy costs by capturing wind for ventilation. One of the questions remaining at the end of the previous work was whether the tower could serve a second, additional purpose by simultaneously generating power, using a wind turbine to extract some of the excess energy from the flow passing through the tower. This paper is an exploration of that question and a continuation of that work.

In this context, it should be understood that the primary function of the tower is for natural ventilation, while the turbine is being added to the tower to provide the secondary benefit of power generation. As such, changes to the already optimized tower should be minimal to preserve the primary function of the tower: the natural ventilation it provides and the optimization already completed. The turbine must be added without interfering with that purpose, but in a way that will maximize power generated. This

basic problem is faced in the design of all ducted turbines, since one of the complications of using ducted turbines is that the turbine itself is a source of blockage in the system, which reduces the amount of air that flows through the duct.

In order to address the growing need for renewable, affordable power generation, this thesis explores adapting wind towers for power production in urban locations numerically. Wind towers, wind turbines, and Computational Fluid Dynamics (CFD) each have their own benefits and limitations, and are all essential to understanding this investigation.

Scope of Research

There are a number of questions to be answered in this investigation. The first and most pressing question is the investigation method itself: how can and should a turbine be placed into a wind tower, and how can such an investigation be conducted? Within the research group, there were two previous attempts to place a turbine into a wind tower for analysis, but both investigations were unable to be completed due to the size and difficulty of the project. Because of this history, the first goal of this thesis is to successfully analyze the performance of a turbine in a wind tower and document the methods used well enough to assist future researchers who may visit the topic. Design choices will be kept as simple as possible to prevent overcomplicating the project, so (for example) there will not be twist on the turbine blade if it is not critically necessary to the function of the turbine or improve total power output. This also allows for a better understanding of the turbine's baseline function in its purest form, so that improvements like the aforementioned twist can be applied judiciously in future work.

The second major question to be examined is whether wind towers can simultaneously provide both natural ventilation and power generation, including the related question of whether existing wind towers might be retrofitted with wind turbines for profit. Thousands of towers already exist in the Middle East, but whether they could be adapted for power generation is yet unknown. Some research has been done to confirm the technical success of putting a turbine into a tower dedicated to wind power [7], but none has investigated using a wind tower designed primarily for natural ventilation being adapted for power generation. It is not clear if introducing a turbine into such a tower would greatly disrupt its normal operation, nor if a tower which was designed for natural ventilation, which typically maximizes mass transfer, would support a turbine, which usually performs better in higher velocities.

A third major question is how to overcome the extreme turbulence of the built environment. Literally millions of dollars have been spent on turbines that do not work in practice as well as was predicted on paper [8]. Understanding the problem so that it can be designed around or compensated for is a critical issue for urban wind power.

The fourth question is what does the wind resource inside the tower look like, so that a suitable turbine can be implemented. To place a turbine inside a wind tower, these details are essential to making sure the turbine is able to be as productive as possible. For this reason, an investigative analysis of several towers will precede the design and analysis of the turbine. A general tower plan optimized in previous research [6] will be used as the basis for these towers.

The fifth and final question to be answered is what kind of turbine should be placed into the tower to optimize power output, and what would the power output be? As

discussed, there are a number of wind turbine designs which work better under different circumstances, and there may be some yet unseen design which would operate even better. Identifying the wind resource and developing a suitable turbine design are central questions to the investigation. The power production will be quantified to put the value of the turbine into perspective and determine whether future work in this area is warranted.

Wind Tower Introduction

Wind towers have a long history. They have been used in the Middle East for many centuries, and modern environmental and power consumption concerns have reinvigorated investigation into them scientifically. The primary function of a wind tower is to provide natural ventilation via mass exchange without the need for electrical power input. Instead, a tower directs wind into the building and exhausts air from inside. Towers are usually evaluated on the criteria of "thermal comfort" or preventing the buildup of CO_2 in occupied buildings. Because of this, the main goal in most wind tower design is the maximization of mass flow (rather than velocity) to optimize the quantity of air being exchanged. Indeed, too much wind speed can be disruptive to occupants, and effort is made to keep exit velocities at vents low and steady.

FIGURE 1 - A typical wind catcher [5]

Wind towers are composed of several parts that work together to catch and direct wind into buildings. The essential parts are the inlet, partition, and diffuser. In this investigation, a nozzle has also been used because previous research [6] indicates it promotes better mass exchange than a tower without a nozzle. A nozzle is also desirable for the turbine to increase wind velocity. While the primary focus of this thesis is power generation using these technologies, one of the goals of this research is to explore using turbines in wind towers that are also providing natural ventilation to support HVAC systems to promote thermal comfort, and so a basic understanding wind tower design from both perspectives is required so that one can understand whether the tower's primary function has been disrupted. Understanding the tower is also essential to understanding how they can facilitate the operation of the turbine.

Inlets

One of the most researched topics in wind towers is the inlet, and this is also the research most useful to the design of a wind tower hosting a turbine. Maximizing mass inflow will promote both maximal mass exchange and promote more power generation. One of the benefits of a tower over a window is the ability to extend above surrounding buildings to gather wind at a higher velocity with more total pressure.

The potential mass flow of a wind tower depends partly on the number of inlets it has. Inlets for square towers are reported to provide more mass flow than round towers, largely due to suction from flow separation on the leeward face [9]. A rounded quarter circle is reported to be the most effective shape for turning the flow [10], therefore circles were used to turn the flow entering the inlet. This was also the shape used in the previous tower investigation [6].

The fewer inlets a tower has, the more mass it will be able to capture when the wind blows in the normal (perpendicular) direction, but the less mass it is able to catch when wind blows in non-optimal directions [9]. An inlet is able to accept wind from angles up to 60^{o} off its inlet normal vector, but there is a marked drop off in capture

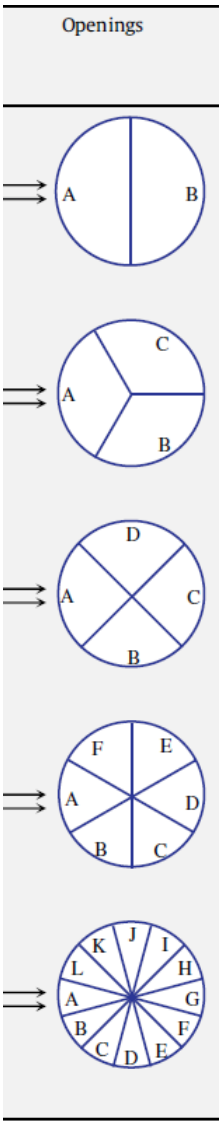

FIGURE 2 - Visual Representations of inlet/partition planforms [9]

beyond 30° [9]. Notably, once a tower has four inlets, the tower becomes omnidirectional, able to accept wind from any direction, because no inlet is ever more than 60° from the prevailing wind. Increasing the number of inlets beyond this decreases total mass flow under ideal conditions, but reduces variation in mass flow depending on which direction the wind is blowing. Refer to Figure 2 for the planform of the wind towers in the experiment, and Figure 3 for a graphical depiction of these results. Note how the total cross section is subdivided equally among all the tower inlets.

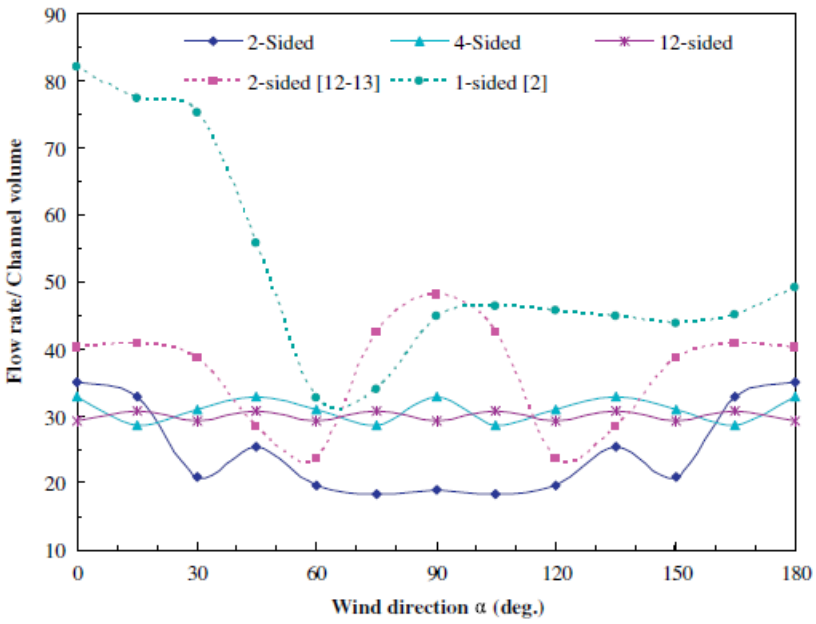

FIGURE 3 -Net Ventilated Airflow per channel volume of the wind catcher for different models [7] (Figure references refer to original paper's references, not references in this thesis)

In a tower with multiple inlets, the inlet or inlets facing into the wind (the "windward inlet") will be an intake, while all the other inlets will see a reduction in pressure as wind blows past them, causing them to behave as "outlets". This allows a single tower with multiple inlets to both intake and exhaust air at the same time without requiring an additional outlet such as a window elsewhere in the building.

It is possible to enhance flow into the tower using inlet vanes or “wing walls” next to the inlet opening, which captures additional wind and directs it into the tower [11]. This effectively increases the inlet area of the tower, and can also be used in areas with low speed wind to enhance the wind resource to something useful for wind towers.

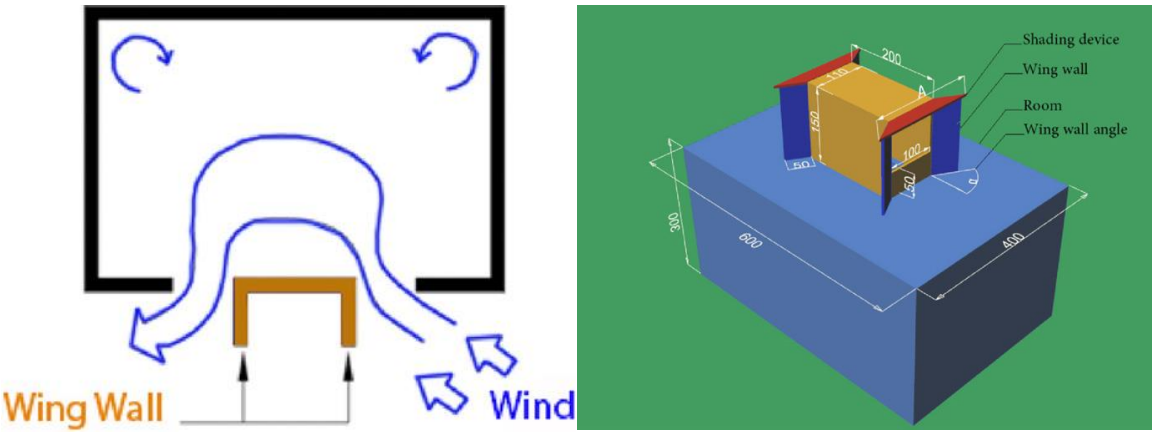

FIGURE 4 - Example of a typical wing wall (left) and the wing wall adaptions investigated in experiment (right) [11].

Partition

In order to prevent wind from simply flowing in one inlet and out another, a partition is required in any tower with more than one inlet. The exact layout of partitions can vary according to local wind patterns, but as noted earlier most research divides the inlet area equally. This is best when no specific wind pattern is being investigated. For the purpose of maximizing the flow intake for general flow patterns, dividing the tower into equal parts is most desirable for this research because it keeps the system symmetric. What this means is that dividing the tower equally between inlets is usually the best approach if considering general wind that is not location specific, but for a specific tower in a specific location the partition could possibly be tailored to the wind resource. For this investigation, the partition will divide the tower equally, as was done in [6].

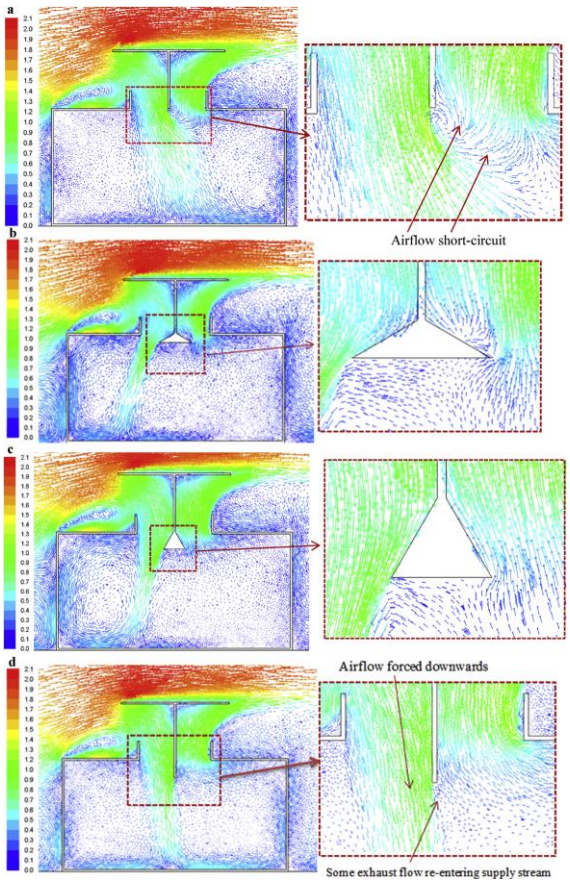

FIGURE 5 - Velocity vectors of mid-plane inside the domain with reference windcatcher (a), windcatcher with 30 ASCD (b), windcatcher with 60 ASCD (c) and windcatcher with 90 ASCD (d). Figure from [12]

Even with a partition, some air flows around the end of the partition to exit the leeward faces. This happens because flow separation around the leeward side of the tower reduces pressure on the leeward inlets, creating suction. The positive aspect of this

is the ability to exhaust air from the same tower, but it does create a problem when air from the windward inlet gets sucked out the leeward inlet. The problem of air flowing in one inlet and out another is referred to as "short circuiting". It is possible to use an "anti-short-circuit device" at the end of the partition to prevent some of that behavior [12]. The device operates by changing the direction of the flow near the end of the partition. The changed momentum carries the flow away from the suction on the leeward side of the tower so that captured fresh air is not wasted; this allows the suction from the leeward side to exhaust air from inside the building. See Figure 6 for visual representation of the anti-short circuit device's functionality.

The partition divides the tower, and in many designs extends the full length of the tower. One of the unusual aspects of the optimization research was that the partition did not extend the full length of the tower, but only went down half way [6]. While there is normally flow down on one side of the tower and up on the opposite side, it is not clear how the partition extending only half way down the tower is going to affect that behavior. The research in [6] indicated that this configuration promoted increased mass flow.

Nozzle

Nozzles increase the velocity in a flow by restricting the area it flows through. According to Bernoulli's law

$$\rho A_1 u_1 = \rho A_2 u_2 \qquad 1$$

thus, the velocity is increased when the flow area becomes restricted. The energy to support the additional velocity comes from the total pressure

$$P_0 = p + q = p + \frac{1}{2}\rho u^2 \qquad 2$$

where P_0 is the total pressure, p is the static pressure, and q is the dynamic pressure defined by $\frac{1}{2}\rho u^2$. In this way, it is sometimes possible to get more kinetic energy than was originally in the flow.

Diffuser

High speed and unsteady airflow can be disruptive to people residing in buildings. To prevent this problem, most wind towers include some kind of diffuser element that reduces the flow velocity before releasing it into the building. In the case of this particular tower, the diffuser is necessary because the nozzle increases the flow velocity, and the turbine is expected to add some unsteady buffeting action to the flow from the motion of the turbine blades. The diffuser preserves the normal function of the wind tower by reducing flow velocity after the nozzle and allowing irregularities in flow to dissipate before it reaches the building.

Wind Turbine Introduction

The Wind Resource

One cannot discuss harvesting wind power using turbines without first discussing the wind resource itself. Most wind farms are built in areas with low turbulence because it improves the amount of power that is produced. For example, off shore wind farms are highly desirable because the open ocean is flat with no obstructions, resulting in clean air with low turbulence. With undisturbed air, wind turbines are able to operate at peak efficiencies.

In stark contrast, the wind resource in cities is extremely turbulent and fraught with wakes behind buildings, or “wind shade”. Called the “built environment”, wind turbines that have been built in urban areas have struggled to produce the power that the

numbers indicate is present [8]. Traditional wind turbines have been deployed, but have consistently underperformed in this environment.

Models for wind behavior often fail to accurately predict turbine behavior, and even when that information is accurate the turbines still only perform as much as 40% as well as predicted [8]. For one specific example of dramatic underperformance, the Museum of Science in Boston, MA installed nine roof-mounted turbines. Although the estimated power production was 20,498 kWh per year (only 15% of total installed capacity), the actual production was only 4,229 kWh per year, or 20% of what was estimated and only 3% of the rated power for the turbines. The power project was converted to a test lab due to the extremely poor performance. This and many other examples from the same source demonstrate that traditional, naked wind turbines are not the best option for power production in high turbulence environments. (Appendix I explores some reasons why this seems to be the case.)

Sometimes, the problem with the installation is deployment in an environment where there is little wind resource to harvest. At the NASA Building 12 location, there was a project to build high-visibility, educational turbines for on-site power production. Because the project was tied to Building 12 and there were a large number of nearby buildings, the turbines were placed into an environment where there was little wind resource to harvest. Because there was little resource to harvest, the turbine power production was minimal.

Turbines cannot be placed without forethought into environments ill suited to power production; and unlike sunlight, the wind resource is not visible to casual observers. Understanding the wind resource prior to construction is critical to the

successful deployment of turbines. Literally millions of dollars have been wasted on projects that do not take the required time to understand the wind resource [8].

The power in the wind can be quantified. Recall that wind in motion is a form of kinetic energy, and that power is energy per unit time. The power in the wind (P_{wind}) is calculated by

$$P_{wind} = \frac{1}{2}\dot{m}u^2 = \frac{1}{2}(\rho A u)u^2 = \frac{1}{2}\rho A u^3 \qquad 3$$

where $\dot{m}$ is the mass flow rate, u is the velocity of the wind, ρ is the density of the flow, and A is the area the mass is flowing through. The most notable feature of this power equation is that power scales with the wind speed cubed. A significant number of cities have typical wind speeds at or above 4 m/s (≈9 mph), which suggests that there could be as much as 39 W/m^2, so this will be the design condition for this exploration of built environment energy production. Some of these cities include Boston, Massachusetts at 5.5 m/s (12.3 mph), Oklahoma City at 5.45 m/s (12.2 mph), and Milwaukee at 5.14 m/s (11.5 mph) [13], among many others. This is also above the wind speed reported to overcome stack effect.

Stack Effect

Putting a turbine into a wind tower is similar to the ducted turbines that have been attempted in the past. One problem that can confound ducted turbines is overcoming "stack effect". Stack effect happens when sunlight warms the exterior of the duct or tower, which then warms the air within the tower, causing it to rise via natural convection and exhaust out all of the inlets simultaneously. In traditional wind tower design, this is

actually a benefit, because the motion of the air upward provides additional ventilation on days that are not windy.

However, for ducted turbine systems, the stack effect can be a critical detriment, causing the flow over the turbine to reverse direction and prevent wind from being able to penetrate into the tower if the windspeed is too low. In one experimental study of the phenomenon, a wind speed of 3 m/s was required to overcome the stack effect [14]. This is lower than the design condition of 4 m/s, but was measured in England (far from the equator). Since stack effect is caused by heating from sunlight, one would expect it to be more important as the intensity of sunlight increases.

It would appear that at least one ducted turbine system was undermined by stack effect. The INVELOX system was designed and tested in Minnesota (roughly 45^{o} N latitude) but implemented in the Palmyra atoll about 1000 miles south of Hawaii and near the equator (about 6^{o} N), among other places. From the description "it acts more like a chimney than a wind turbine", it appears that the INVELOX system failed to perform to expectation in part because of this effect [15,16], so it would be prudent to bear it in mind for design consideration, even though the stack effect is not explicitly modeled in this investigation. SheerWind, the company that designed the INVELOX system, went bankrupt in December 2017.

Investigating stack effect would best be done for each tower on an individual basis before construction on site, considering the direction of the sun and local winds. Trying to do so now would be impractical, and would drastically overcomplicate this early, more general investigation. The effect is important to note for future work.

Efficiency and The Betz Limit

The constraints of reality mean that a wind turbine is never able to extract 100% of the energy from the wind. Conceptually, if a turbine did extract all the energy from the wind, the wind would stop moving and prevent further wind from being able to pass through the turbine. The Betz limit sets a theoretical upper limit for the expected efficiency of a turbine and is an accepted estimation of idealized flow potential.

Written in 1920 by Albert Betz, the limit is equal to 16/27 of the energy in the flow, or about 59% of the energy contained in the wind for an area equal to the rotor area [18]. Returning to the earlier result from equation 3, if there are 39 W/m^2 in a flow at 4 m/s, then the most energy one would be able to extract would be about 23 W/m^2. This sets a reasonable upper limit for the power production of a turbine in much the same way that the Carnot cycle sets a theoretical limit on heat engines. The actual efficiency of any given wind turbine will vary according to the specifics of that turbine.

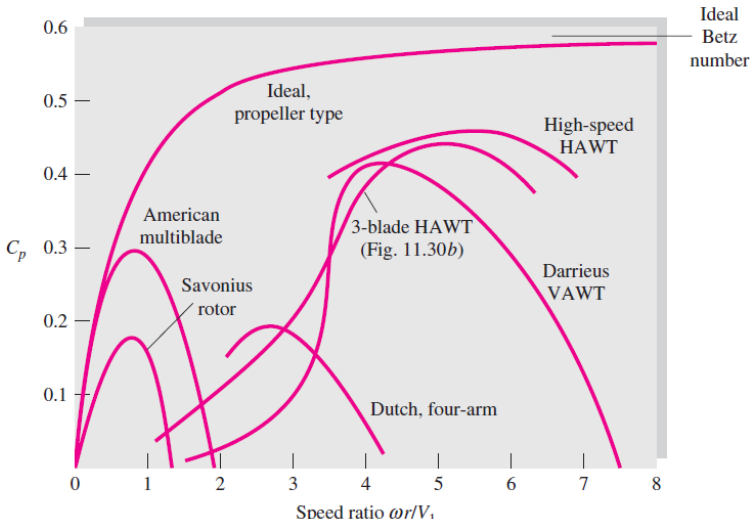

FIGURE 6- Graph of various turbine efficiencies [18]

The Betz limit is a limit based on actuator disk theory, where the turbine is conceived of as an infinitesimally thin disk, and works well for traditional horizontal wind turbines. Savonius turbines have found some success in the built environment. Savonius turbines, also known as S-type turbines, are drag based vertical axis wind

turbines. They are known for having low power coefficients (see Figure 7), but are robust in turbulence. Turbine configurations will be discussed for clarity.

Turbines

Wind turbines are devices used to convert the physical motion of the wind into useful power. Wind moving over the turbine blades produces lift and drag, forces that put torque on the turbine blades and turn the rotor. The rotor is usually attached to a shaft and a gearbox, and ultimately to a magnet that rotates in a coil to produce electricity. The focus of this investigation is on the rotor and the aerodynamic forces it produces to estimate the final power output. Other components, when relevant, will be estimated. Turbines come in many varieties; a basic understanding of the options is required to make informed decisions.

Rotor Configurations

There are two main configurations of wind turbine, the Horizontal Axis Wind Turbine (HAWT) and the Vertical Axis Wind Turbine (VAWT). As the name implies, the HAWT rotates about an axis that is horizontal and parallel to the velocity vector of incoming wind. The familiar three-blade design is the most commonly encountered wind turbine design, and is an example of a HAWT. In contrast, the VAWT rotates about an axis that is "vertical", or perpendicular to the incoming flow of wind. This turbine configuration is illustrated in Figure 8.

FIGURE 7- A Typical Horizontal Axis Wind Turbine (left) [19] and a Darrieus Type Vertical Axis Wind Turbine (right) [20]

The HAWT has a few major advantages. First, the blades can be optimized for a single operational condition for a given uniform wind. This results in relatively smooth, even torque on the rotor as the turbine spins as long as the wind is clean and steady. For commercial power projects, the blades can be actively managed to optimize performance for the incoming wind condition, which maximizes the efficiency and productivity of the turbine. For commercial projects, actively managed turbine blades are standard because improving the performance of a megawatt turbine is worth the cost and effort.

The HAWT is a mature technology, which is an advantage for that configuration. The design of the turbine blades is advanced, with twist and airfoil shapes that change over the length of the blade to take advantage of variations in relative wind along the length of the blade. The velocity triangles are well defined and described, and many advanced turbine designs would be available off the shelf for implementation, if a HAWT were viable.

The main disadvantage for HAWT is that they have been attempted many times before in the built environment, and have consistently underperformed compared to even modest expectations [8].

The VAWT offers different advantages. First, it is "omnidirectional", meaning that it can accept a flow from any direction, so there is no need to rotate the turbine to orient it into the wind. However, a uniform flow acting on a VAWT only produces useful aerodynamic forces over half the turbine, while the other half still produces drag that retards the motion [21] (see Figure 9). In free flows, a drag shield can be implemented over the unproductive section of the turbine to reduce the problem and even direct the flow toward the productive side [22].

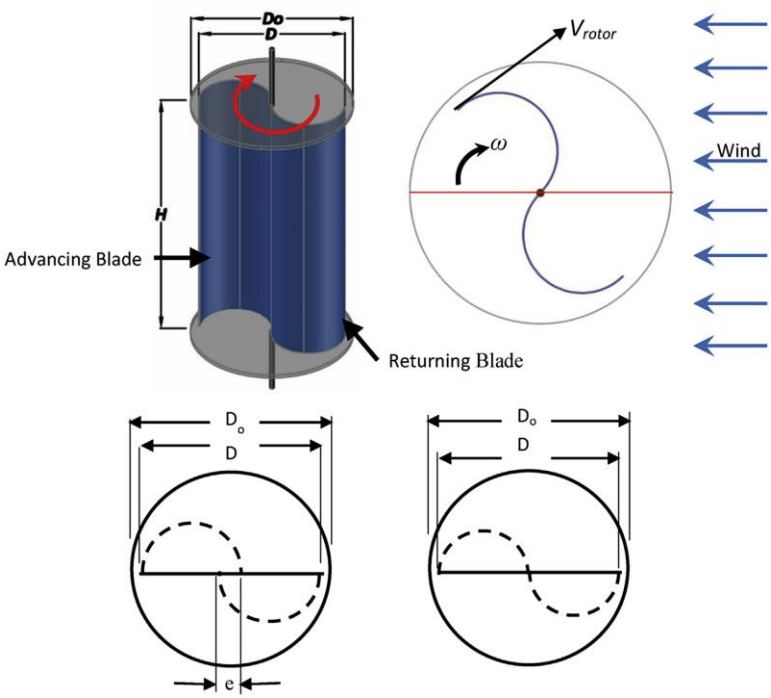

FIGURE 8 - A typical Savonius turbine design with or without overlapping blades. [21]

Second, VAWT can be designed as either a drag-based turbine, or as a lift-based turbine. The turbine design varies based on whether most of the torque comes from drag or lift. The most common drag-based turbines are the Savonius turbine, which provides strong torques, is self-starting, and works well at low tip speed ratios and operational velocities. Savonius turbines are sometimes referred to as "S-type" turbines, and two variants were pictured in Figure 9. An alternative version of the Savonius turbine is the Bach turbine, which modifies the blades for improved efficiency and power production [23].

VAWT can also be Darrieus turbines, or D-type turbines. Darrieus type turbines use lift to produce power, but are not self-starting. A Darrius turbine requires either an outside power source to start it, or an additional turbine to provide the starting torque. Sometimes referred to as "egg-beater" turbines, the Darrieus turbine has two thin blades attached to a central shaft to provide torque. A Darrius turbine can be seen in Figure 7 (right image).

One last type of turbine is a barrel-type turbine, which is often lift based but uses multiple blades in a barrel shape. This was implemented in [7].

Regardless of the type of turbine, one of the most often compared characteristics is the "tip speed ratio" (TSR), defined

$$\lambda \equiv \frac{\omega R}{u} \tag{4}$$

where λ or TSR are the tip speed ratio, ω is angular velocity, R is the radius at the tip of the blade, and u is the velocity of the freestream.

Aerodynamic Forces

There are two primary aerodynamic forces: lift and drag. Drag is defined as the force produced in the same direction as the wind, while lift is perpendicular to the wind. Lift and drag are often described using lift and drag coefficients rather than direct forces, and those coefficients are defined

$$C_L = \frac{L}{\frac{1}{2}\rho u^2 A} \tag{5}$$

$$C_D = \frac{D}{\frac{1}{2}\rho u^2 A} \tag{6}$$

$$C_M = \frac{M}{\frac{1}{2}\rho u^2 Ac} \qquad 7$$

where L is the lift force and D is the drag force, normalized using the dynamic pressure and a "characteristic area", usually the area of the airfoil or body of interest.

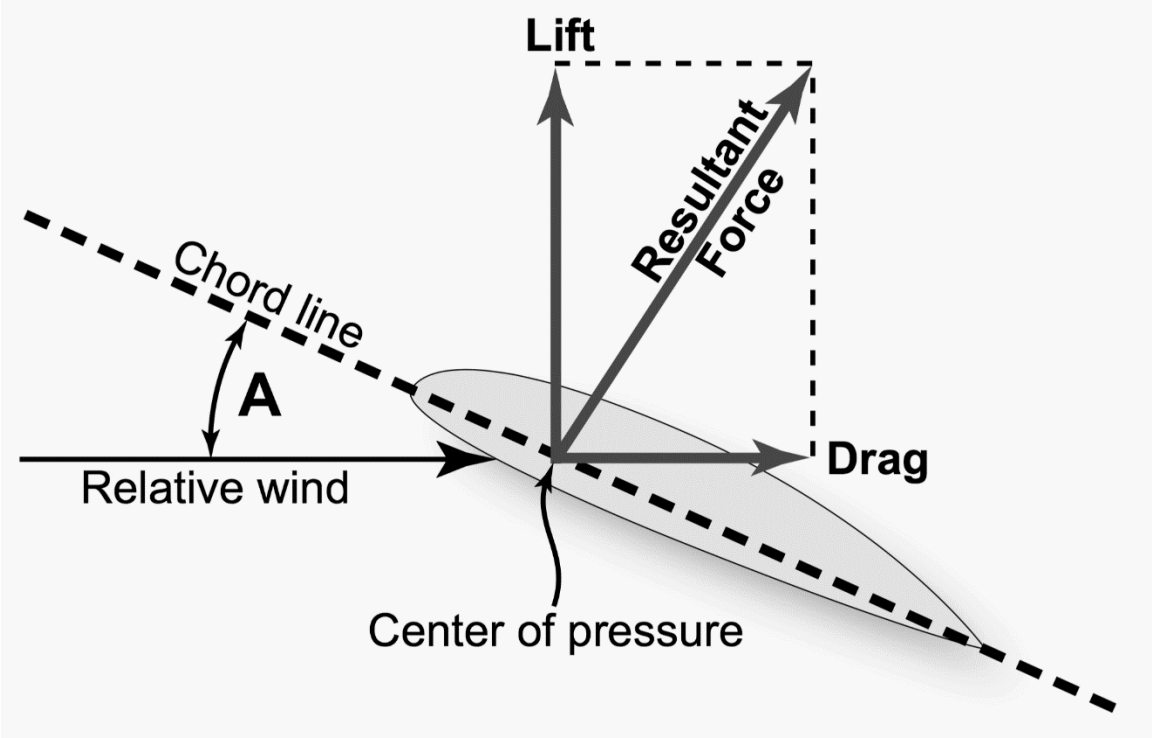

FIGURE 9 - Lift and Drag force diagram [24]

For most airfoils, there is a region at small angles of attack (α) that will produce high lift with very low drag, and in many applications (including HAWT turbines) this is the preferred operational regime because it offers the highest lift-to-drag ratio. As the angle of attack increases, eventually an airfoil will reach "stall", where the flow separates from the airfoil. At that point, there will be a dramatic loss of lift, and drag will suddenly increase [25]. Sometimes, lift and drag coefficients are only reported to this point,

because for many applications such as aircraft, the ratio of lift to drag is the critical criteria, not the maximization of lift. Such reports resemble the functional diagram in Figure 10.

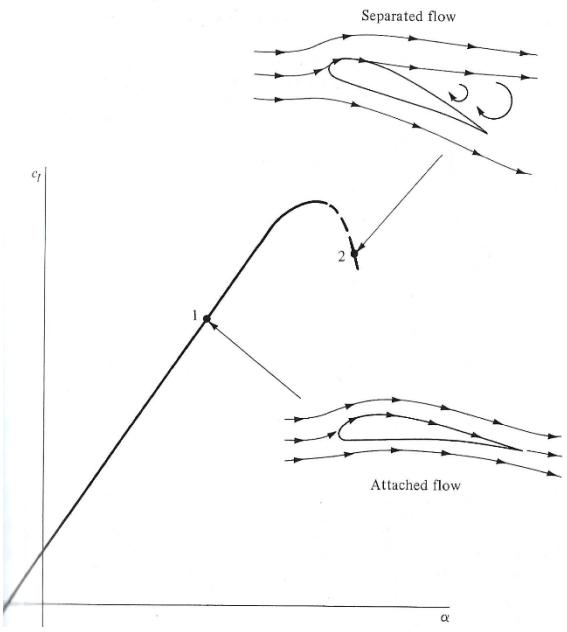

FIGURE 10 - Functional Diagram of lift coefficient for a cambered airfoil [25]

After stalling, as the angle of attack continues to increase the lift and drag also continue to increase. The maximum value for lift coefficient in this region peaks at 45^o while the maximum value for drag coefficient peaks at 90^o. While many lift and drag curves only display the portion of performance leading up to stall, for VAWT one needs to consider the entire 360^o lift and drag curve, since the airfoil will pass through all of those angles and will need to be understood at each of those points. For a symmetric airfoil, a 180^o report is functionally identical to a 360^o report, because the symmetry of the airfoil means that 181^o-360^o are the mirrored values as reported for 1^o-180^o. A 180^o lift and drag curve for the NACA 0012 can be seen in Figure 11, which was generated using data from Sandia National Labs [26]. The NACA 00-series are symmetric airfoils.

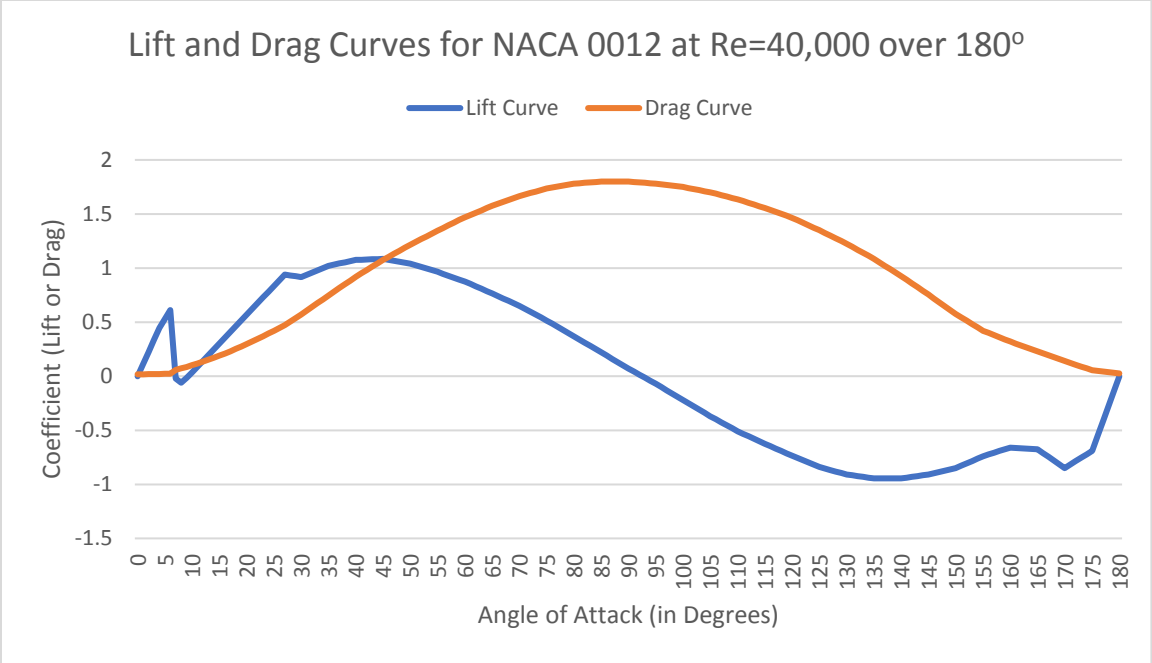

FIGURE 11 - Lift and Drag curve for NACA 0012 over 180 degrees
Note the sharp drop off around 10 degrees; that is where the airfoil reaches stall.
Data from Sandia report [26].
Note the difference between maximum lift coefficient and drag coefficient.

Velocity Triangles

For a turbine, the incoming freestream wind is not the only wind acting on the turbine blade. In a rotating turbine, the wind that is "seen" by the turbine blade is a combination of real freestream velocity and an induced velocity resulting from the rotation of the turbine. This is described by

$$\vec{u}_{tot} = \vec{u}_w + \vec{u}_{rel} \qquad 8$$

with the induced wind defined by

$$\vec{u}_{rel} = -\vec{\omega} \times \vec{r} \qquad 9$$

where ω is the angular velocity vector (*i.e.* rotation speed) and r is the radius. The cross product of these two variables is the physical motion of the blade tip, while the apparent wind will be in the opposite direction to the motion (hence the negative). As seen in

equation 7, the larger the radius and the faster the angular velocity, the larger the relative component of the wind. For a HAWT, because the radius varies significantly along the length of the blade, a twist is sometimes applied to the blade so that each part of the blade is generating as much lift as possible at the optimal angle of attack.

The power generated by a turbine is calculated using

$$P_{turb} = \tau\omega \tag{10}$$

where τ is the torque or moment acting on the turbine and ω is the angular velocity. By taking the ratio of the power produced to the power in the flow (or the freestream), one can determine the power coefficient of the system using

$$C_p = \frac{P_{turb}}{P_{wind}} \tag{11}$$

which describes the fraction of the energy actually captured by the turbine. Using the power coefficient, the efficiency of different wind turbines can be compared. For example, the power coefficient for a perfect turbine at the Betz limit would be 0.59.

Computational Fluid Dynamics (CFD) Introduction

Computational Fluid Dynamics (CFD) is a solution method for fluid dynamics that solves large, complex problems by breaking them into many small, simple problems, then assembling an answer from the collective solutions. Also referred to as a "numerical analysis", the technique enables the investigation of advanced fluid phenomena that would be expensive or physically impractical to investigate using experimental means, but also requires that the initial set up for the problem be a reasonable approximation for the reality being investigated. If a solution is set up incorrectly, CFD will still produce a solution, but the solution will be wrong. Therefore, it is critical that problems

approached using CFD be defined correctly. In order to ensure that the data generated are useful, it is important to understand the basics of how CFD problems are defined, and how each of those steps contributes to an accurate solution.

Computer-Aided Design (CAD)

The first step to a numerical solution is to set up the geometry using a CAD program of some kind. Programs such as SolidWorks and DesignModeler allow users to define the physical boundaries of a fluid dynamics problem. When flow over a solid body is considered, often the solid body of interest is modeled first. Then, the solid body is subtracted from a fluid domain in order to leave behind only the fluid – the air or water which is the real body of interest in a CFD investigation.

When setting up geometry, it is important to ensure that the fluid domain is large enough that restriction within the domain itself will not greatly influence the solution. If fluid is flowing over a physical body, the body behaves like an obstruction. If the fluid domain is too narrow, the blockage will reduce the flow area substantially and distort the flow field over the body. This is similar to the problem faced in wind tunnels where models too large for the tunnel generate incorrect results. As long as the blockage ratio is not too large, there should not be a problem. Usually, a blockage ratio between 5% and 10% is considered acceptable [27].

Meshing

The second step in CFD is meshing, where the problem is broken into many small parts. The primary tradeoff driving most meshing decisions is the conflict between the need to accurately model an unknown flow and the time (and computational power) available to calculate the solution of the resulting problem. Reducing elements to only

80% of their original size roughly doubles the number of elements, but failing to have enough resolution in critical areas will cause the solution to be wrong. This problem can be investigated using a mesh analysis. The problem is initially solved using a loose mesh to generate a baseline solution, then repeatedly solved with more refined meshes until the solution stops changing with improved resolution. The solution is quantified by measuring a specific value and area of interest until the value of interest does not change with greater refinement. This does not guarantee a "correct answer", but a mesh analysis does confirm that the solution generated is independent of the mesh being used to investigate the problem. In other words, a mesh analysis confirms that the answer is not a fluke of how the problem was broken up before solving.

Solving

Solving the fluid flow in question is done using a solver, such as CFX, Star CCM+, or Fluent. A solver allows the user to specify boundary conditions and equations used to solve the fluid flow problems in the mesh. The equations used vary depending on solver; the most common solution methods use Reynolds Averaged Navier-Stokes (RANS) to determine the flow behavior by modeling rather than calculating all the details of the flow. Various models work well with varying levels of accuracy under different circumstances, depending on which equations the method prioritizes and the conditions in the flow.

There are two popular two-equation turbulence models. The first is the k-ε model [28], which solves for the turbulent kinetic energy and the dissipation rate of turbulent energy. This model excels at modeling free flows, but sometimes fails to accurately capture flow separation. In contrast, the k-ω model excels in the near-wall region, but

fails to capture behavior further from the wall accurately. The shear stress transport k-ω model, which uses the k-ω model together with two other transport equations, one for intermittency and one for transition onset criteria, to blend accurate models near and far from walls [29]. Models using additional equations can improve the ability to model accurately, at the expense of increased simulation runtime. The Transition SST model available in Fluent uses 4 equations to improve the prediction separated flows.

To generate useful data for a VAWT, it is important to apply a method that is able to model the flow over an airfoil at extreme angles of attack and produce lift and drag results of satisfactory accuracy even when the flow is separated. It is possible to model separated flows using other models as well, such as a Large Eddy Simulation (LES) or Detached Eddy Simulation (DES), but those methods are more computationally expensive. As described by Fu [30]:

> "[The author of a paper] performed Delayed Detached Eddy Simulation (DDES) using an Audi RS5 DTM model in order to investigate the interference of the moving belt geometry on racecar aerodynamics. Their CFD model consists of 90 million cells, and a 512 core cluster took 130 [hours] to complete one simulation. In comparison to that, a 115-million cell RANS simulation of a NASCAR racecar would have taken about 8 [hours] to be completed on the same cluster."

The cost of more complex models is high, and for an initial exploratory investigation may not be worth the computational cost. This cost would be magnified as the number of simulations increased. LES or DDES would be appropriate to analyzing a complete or nearly complete design which could not be improved using simulations run using a RANS method, but should be reserved to that time.

Post Processing

Post Processing refers to the information extracted from a simulation after it has been solved. Often, post processing involves visualizing data so it can be interpreted and understood more clearly by humans. Most of the visual figures featured later depicting the flow over the tower and turbine were developed using post processing.

The Structure of This Paper

One of the major goals of this paper is to ensure that following researchers from the group will be able to understand, duplicate, and build on this work. This paper is primarily structured as a series of projects in each chapter, with the analysis from earlier projects informing decisions made in later projects. Tower investigations are collected first because understanding the tower is required to make informed decisions about the turbine. Turbine investigations are in later chapters. To better organize the methodology and results of multiple projects, each individual investigation is in its own chapter with its own brief Methodology, Results, and Conclusion sections. When applicable, the strengths and weaknesses of each investigation are discussed.

CHAPTER 2: ANALYSIS OF FLOW IN VARIOUS WIND TOWERS

In order to implement a turbine in a wind tower, it was necessary to gain an understanding of the flow behavior inside the wind tower to inform the choice of turbine. This first investigation started with the same techniques and tower design where the previous research left off.

Various Wind Towers: Methodology

The general plan for the tower's design had been determined by previous research [6]; what was not clear was how many inlets should be used, how the number of inlets would affect the behavior of the flow inside the tower, or how the shape of the tower cross section would affect the flow through the tower. The specific flow behavior within each tower was also uncertain, so it was not clear whether a HAWT or a VAWT would be a better choice for the flow conditions. Before beginning design on a turbine, it was necessary to understand the behavior of the flow which would be harvested; this is a necessary step which caused

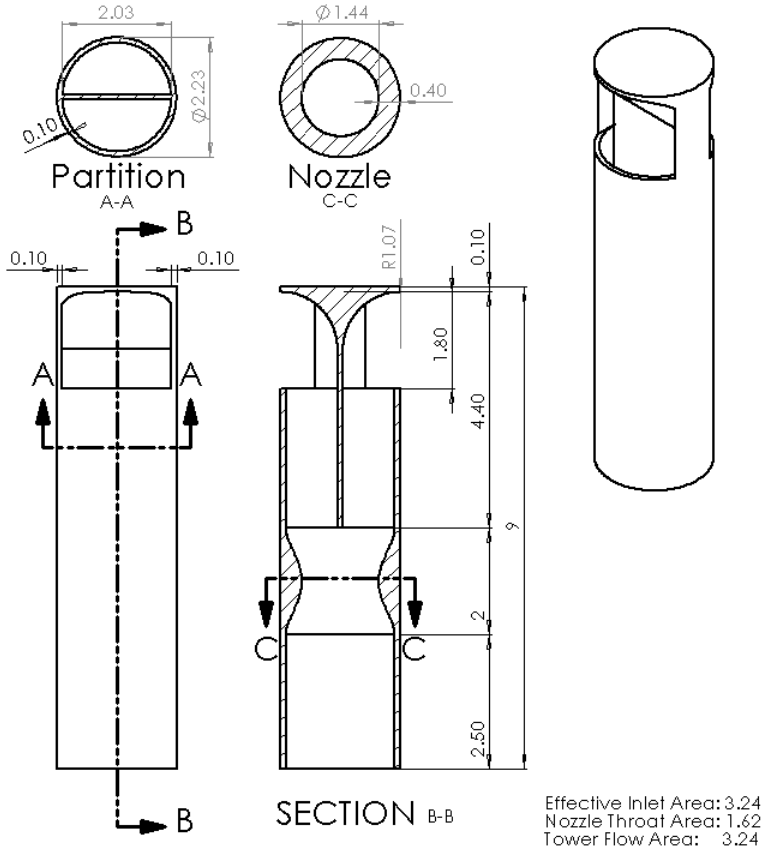

FIGURE 12- Dimensions for the Two-Sided Circular Tower Lengths in meters, areas in m^2

multiple professional projects to fail [8].

First, the general planform from previous research [6] was used. Each tower would be 9 meters tall, have a cross sectional area of 4 m^2, and use both a partition and a nozzle to guide and enhance the flow in the tower. All walls were 0.10 m thick; thus the area of the flow beyond the partitioned area in square towers was 3.24 m^2. The nozzle area was half the undivided tower cross sectional area. The throat of the nozzle was 3.5 m over the ground, and the converging-diverging nozzle was 2 m long. One improvement in these models over previous work was the use of a spline curve to define the nozzle. This improvement was possible by using SolidWorks instead of the ANSYS DesignModeler, which did not easily support spline curves. The spline is visible in Figure 13. The shape was extruded using "up to next", then a circular pattern was applied to achieve the final nozzle shape. This means that the shape of the nozzle matches the shape of the tower.

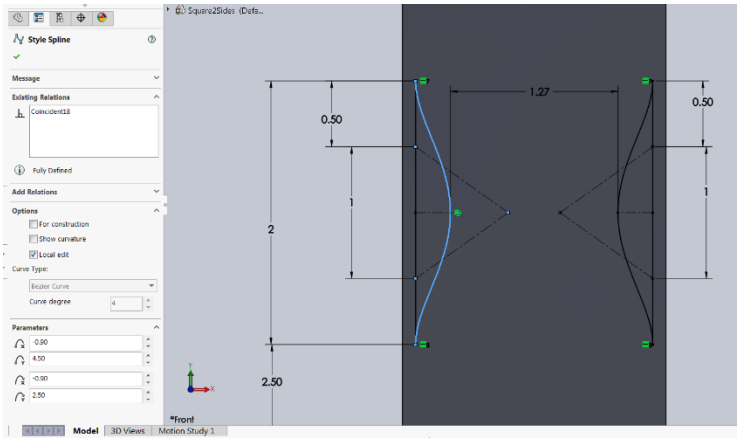

FIGURE 13 - View of spline curve definition for nozzle in a square tower.

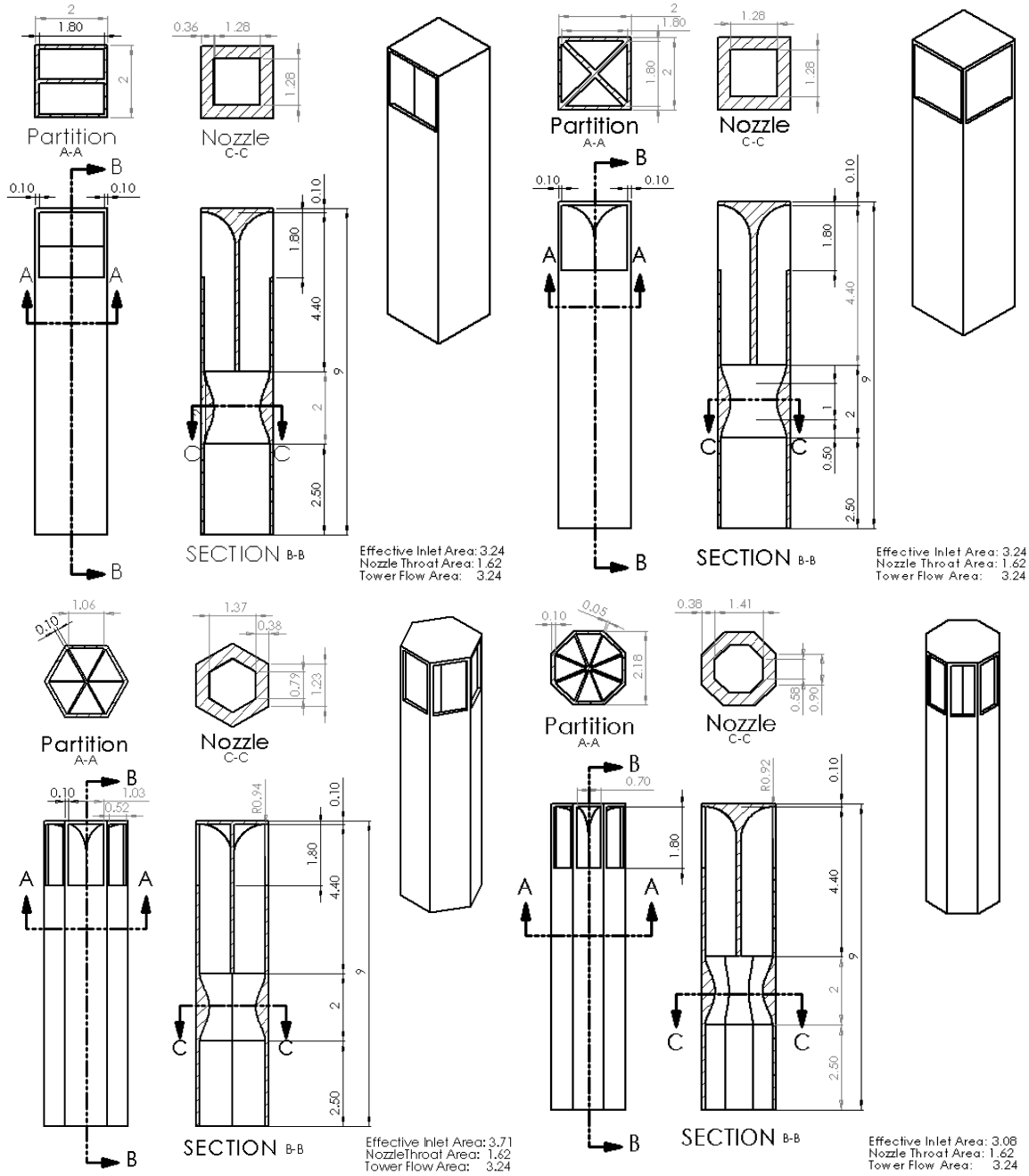

FIGURE 14- Dimensions for Two-Sided Square (top left), Four-Sided Square (top right), Six-Sided Hexagon (bottom left), and Eight-Sided Octagon (bottom right). Length dimensions in meters (m), areas in meters squared (m^2).

The base of the tower had an opening which served as a pressure outlet and represented the tower's connection to the building it was likely to be attached to. The

pressure at the outlet was assumed to be 1 atm (0 gauge pressure). The fully detailed towers with dimensions are visible in Figures 12 and 14.

The towers were modeled in SolidWorks, then imported to ANSYS Workbench 19.0 for analysis as initial graphics exchange specification (.IGS) files. The fluid interior was added using Design Modeler by using a Boolean to subtract the modeled tower from a solid volume of air equal to the exterior dimensions of the tower. The simulation was meshed using ANSYS Workbench using 8 cm sized elements for most of the tower, and 5 cm sized elements in the nozzle. The boundary layer by default was modeled using 5 inflation layers with 1 mm for the first layer thickness and a growth factor of 1.2. The tower nozzle was almost the same, with 7 inflation layers instead of 5.

The mesh was imported to ANSYS CFX, where the boundary conditions were set. One inlet was taken to be normal to the incoming flow, and was set as a velocity inlet at 4 m/s normal to the inlet. For towers with more than one inlet on the windward side, such as the 6-sided hexagonal tower, the other inlets were set with wind velocity component-wise in the same direction as the wind at the windward inlet. In other words, all of the inlets facing the wind were set to have wind blowing at 4 m/s blowing in the same direction. Inlet turbulence intensity at the inlet was set at 5%.

Using 4 m/s for the windward inlets corresponds to 100% capture of the freestream mass flow, and was the design condition originally used by the NADGOD research group to optimize the tower in [6]. This dramatically reduced simulation times compared to modeling the tower with an enclosure. Using this as the initial design condition does require caution because it is extremely unlikely that 100% of the freestream will actually be captured by the tower, but the tradeoff for quickly

understanding the general flow profile was deemed acceptable for the first investigation. (This method of operating is not recommended for future work.)

The other inlets, which did not face into the wind at all, were set as entrainment with 1 atmosphere of back pressure (*i.e.* 0 gauge pressure), meaning that they were able to function as either an inlet or an outlet as determined by flow conditions in the rest of the tower. This was also consistent with the model used in previous work to optimize the tower. The outlet at the bottom of the tower was a pressure outlet, also at 1 atm (0 gauge) pressure. The walls of the tower were set as "walls" with the no slip condition. A mesh analysis was performed on the two-sided tower's mesh, and other towers were meshed using the same criteria. The number of mesh elements (*i.e.* cells) for each tower are listed Table 1.

TABLE 1 - Number of elements for each wind catcher cross section used in CFD simulations

Tower	Elements
2-Sided Circular	421k
2-Sided Square	520k
4-Sided Square	739k
Hexagonal	1,465k
Octagonal	1,372k

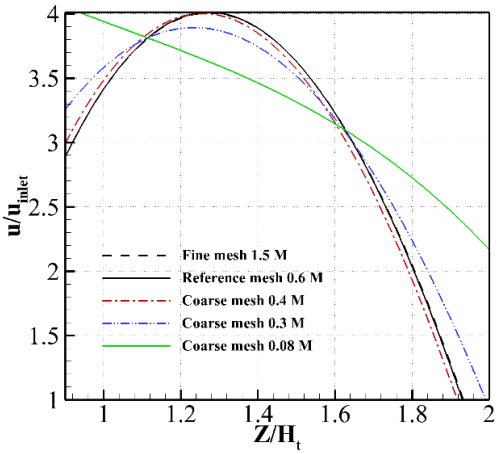

FIGURE 15- Grid-sensitivity analysis, profiles of normalized velocities at the nozzle throat area for different grid sizes

The solver then solved each tower to determine the flow profile through the tower. An SST k-ω model was used to analyze the flow in the tower. The results are summarized below.

Various Wind Towers: Results and Analysis

Because power scales with the velocity cubed, the velocity is the most important flow characteristic to consider for power production. The two towers with the highest velocities in these simulations were the four-sided square and the hexagonal tower, as seen in Figure 16 and Table 2. The four-sided square had a higher peak velocity, but the wind resource was confined to a limited area near the walls where it might be difficult to harvest. The hexagonal tower had more power closer to the center of the flow field and a more even velocity distribution, which would be more desirable for a HAWT if the data supported that option. The high velocity flow in the four-sided square tower is clearly visible, as is the asymmetric velocity distribution within the nozzle of the tower.

TABLE 2 - General Tower Summary of Relevant Characteristics

Tower	Max *V* (m/s)	Average *V* (m/s)	Mass Flow (kg/s)
Two-Sided Square	16.95	10.07	19.25
Two-Sided Circular	15.96	11.18	21.41
Four-Sided Square	31.64	10.74	19.77
Hexagonal (6-sided)	23.65	11.18	21.27
Octagonal (8-sided)	21.41	9.79	18.64

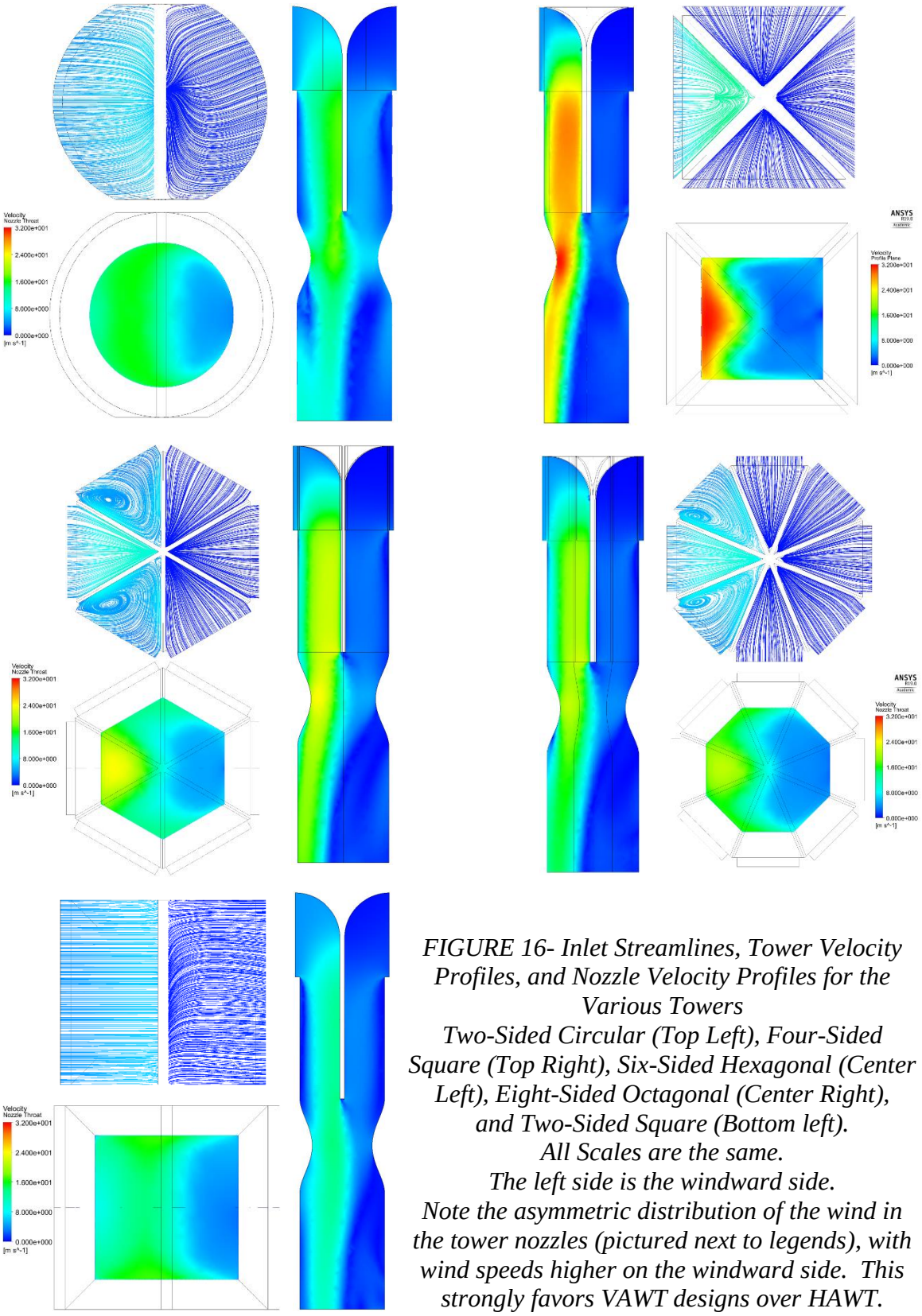

FIGURE 16- Inlet Streamlines, Tower Velocity Profiles, and Nozzle Velocity Profiles for the Various Towers
Two-Sided Circular (Top Left), Four-Sided Square (Top Right), Six-Sided Hexagonal (Center Left), Eight-Sided Octagonal (Center Right), and Two-Sided Square (Bottom left).
All Scales are the same.
The left side is the windward side.
Note the asymmetric distribution of the wind in the tower nozzles (pictured next to legends), with wind speeds higher on the windward side. This strongly favors VAWT designs over HAWT.

Energy Analysis

Once the two towers most likely to have the most energy had been identified, a more detailed method of analysis of the energy available in the throat of the nozzle was developed and conducted. Because power scales with the cube of velocity, looking at the average velocity alone will not account for all of the available power. For the four-sided square and six-sided hexagonal towers, each nozzle was sampled twice, once with the tower profile shape (the profile for a VAWT) and once with a circle (the profile for a HAWT) to determine the amount of power which was in the flow. The square sample in the square tower was sampled every 1 cm in a square 1.28 m by 1.28 m, for a total of 16641 points (end points inclusive). The hexagonal sample in the hexagonal tower was

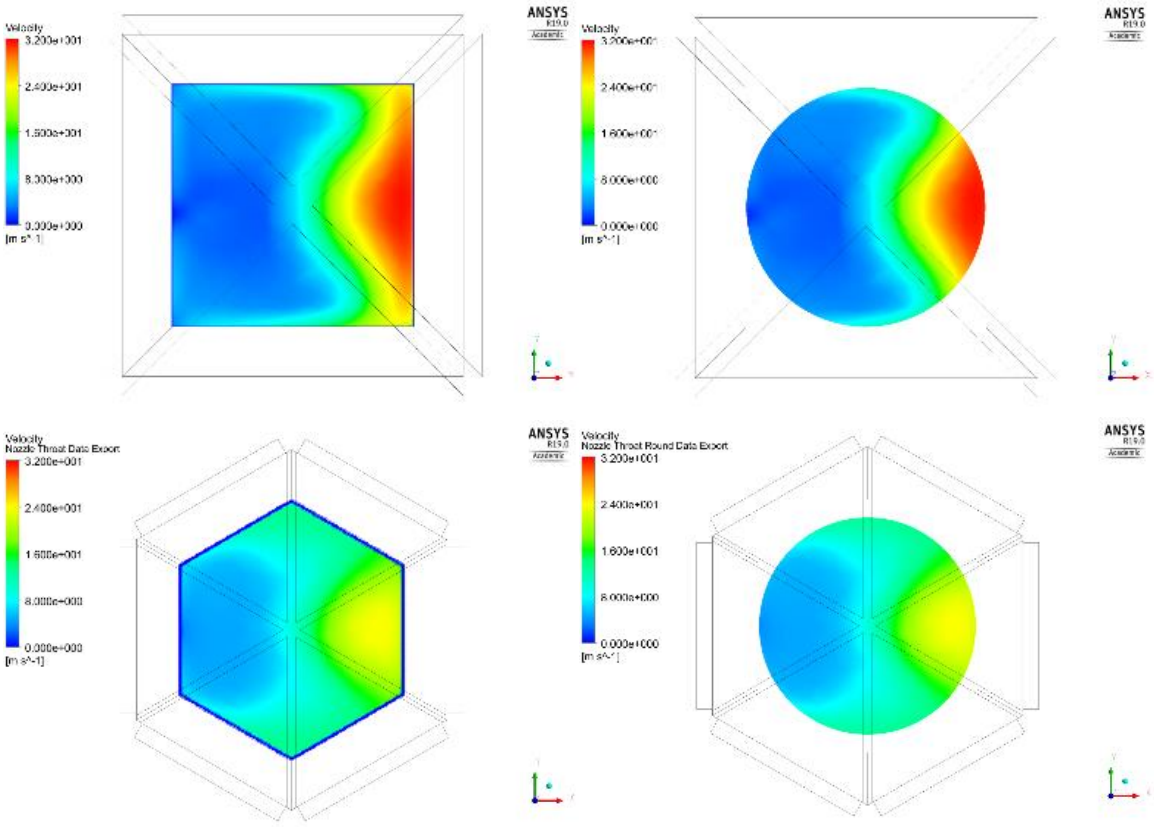

FIGURE 17 - Exported Velocity Profiles for tower nozzles with high velocities. Square VAWT (top left) and HAWT (top right) and Hexagonal VAWT (bottom left) and Hexagonal HAWT (bottom right) profiles.

also sampled every 1 cm; the sample plane was a rectangle large enough to encompass the entire cross section, with 17149 points inside the tower (sample points outside the tower with no velocity were discarded when the data was exported from ANSYS CFD-Post). For each of these cases, the area of the nozzle throat was algebraically divided equally among the sample points, so that each sample velocity was given equal weight. The energy in each sample area was summed then summed to find the total flow energy available to a VAWT.

The second part of the analysis was for a circular sample area, since that is the profile of a HAWT in the flow. For that sampling, each of the towers was sampled using a polar coordinate frame, with 360 samples in the θ-direction and 101 samples in the r-direction, for a total of 36001 sample points (100 in each direction and one center point). The radius of the circle for the square tower was 0.63 meters and for the hexagonal tower was 0.675 meters.

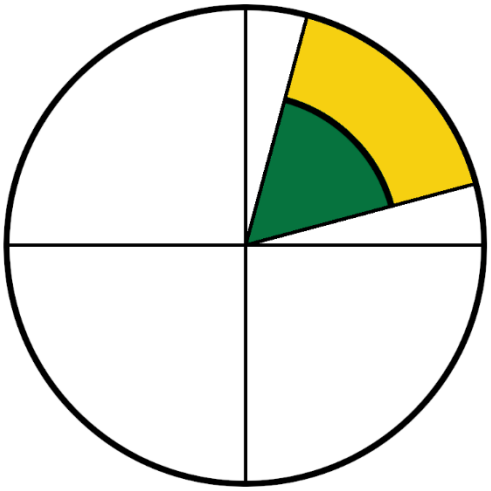

FIGURE 18 - Visual representation of the difference of two sectors of different radii but equal angle. The difference is in gold.

Because the sample area for each point was not quite the same (samples increase in size as the radius increases), the sample area was calculated per point in Excel using an area formula. Recall the area of a sector is

$$A = \left(\frac{\theta}{2}\right) r^2 \qquad 12$$

and taking the difference between two sectors of different radii r_0 and r_1 but equal angle yields

$$A = \left(\frac{\theta}{2}\right)(r_1{}^2 - r_0{}^2) \quad (13)$$

where r_1 is the outer radius of the area, r_0 is the inner radius, and θ is the polar coordinate. This expression is the difference of two sectors with equal angle (θ) but different radii (r_0 and r_1). See Figure 18 for visual representation of the difference of two sectors. This allows sample points further from the center to reflect their larger area accurately, which is important since the high energy part of the flow is far from the center.

The samples exported from the cross sections included data for total velocity magnitude and each velocity component. Using the power formula from Equation 3, the total power within the flow could be calculated. The square and hexagonal samples were weighted equally because the sampling was evenly distributed, and each sample point had an area equal to the cross section divided by the number of sample points. The results are summarized in Table 4.

TABLE 3 - Detailed Energy Analysis Results

Tower	Turbine Profile	Power (kW)
Four-Sided Square	VAWT (Square)	4.866
Four-Sided Square	HAWT (Round)	3.300
Hexagonal	VAWT (Hexagonal)	2.500
Hexagonal	HAWT (Round)	2.263

Various Wind Towers: Conclusion

Based on these results, it appeared clear that a vertical axis wind turbine (VAWT) of some kind would be the most suitable option for power generation. The asymmetric

flow field strongly suggested the use of a VAWT over a HAWT because of the asymmetric flow pattern, and the power analysis for the towers supported that decision. While it might hypothetically be possible to redesign the towers to change the nozzle shape to better accommodate a HAWT, that would not change the asymmetric flow field, and a HAWT would not operate well in an asymmetric flow such as is found in these towers.

This work led into Chapter 3, understanding the tower using an enclosure; and into Chapter 4, where a VAWT investigation began. Assuming full capture at the inlet allowed for running simulations quickly, but was not an effective method of investigation because the data which were generated were not representative of reality, as will be seen in Chapter 3. The method used to extract and understand power remained useful throughout the investigation.

CHAPTER 3: TOWER WITH ENCLOSURE

Tower with Enclosure: Introduction

It was known when running the initial analysis that there would not be complete capture of the freestream velocity. To get a better understanding of how a tower would behave in reality, a simulation using an enclosure was run to more accurately model tower behavior from the first investigation.

Tower with Enclosure: Methodology

A simulation with an enclosure was prepared for the four-sided square tower. The tower from the previous investigation was used. Recall the tower was a 2m by 2m square and 9m tall. The enclosure extended 10 m before the tower, 20 m behind the tower, and 7 m to either side of the tower. The simulated volume was 30 m tall. Figure 20 shows the simulation set up visually.

The face before the tower (10 m from the tower) served as a velocity inlet, with wind at 4 m/s and 5% turbulence. The opposite face (20 m behind the tower) and the inside base of the tower were pressure outlets at 1 atm. For the external pressure outlet, 1 atm is the standard pressure. The outlet at the bottom of the tower represents its connection to whatever building to which it would be attached. The ground and the tower walls were walls with the no-slip condition.

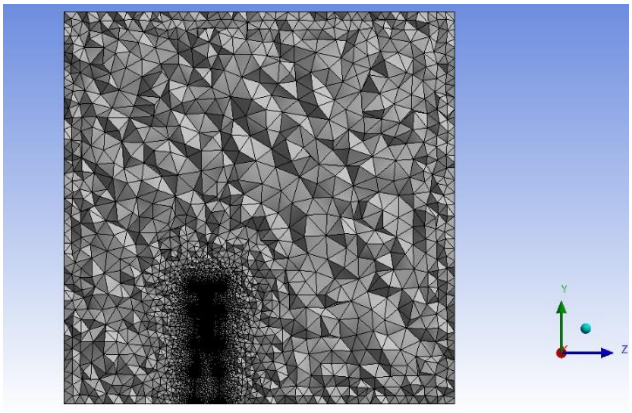

FIGURE 19 - Section view of meshed tower

The volume was meshed using many refinements around the inlet and

partition to ensure accurate representation of the flow. The final element count was 15 million cells, with most of the refinement within the tower itself. The mesh was then solved using the SST Transition model.

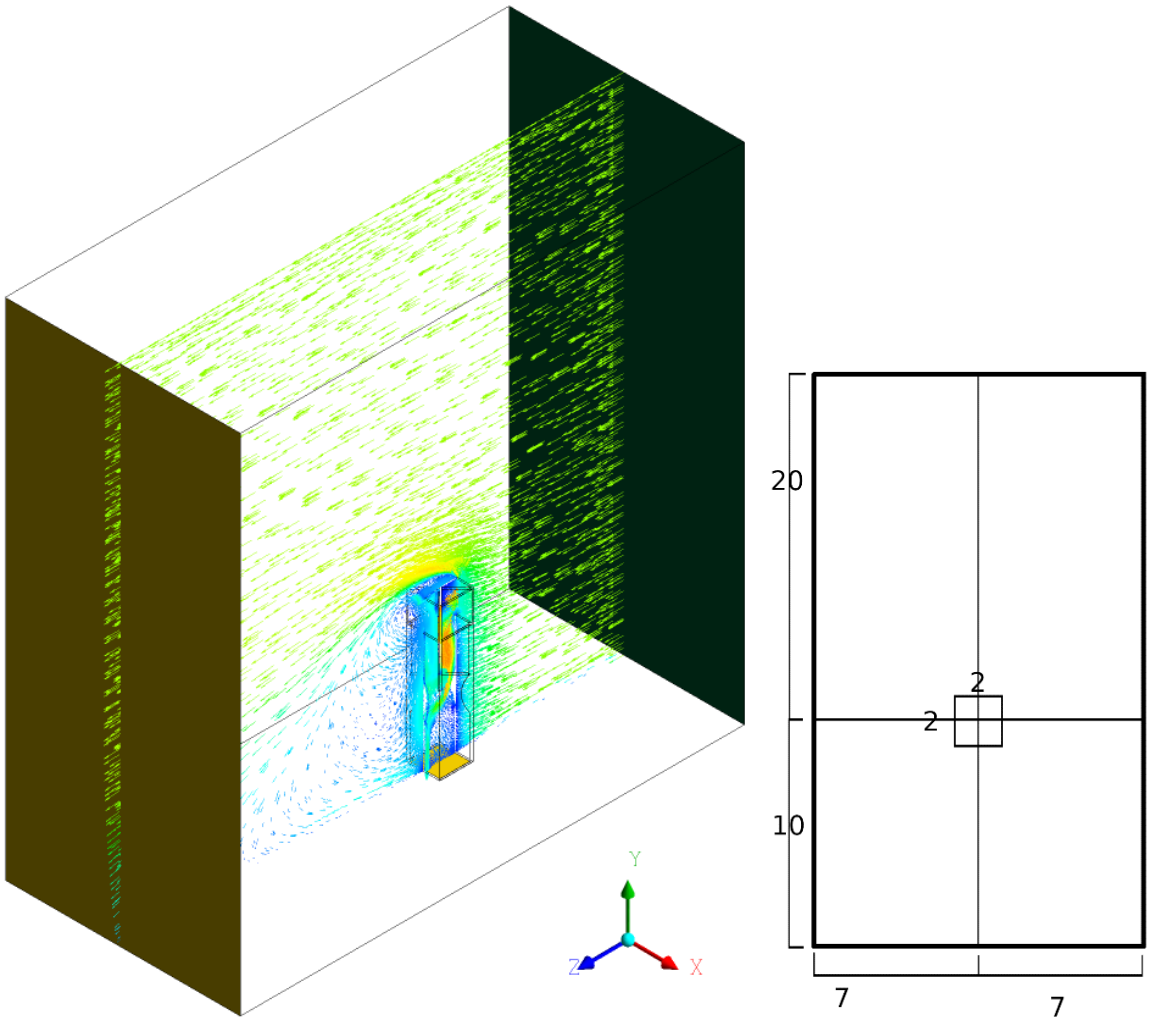

FIGURE 20 - Computational Domain of Second CFD Analysis.
Velocity inlet in dark green; pressure outlets at bottom of tower and rear in gold (left).
Top view of Enclosure (right). All lengths in meters; enclosure is 30 m tall

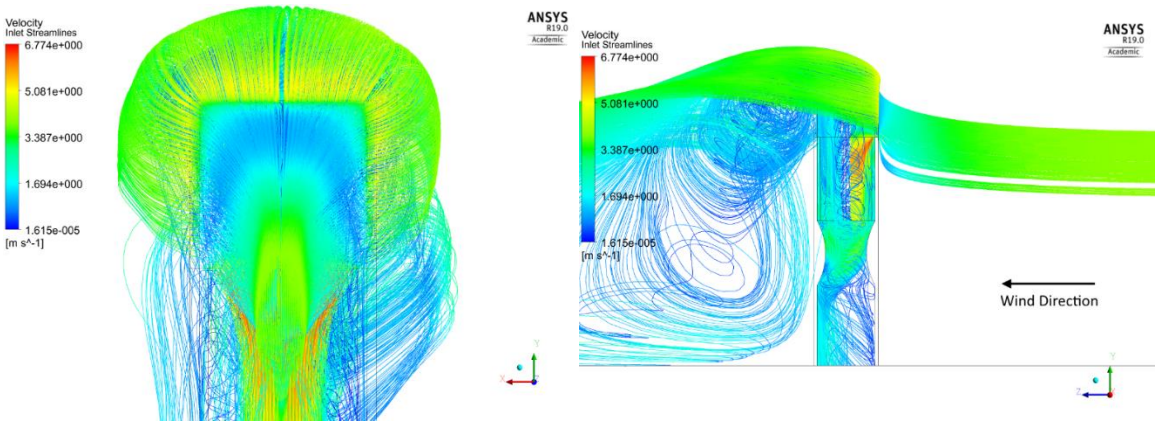

FIGURE 21- Front View (left) and Side View (right) of Inlet Streamlines of tower in Enclosure, showing inlet spillage around tower with flow going in the inlet, reversing, and flowing back out and around the inlet.

The results indicated that the assumption of full capture was extremely wrong. Figure 21 shows the flow in the windward inlet, where some of the wind which had been captured reversed direction, exited, and flowed out and around the tower. Note the horseshoe pattern in Figure 21 (left) indicating that the flow has encountered a region of high pressure that pushed it back out the inlet. This suggests the inlet can be improved to capture more of the flow. Figure 22 shows the updraft from the bottom outlet (at 1 atmosphere) up through the tower and out the "inlet" at the top of the tower on the leeward

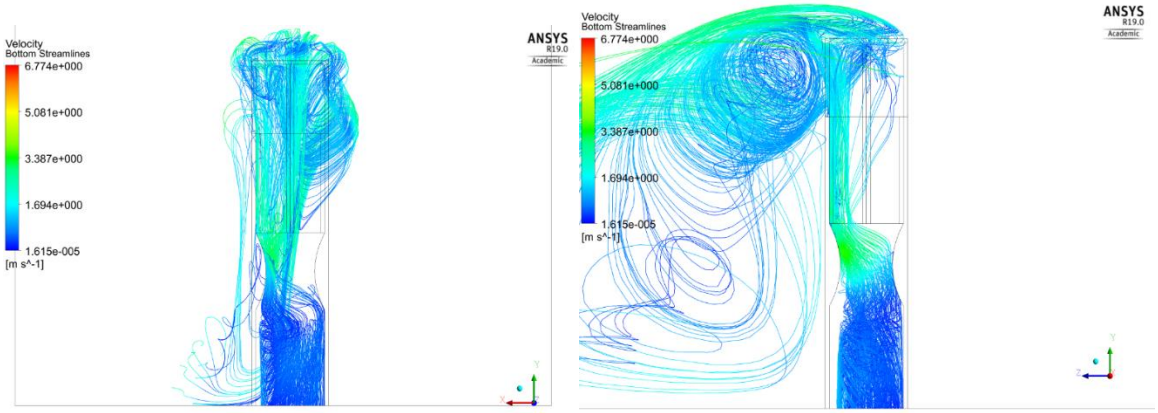

FIGURE 22 – Front (left) and Side (right) views of streamlines originating from pressure outlet at base of tower and exiting the leeward side of tower

side, showing the path of reversed flow from the bottom "outlet". This is important to describe because it informs the choice of turbine, most importantly whether to opt for a lift-based or drag-based turbine.

Figure 23 shows the vertical velocity (v-component) distribution for the tower at the nozzle throat. It suggests that the location of the turbine (in this case, a VAWT) should be centered in the nozzle throat, rotating about an axis in the x-direction so that the two flows in opposite directions will both be able to provide torque about the center. Because the region between these two flows appears to be a region with very little velocity resource, the productivity of lift would be limited. Therefore, the turbine should be designed using drag-based turbine blades. The negative velocity (blue) in Figure 19 shows the flow down the tower, while the red shows the flow moving up the tower.

One of the major problems revealed by this simulation was how little mass would actually be captured by this tower design. The four-sided tower only captured 19% of the incoming flow, and power potential was dramatically reduced compared to the estimation developed from the full capture assumption. Adjustments to the basic tower structure were

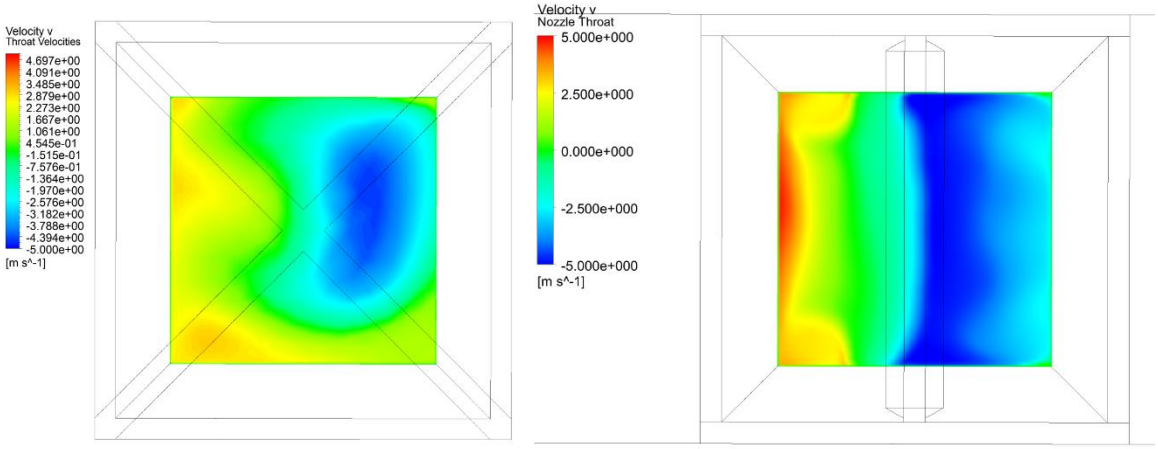

FIGURE 23 - Nozzle throat before (left) and after (right) changing from four-sided to two-sided tower. In this figure, the windward side is on the right.

unavoidable, because energy in the flow at the throat was 24W, which was too little to support power generation.

This does highlight a critical limitation of the initial investigation. The incorrect assumption of full capture, which was also used during the original design of the tower, led to an extremely wrong conclusion regarding the function of the tower. Assuming full capture of the flow should never be applied to future investigations; instead, start with the tower in an enclosure. No time is saved because the second simulation is always necessary, and no novel insights were generated by considering the towers in that way that could not have been developed using the more rigorous tower-in-enclosure technique.

Tower Adjustments

With the analysis of towers complete, it was clear that the optimized tower was not performing as well as [6] had described when properly analyzed in an enclosure. A complete redesign of the tower was time prohibitive, but some adjustments were necessary to ensure an appreciable amount of energy was present in the system so that a turbine could be analyzed. Several changes were made to improve the ability of the wind tower to capture wind. First, because the flow capture depends strongly on the number of inlets, the tower was changed from the four-sided to the two-sided square. This dependence does appear to be strongly connected to the fact that the tower area is being subdivided several times; these subdivisions are a typical way to divide such a tower, so in order to analyze the tower in the context of retrofitting existing towers this is the way the tower must be divided. Based on data in Figure 2 [9], this should increase the flow in the inlet compared to the four-sided option. Several small adjustments were made to the tower, since a complete redesign was time prohibitive. An overhang was added to the top of the tower,

similar to the wing-walls which were used to improve productivity with low speed wind [11]. While changing the "footprint" of the tower was not an acceptable design change, adding a small attachment to the top of the tower would not likely interfere with any surrounding architecture, if there were any. The inlet curvature was also modified from a quarter circle tangent to both the back wall and the top of the inlet to a circle which was tangent to the back wall and coincident with the tower inlet. This allowed the circle to extend all the way down the length of the inlet. Lastly, short circuit protection was added to reduce the amount of flow short-circuiting past the partition. The partition was also extended into the nozzle. The length of this extension was based on the maximum possible size of a turbine centered in the nozzle. This also had the unplanned benefit of creating a miniature nozzle before the main nozzle which increased the flow velocity, allowing momentum to carry it downward in a small jet. With these adjustments, the mass flow captured was increased to an amount that literature suggests should be reasonable for a 2-sided wind tower. Literature [9] suggested that as much as 35-45% of the mass flow should be captured by a 2-sided tower, while 34.8% was being captured here. To see the impact of tower adjustments visually, review Figures 24-25.

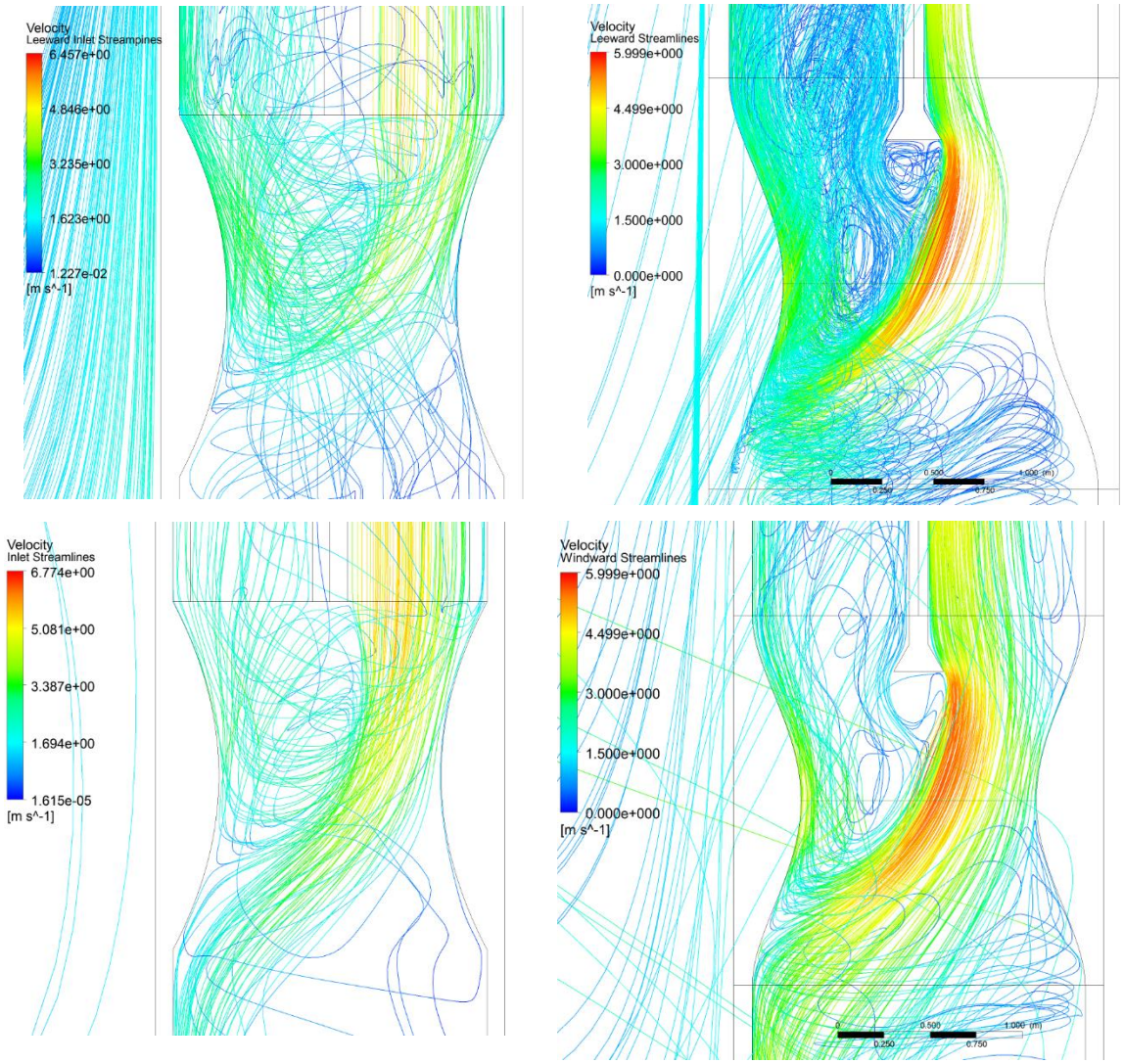

FIGURE 24 - Streamlines traced backward from the leeward inlet show a significant amount of short-circuiting before changing (top left), while after changing (top right) short circuiting only happened for part of the windward side. After adjustments, there was also a dramatic reduction to the number of streamlines from outside the tower finding their way into the leeward inlet.

Compare leeward streamlines backward (top) to corresponding windward streamlines forward (bottom) to see short-circuiting and the difference that short circuit protection made.

For all figures, 250 streamlines were traced from an inlet. The right side (after adjustments) has more streamlines in the nozzle because there was more flow through the tower and less spillage at the windward inlet. (See Figure 30 for capture comparison)

Tower with Enclosure: Conclusions

With these adjustments, the mass flow rate was increased from 3.78 kg/s (24% of the freestream) to 5.53 kg/s (34.8% of the freestream). The power in the nozzle area was increased from 24 W (19% of freestream) to 49 W (34.8% of freestream). As can be seen in Figure 30, the inlet profile was changed from a horseshoe shape to a distinct vertical triangle shape. There is substantial room for improvement to the design of the tower, but redesigning the tower from the ground up would be a complete project unto itself. Initial assessments of tower performance should not be done without the use of an enclosure, because the data generated are not representative of reality. Inlet performance is critical, but cannot be assessed applying the assumption of 100% flow capture. The area of the channel immediately behind the inlet appears to have a strong influence on the amount of mass flow being captured.

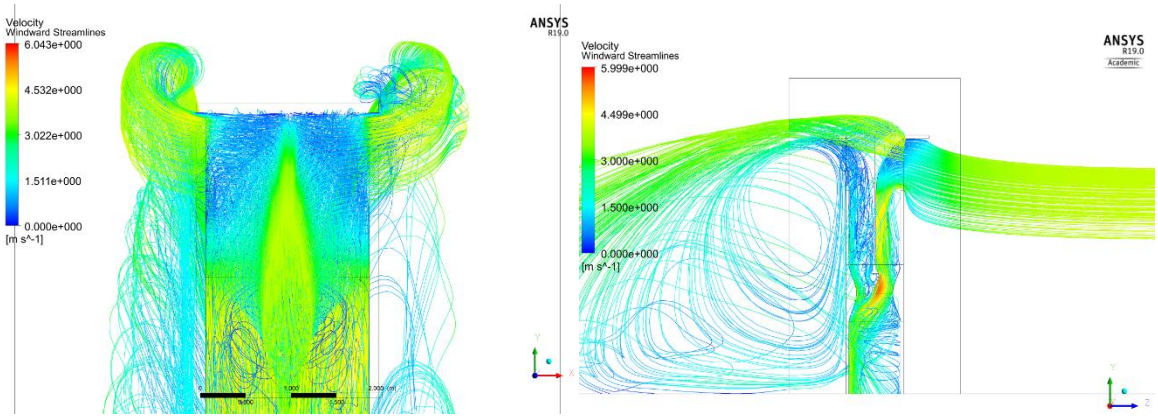

FIGURE 25 - Inlet Streamlines front view (left) and side view (right) following tower revisions and showing more flow through the tower.

CHAPTER 4: ANALYSIS OF THE CHARACTERISTICS OF VAWT TURBINES

Turbine Analysis: Introduction

The design and development of a VAWT for use in a wind tower required multiple design decisions to be made, including choice of airfoil, attachment angle of the airfoil to the turbine, operational angular velocity, and chord length (among others). The data indicated that a VAWT would likely outperform a HAWT under the flow conditions found within the towers, but there was not enough data to choose between a lift-based or drag-based VAWT design. Further, factors such as chord length, angle of attachment between the turbine blade and the turbine, and operational rotation speed were critical decisions that needed to be made in an informed way. An optimization investigation was conducted to determine what the ideal configuration would be under a given set of circumstances. The goal was to develop a method for rapidly comparing different configurations so that the best could be identified more quickly.

While there are many various methods of optimization available, the simplest of all methods is "brute force optimization" where the end result for every possible outcome is considered. With brute force optimization, all of the possible configurations are calculated and compared to each other. This method sometimes suffers because as the size and complexity of the problem increases, the number of configurations increases exponentially. However, because of the relatively small number of variables and well-defined formula for the impact of each criteria on power production, this approach seemed viable. Using lift and drag coefficients from published data, an extremely large number of designs could hypothetically be considered in a short period of time.

Developing a script for that purpose would also require developing a thorough understanding of the underlying equations, which was an additional goal of the research.

Turbine Analysis: Methodology

In order to optimize the turbine, a MATLAB code was developed to quickly determine the ideal attachment angle and angular velocity of operation for a given turbine blade for a VAWT, based on lift and drag coefficients. The prototype program considered a uniform flow field, but could be updated for a provided flow field condition.

This was a "brute force" optimization which calculated lift and drag at each degree around the turbine, then compared the expected power production for the turbine. Because the equations are relatively simple and the problem domain is well defined, more advanced optimization techniques were not required. Part of the benefit of this method was that determining whether a lift or drag based turbine would provide more power would be obvious from the calculation results, and the decision between a lift or drag based turbine could be entirely data driven. If successful, it would be possible to quickly compare optimized configurations for many different turbine blades to quickly arrive at a conclusion.

To develop the code, it was necessary to develop the equations describing lift and drag on the turbine blades so that the resulting moment could be calculated. The velocity triangle for a HAWT is already well defined and understood, but the formula for VAWT are more complex and not readily available in literature, so it was necessary to develop them. This is because for a HAWT, the relative wind changes along the length of the blade but does not change as the turbine rotates. In contrast, relative wind does change for a VAWT as each turbine blade passes through each angle around the turbine.

The ultimate objective was to calculate the power produced by a turbine configuration in one rotation. To do this, the program needed to find the lift and drag at each degree around the wind turbine, calculate the moment at that point, then combine the results to get the total moment for one rotation of the turbine. Using this information, the power production was calculated for a given angle of attachment and angular velocity would be calculated. Different airfoils can be compared by loading the appropriate lift and drag coefficients for that airfoil. Once the productivity had been calculated for multiple angular velocities, it would be trivial to locate the largest power production configuration using a spreadsheet. In this way, it would be possible to determine the ideal angle of attachment for a given airfoil quickly, given the C_L and C_D values for the airfoil. Once completed, it would be possible to quickly run multiple different airfoils to calculate ideal projected power output for that airfoil and select the optimal configuration. The different optimized turbines with different blades could then be compared simply and easily, reducing the number of variables being considered at any given time.

The velocity triangle for a VAWT is significantly more complicated than for a HAWT. The premise that the total wind "seen" by an airfoil is a combination of the freestream velocity and the rotational velocity remains the same as in equation 6 (see Introduction), but because the orientation of the VAWT blade changes as the turbine rotates, the angle of attack is constantly changing, and thus the velocity triangle is different at every point during the rotation. See Figure 26 for a visual representation of the velocity triangles for a VAWT.

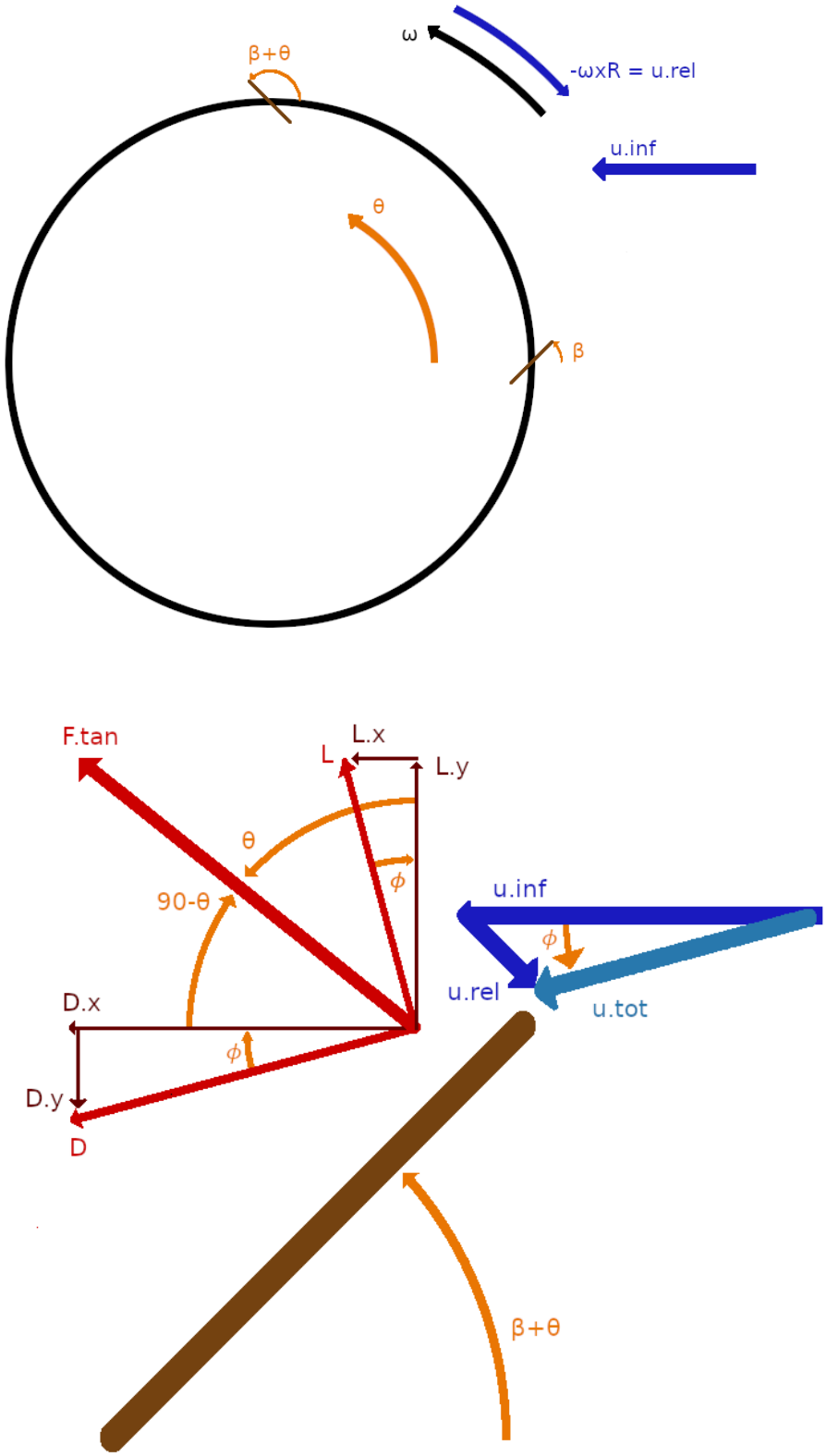

FIGURE 26 - Diagram of Rotating Section (top) and determination of velocity triangle and torque component F_{tan}. The period in the diagram denotes a subscript.

In order to look up the correct C_L and C_D value from published information, the angle of attack (α) is required. Consider the diagram in Figure 26. In this example, the velocity of the wind is constant, but the turbine is rotating. The chord's position around the rotor is θ, and the angle of attachment of the chord to the rotor is β, so that if θ=0 and β=0, then the airfoil's chord will be parallel to the freestream velocity (but not necessarily to the relative wind velocity, because of the motion of the turbine). The angle of the chord relative to the freestream wind then is

$$\theta + \beta = \psi \tag{14}$$

The direction of the relative wind is a combination of the freestream wind and induced wind from the motion of the turbine. Because a VAWT is able to accept wind from any direction, the coordinate system can always be oriented such that the incoming wind is parallel to one of the axes; therefore, the relative angle of the wind is entirely due to the rotation of the motion of the turbine. This angle is

$$\arctan\left(\frac{u_{rel}}{u_w}\right) = \varphi \tag{15}$$

and the angle of attack (α) for any point around the turbine is

$$\psi - \varphi = \theta + \beta - \arctan\left(\frac{u_{rel}}{u_w}\right) = \alpha \tag{16}$$

This equation allows for the calculation of angle of attack, and by extension lift and drag, at any point around the turbine. As described in equations 4 and 5, lift and drag can be calculated using the lift coefficient (C_L) and drag coefficient (C_D), where α is a reference value to determine the correct coefficient in a table. Since the direction of lift and drag are defined by the direction of the relative wind, the lift (L) and drag (D) need to be translated back to the primary coordinate frame for the program to take the summation

of moments. Recall that by definition drag is in the same direction as relative wind, while lift is by definition perpendicular to it. The lift in the primary coordinate frame is

$$L_x = L \sin \varphi \quad (17)$$

$$L_y = L \cos \varphi \quad (18)$$

while the drag translated to the primary coordinate frame is

$$D_x = D \cos \varphi \quad (19)$$

$$D_y = D \sin \varphi \quad (20)$$

To calculate the moment about the center of the turbine, and taking the origin to be located at the center of that turbine, one can find the part of the lift or drag in the x or y-direction tangent to the radius for the particular angle θ using

$$L_{xtan} = Lsin\varphi cos\theta \quad (21)$$

$$L_{ytan} = Lcos\varphi sin\theta \quad (22)$$

$$D_{xtan} = Dcos\varphi sin\theta \quad (23)$$

$$D_{ytan} = Dsin\varphi cos\theta \quad (24)$$

These equations yield the component of the lift and drag in the x-direction and y-direction tangent to the circle of rotation, which is the portion relevant to computing the moment on the turbine and the power generated by it. The moment and subsequent power per turbine blade can be calculated

$$M_{tot} = \frac{\sum_0^{359} L_{xtan} + L_{ytan} + D_{xtan} + D_{ytan}}{360} * (r - 0.25c) \quad (25)$$

$$P_{turb} = M_{tot} * \omega \quad (26)$$

where M_{tot} is the moment about the turbine, and P_{turb} is the power produced by the turbine. The sum of the average of the forces for a one rotation of the turbine is multiplied by the distance from the center of rotation to the quarter-chord of the airfoil. Whenever uncertain of the center of pressure for a lifting airfoil in low speed, subsonic flow, it can be estimated using the quarter-chord [20]. Using a pair of for loops, these equations can be summed at each degree over the turbine for all 360 degrees to determine how much torque a particular airfoil would produce per rotation, then the process can be repeated for multiple angular velocities and angles of attachment to generate a spreadsheet of power production values.

There are some limitations to the effectiveness of the process. This code neglects the effect of wakes (when one turbine blade passes behind another), so an accurate design prediction requires that wakes not extend from the front turbine blades to the rear turbine blades. The program also requires the coefficient of lift and drag to be known *a priori*, and thus is not able to analyze novel airfoil geometries without that information. The version of the code which was completed considers a uniform flow field, but could be modified to read velocity from a table for non-uniform flow conditions.

In operation, the code calculated 18281 configurations for attachment angle β and angular velocity ω in roughly 30 seconds, then charted the data in a spreadsheet. Using Excel, the optimal blade configuration can be located quickly using the MAX function. As long as the airfoil lift and drag coefficients are available and the design would not suffer from wakes, the program should quickly and accurately locate the optimal operating configuration for any given airfoil.

The chord length, the operational radius, and the free stream velocity were variables within the program and would be constant for each run of the program. Each could be investigated by changing the value manually for each run. The operational radius was confined by the size of the tower and the chord length would be limited by wake considerations, so no for loop was considered for those variables. The freestream velocity was estimated using the previous investigation.

To test the program, data for the NACA 0012 was located in a Sandia report [26] and entered into a spreadsheet (saved as a CSV text file; see Appendix II for data). The report provided data for every degree from 0 to 27 degrees, then for every five degrees from 30 to 180 degrees. For missing data points, the coefficients were linearly interpolated from the adjacent points in the report.

Turbine Analysis: Results and Conclusions

When the MATLAB code was run, the output suggested that an attachment angle β of -7 degrees and angular velocity ω of 0.5 radians per second would be ideal for operating a NACA0012 in a 20 m/s flow. This result was extremely counter intuitive, because at that angle of attachment the airfoil would be producing downforce on the front of the turbine where lift would normally be expected to be most productive, and lift on the rear of the turbine

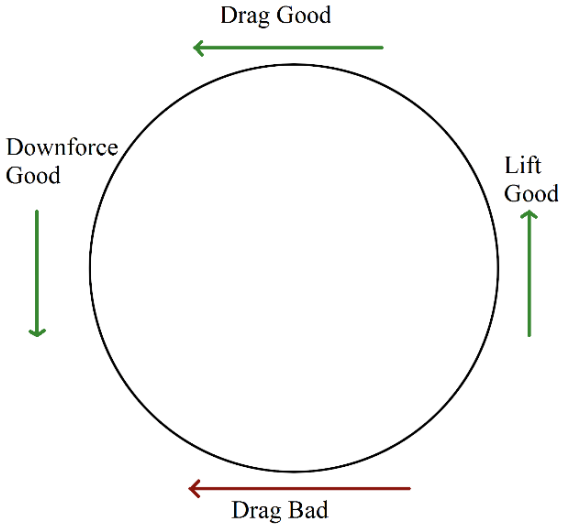

FIGURE 27- Diagram of helpful and harmful forces acting on a VAWT and where they can be found; wind from the right and rotating counter clockwise.

where downforce would be productive (see Figure 27 for diagram of VAWT productivity in a uniform flow field). After several attempts at debugging the code did not locate an error in logic nor a misplaced negative, other problems were considered. One of the limitations of the data available was the resolution on data between 150 and 180 degrees. The lift and drag coefficients varied greatly over the range of 0 to 27 degrees, and it would be reasonable to expect similar behavior when the airfoil was rotated to 180 degrees. In this region, the experiment only considered values every five degrees, not every degree as it did from 0 to 27. It must be noted that the lift and drag coefficients from 0 to 27 degrees cannot simply be reflected and used for the missing values because the airfoil is not symmetric along that dimension; the tail of the NACA 0012 is a sharp point, while the leading edge is curved.

It was decided to analyze the problem using CFD. This would provide a point of comparison for the MATLAB code to validate (or invalidate) the program result.

CHAPTER 5: CHOOSING A CFD TURBULENCE MODEL

Choosing a CFD Turbulence Model: Introduction

One of the concerns using CFD (Computational Fluid Dynamics) to model a turbulent flow is that it does not always accurately model flows which are separated, which can lead to inaccuracies when trying to predict aerodynamic forces acting on those surfaces. Choosing the correct turbulence model is important for making sure the data produced reflects reality. Computational fluid dynamics has advanced significantly in recent years such that some models are able to accurately predict aerodynamic forces, even for separated flows. To confirm that a CFD simulation would be able to verify or debunk the results from the MATLAB Optimization code, an investigation was conducted to determine an acceptably accurate turbulence model for the simulation to ensure that the CFD would produce a correct answer itself.

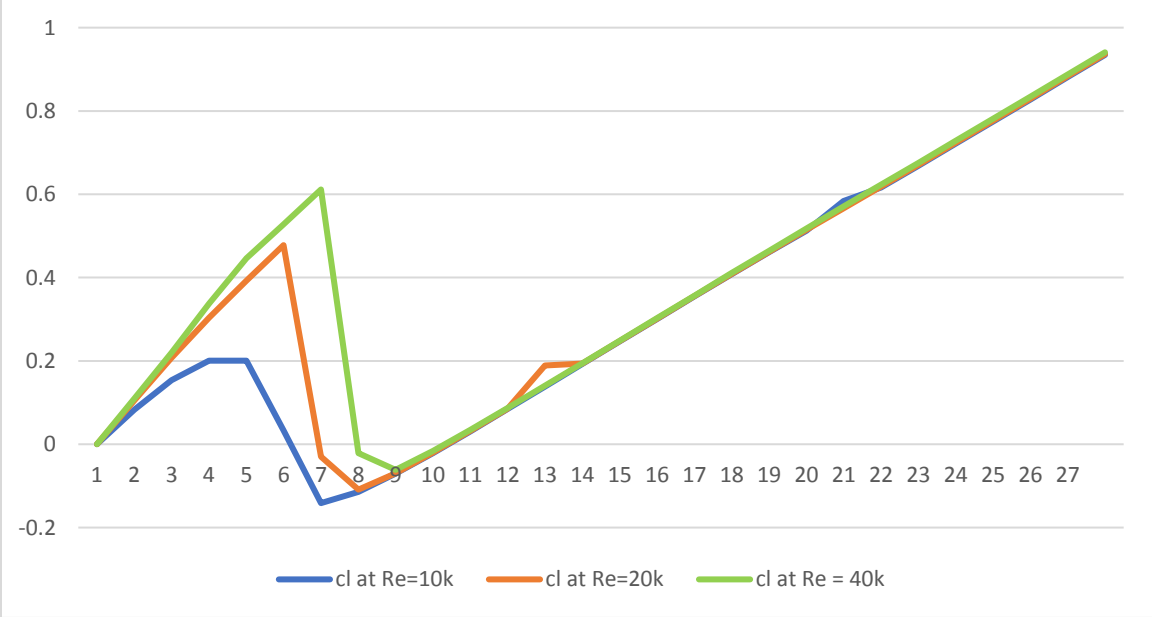

FIGURE 28 - Plot of Lift Coefficients for NACA 0012 from 0 to 27 degrees, generated using data from Sandia report SAND80-2114 [23]

Airfoils at large angles of attack (α) experience flow separation (see Figure 6). Flow separation can be delayed by higher Reynolds numbers, but for a VAWT it is inevitable that eventually the flow will become separated because the airfoil passes through all 360 possible degrees as it rotates about the vertical axis. Furthermore, because of the smaller size of turbines required for operation in cities and relatively low wind speeds compared to commercial projects, the Reynolds number for built environment turbines is likely to separate very quickly. Once an airfoil reaches the stalling angle of attack, the flow becomes separated, marked by a sharp decrease in lift and an increase in drag [20]; the effect is visible on both the C_L and C_D curves. As seen in Figure 7, the sharp drop off near 7^o indicates that the flow has separated from the airfoil. Exactly when and where the flow separates depends in part on the Reynolds number of the flow; see Figure 16. For the NACA 0012, the flow separates at 5, 6, or 7 degrees depending on the Reynolds number of 10,000; 20,000; or 40,000, respectively. At 45 degrees, the flow will definitely have separated for any of the low speed flows which would be of interest to this design process.

This is important to this research because for the vast majority of the time, the flow over the airfoils of the turbine is likely to be separated. Put another way, the wind over the airfoil is likely only attached between $\pm 7^o$ and possibly some values around 180^o but separated everywhere else. In other words, the flow is likely to be attached for less than 30^o out of 360^o. Because separated flow is so prevalent due to the VAWT design, it is important that the model represent the effect accurately enough to correctly estimate the forces acting on the turbine blades. A second goal is to predict the size of the wake behind the blades, so that whether "wind shade" affects the rear turbine blades or not can

be known. If at least the lift and drag coefficients cannot be obtained accurately when the flow is separated, then CFD modeling would not be useful for this research. If a competent model were found, it would be possible to proceed to the next step.

At the time of this part of the research, the goal was to find a method that would work effectively. Because of the need to run many simulations in a short time to generate large amounts of data, a significant amount of which is likely to become obsolete as understanding of the system grows, it would be preferable to use RANS simulations if at all possible, because the more rapid simulation run times allow for the consideration of a larger number of design possibilities in a shorter amount of time. This does come at a trade off of accuracy, and the inaccuracy of the technique must be considered.

However, simulating separated flows with high accuracy would likely require either a detached eddy simulation (DES) or a large eddy simulation (LES) to more accurately understand the flow behavior. Future work should strongly consider those simulation techniques for their improved accuracy, once there is a need to develop more precise information about the optimized configuration. Applying these techniques now would be expensive in terms of time, and the improved precision is not likely to be of a benefit to the early decision-making process where relative performance is far more important than accurate prediction.

Choosing a CFD Turbulence Model: Methodology

To determine which models are accurate, an airfoil was modeled at 45^{o} angle of attack in a freestream. This angle was chosen because the flow would certainly be separated, and also because the lift coefficient and drag coefficient should both be large. Trying to compare small numbers in numerical simulations can potentially cause errors,

and this is to avoid those problems. The result of the simulation would then be compared to the published values found in SAND80-2114 [26] for C_L and C_D to determine which models are accurate and which are insufficiently accurate for separated flows.

The chord length was 0.20 m, and the airfoil was 0.5 m wide; the simulation was run in 3D. A side view is available in Figure 30. Because the simulation was run using a student license, the mesh size was limited to less than 500,000 elements; the mesh had 443,334 elements with no special refinements (unstructured tetrahedral mesh). The inflation layer was the default 5 layers with a 1.2 growth factor. The density was 1.225 kg/m^3, per STP. The viscosity used was the default for Fluent simulations, 1.7894×10^{-5} kg/ms. The inlet velocity was set to 0.907 m/s for the k-ε simulation and 2.938 for the k-ω simulation; this corresponded to Reynolds numbers of roughly 10,000 and 40,000. The airfoil was solved using the k-ε model (2-equation) and the SST Transition (4-equation) models. This topic was eventually revisited and additional simulations were run using the SST Transition model to determine its accuracy. The results are tabulated in table 5. The "default settings" used in all SST Transition simulations are shown in a screen capture in Figure 29.

Choosing a CFD Turbulence Model: Results

The result was that the k-ε model was unable to correctly predict lift and drag for an airfoil at extreme angles of attack by a very large margin, but the SST k-ω model provided lift and drag predictions that were within 1% of the published values on the first investigation. Because of this, the SST Transition model was used for all further simulations to reasonably accurate predictions of lift and drag. Subsequent investigations with greater detail suggested that the lift and/or drag coefficient may be off by as much as

It should be noted that the first mesh was extremely loose. Later analysis with smaller airfoils suggested error may be as large as 20.36%, depending slightly on the scale of the model. For case 1, the airfoil chord length was 0.06 m and u_w was 4 m/s; for case 2, the airfoil was 1 m and u_w was 4 m/s. The difference from experimental values can largely be attributed to differences in the transition length in the SST model. The "accuracy" of the original simulation may have been a fluke of the restricted mesh and geometry. With correct tuning, a simulation should be able to accurately represent the lift and drag produced by the airfoil accurately. It appears that the forces are more likely to be underestimated than over-estimated, since all of the large errors are underestimations.

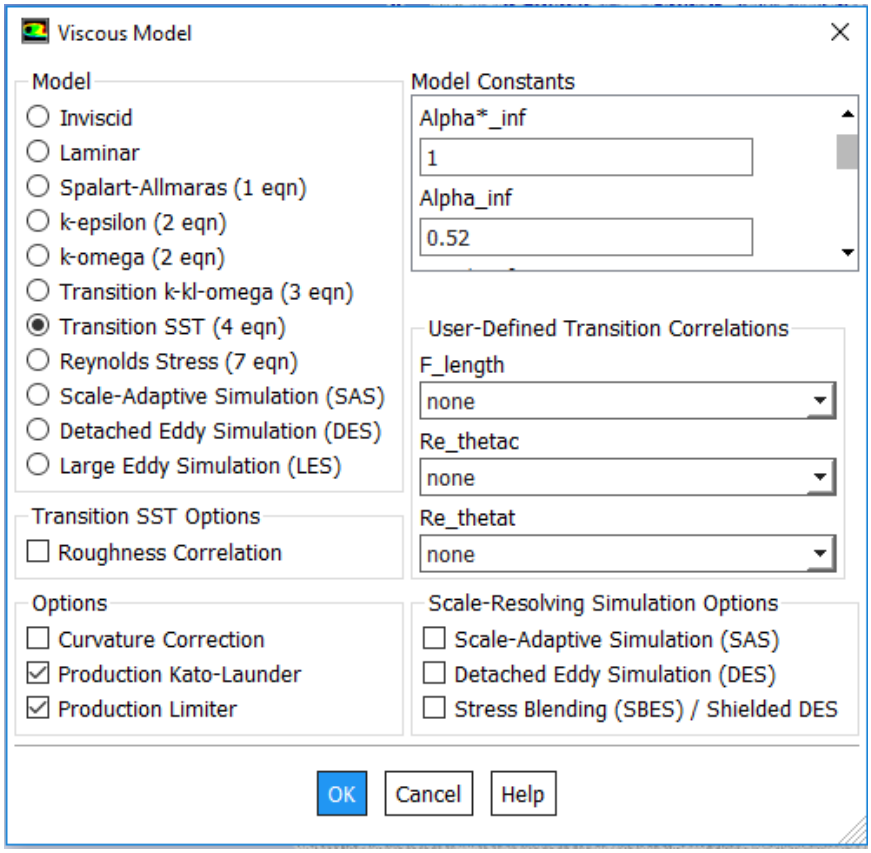

FIGURE 29 - Default settings for Transition SST (4 eqn) as listed in ANSYS Fluent 19.0

TABLE 4 - Table of Coefficients

Model	Lift Coefficient	Drag Coefficient
Sandia Report	1.085	1.075
k-epsilon	0.103	-0.103565004
SST Transition	1.095493982	1.051964181

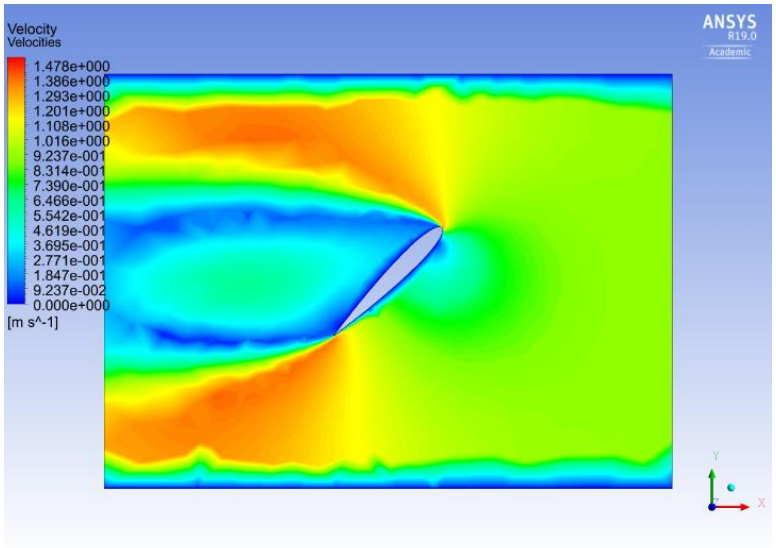

FIGURE 30 - Side view of NACA 0012 at 45 degrees to freestream

TABLE 5 - Later case examinations of airfoils at 45 degrees angle of attack under various chord lengths and Reynolds numbers.

	Lift Coeff	Drag Coeff	Error Fraction Lift	Error Fraction Drag
Published	1.085	1.075	0	0
1st	0.892397	0.857806	-0.17751	-0.20204
2nd	0.890171	0.856118	-0.17957	-0.20361

CHAPTER 6: SLIDING MESH SIMULATIONS

Sliding Mesh Simulation: Introduction

With confirmation that a CFD solution could accurately model the turbine, even when flow over the turbine blades became separated, simulation work began to determine whether the MATLAB code had a programming error, whether intuition was incorrect, or whether something else was the problem.

A sliding mesh simulation was explored because sliding mesh simulations are able to model wake effects, unlike moving reference frame (MRF) simulations. MRF simulations also "smear out" and average the forces acting on the rotor. Because it is desirable to understand the forces acting on the turbine blades at every point around the rotation, MRF is inadequate for meeting both the immediate goal of validating the script and long-term design goals.

A 6-degree of freedom (6 DOF) simulation would allow the system to rotate freely, but would not match the MATLAB code's operational assumptions (constant angular velocity), and would not allow for the simulation of power extraction from the system. With a 6 DOF system, the turbine would rotate freely until the aerodynamic forces acting on the turbine were balanced, with the torque provided to the rotor exactly balanced by the drag acting on the blades outside operational regions. However, a 6 DOF could not capture the retarding effect of power extraction. In effect, the 6 DOF model would be great for locating the operational condition where the power curve intersects the axis, or for modeling start-up behavior, but would be unable to model the operational condition of interest here. In real operation, the generator will be providing a retarding torque on the rotor shaft in addition to the aerodynamic drag. The sliding mesh model

captures this effect by prescribing a fixed angular velocity. For these reasons, the sliding mesh simulation was the preferred method for modeling the turbine.

Sliding Mesh Model

With this method, the turbine and some of the surrounding air are contained within a rotating volume. That volume rotates at a fixed angular velocity (ω) so that aerodynamic forces acting on the turbine can be measured and recorded. The primary reason this method will be used to analyze the turbine in this research is because a central interest is how far the wake extends behind the turbine blades and whether that is disruptive to the tower's normal operation for natural ventilation. One major advantage of this method is that it is able to model any operating condition, even operating conditions that might be unrealistic, such as a rotor rotating faster than aerodynamic forces and physical limitations would be able to turn it. In this way, one can investigate multiple points along the power curve simply by changing the angular velocity of the turbine section. This saves some set up time on for each simulation, which is a small operational benefit.

Sliding Mesh Simulation: Methodology

A six-blade turbine using NACA 0012 airfoils was modeled using SolidWorks and ANSYS Fluent to determine what the moment acting on the turbine blades would be. This work was done in 2-dimensions because the computer doing the processing only had access to a limited academic license and would not be able to run a simulation with a larger number of cells. Working in 2 dimensions at this point was an acceptable compromise to reduce the number of cells being considered.

The turbine would be designed to match the conditions that had been entered into the MATLAB program and the optimal operational conditions as recommended by the script so that the results could be compared directly. The NACA0012 airfoil was obtained from an online source [31]. The airfoils were modeled in SolidWorks with an angle of attachment β of -7 degrees, as recommended by the MATLAB program results. The airfoil as given in [31] was rotated -7 degrees using the Airfoil Rotator script in Appendix III. The mesh for this simulation used a minimum face size of 0.0005 m and max face size of 0.01 m. The domain was a 2m by 2m square with 44k elements. The inflation layer was the default 4 layers smooth transition with growth rate of 1.2.

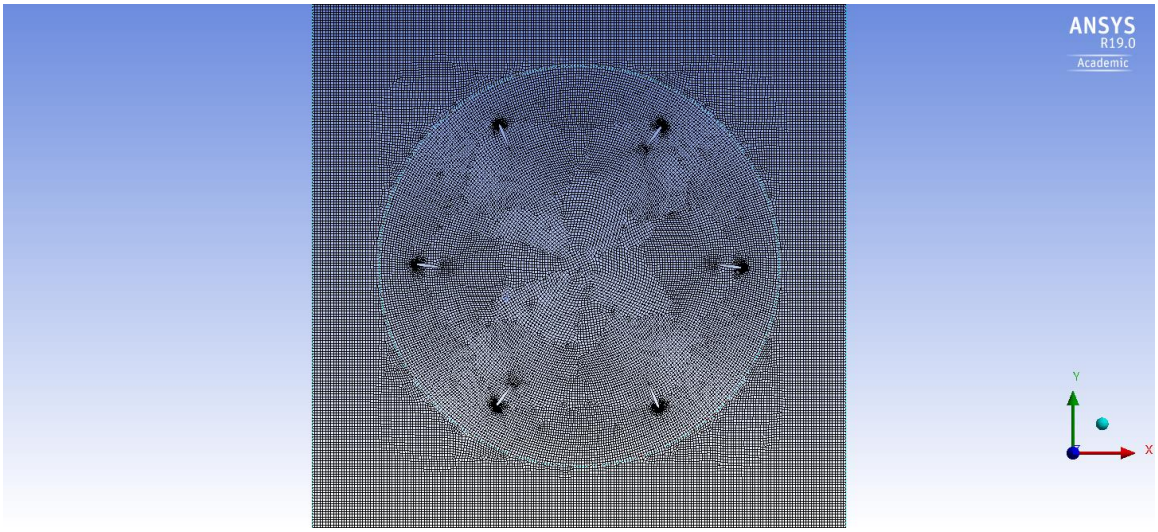

FIGURE 31 - 2D Mesh Domain for 6-blade Turbine

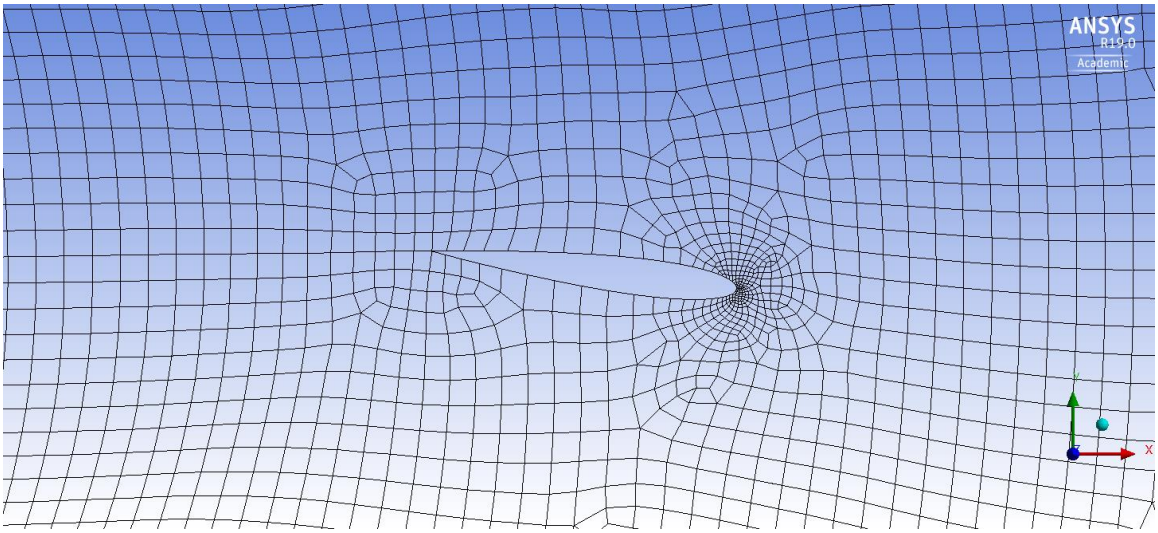

FIGURE 32 - Close up of mesh on a single airfoil

The turbulence model was SST Transition, with the circular portion of the mesh rotating counterclockwise at 0.5 rad/s. The velocity inlet on the right side was set to 20 m/s because this was close to some of the simulation values from the wind tower investigation (see Chapter 2), and the analysis with the enclosure was not yet complete. The timestep size was 0.01 s. The element report in Fluent indicates face element sizes varied from .00038 m^2 to .018 m^2. The simulation was run for 1257 timesteps.

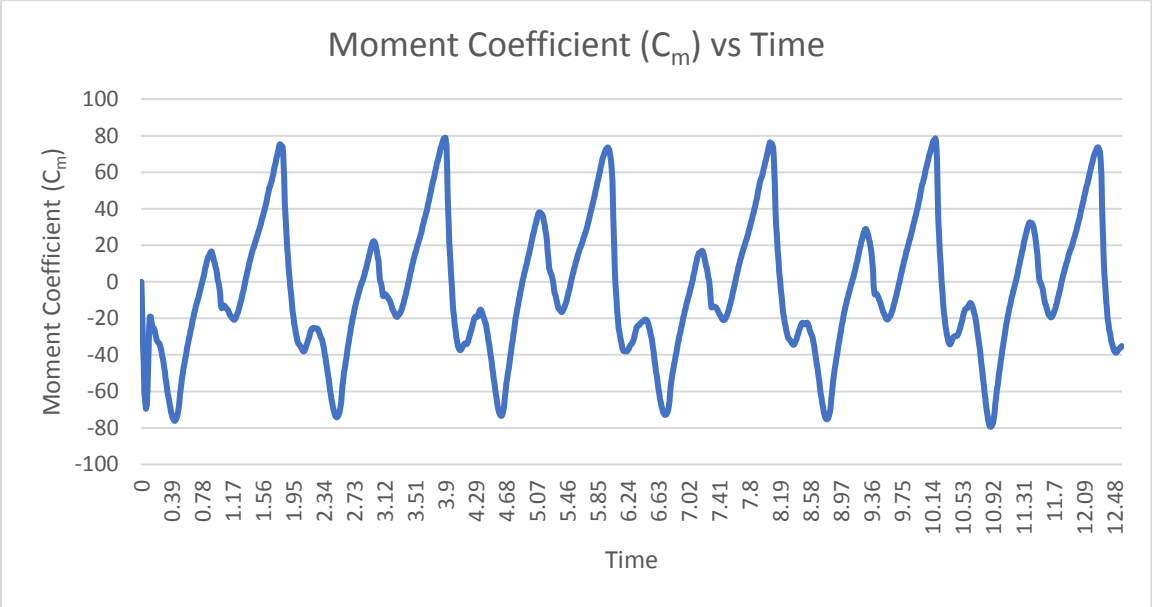

FIGURE 35 - Moment Coefficient vs. Timestep for combined six blades of turbine

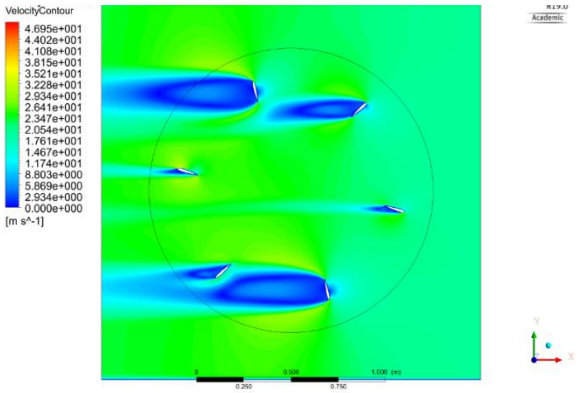

FIGURE 34 - t=2.05 Influence of wakes causing a moment drop sharply as leeward blades enter wake of windward blades. [32]

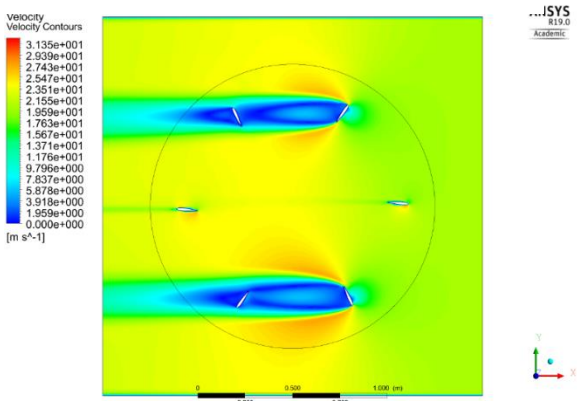

FIGURE 33 - t=1.74 Velocity Contours at Time of Maximum Positive Moment [32]

As seen in Figures 33-35, the wakes from the turbine blades were extremely large, and extended further behind the turbine blades than anticipated. The blades had been placed six chord lengths apart based on an estimation about wake distance and recovery behind buildings [33], which suggested that in some cases the wake behind a building would recover after 6 to 8 side lengths behind a cube (a “side length” is the length of one

cube's side). At 6 characteristic lengths, this was not the case for the airfoils; the wakes extended well behind these airfoils. As is clearly visible, the low velocity wake behind the windward blades is obscuring the leeward blades with wind shade at several points during the rotation, causing dramatic fluctuations in torque as the turbine blades enter and leave wind-shade. These simulations highlighted the importance of wake modeling to the design of the turbine.

The very large and rapid changes to moment coefficient suggest that vibration would be severe using this particular design. Future designs should seek to reduce vibration by eliminating wind shade effects. If wind shade is allowed to persist, it should be consistent on the rear blades to reduce the dramatic changes to torque on the turbine. Note that the moment coefficient (C_m) is quite large. This is because the moment coefficient is defined

$$C_m \equiv \frac{M}{\frac{1}{2}\rho u^2 Ac} \qquad 27$$

where the moment (M) is divided by the dynamic pressure ($1/2\ \rho\ u^2$), the area of the airfoil (A), and the characteristic length (c). In this case, the chord length is the characteristic length. When the radius is larger than the chord, the moment coefficient can be much larger than 1.

Taking the average moment coefficient for the turbine from timestep 47 to timestep 255 yields a moment coefficient of -0.08, suggesting that the MATLAB optimization program may not be working correctly, although it does not suggest why. This corresponds to power consumption of 0.48 W, suggesting this particular configuration would not produce power at all but would require power to function under these conditions.

Sliding Mesh Simulation: Conclusions

This simulation identified several problems which wind shade could cause a turbine, and confirmed that sliding mesh is an appropriate way to analyze a turbine when obtaining power production at a specific operating condition is the goal. In particular, the ability to model and investigate when a wake might be a problem is extremely valuable. The problems of wind shade were identified as reduced power output and increased vibration from sudden changes in torque. A distance of six chord lengths was found to be inadequate to prevent wind shade from extending from the front blade to the rear blades.

The optimization result of -7 degrees was determined not to produce power. This is consistent with the mathematical analysis, which suggests the problem is not with the concepts developed. The result seems to come from limitations in the C_L and C_D data available. For values from 150 to 180, the C_L and C_D were only published for every 5^{th} degree (instead of every degree). The low-resolution data appears to inflate the benefit of downforce on the rear half of the turbine in an unrealistic way because the magnitude of the lift coefficient appears to be larger than would be guessed, based on typical airfoil behavior at low angles of attack and the data from 0-10 degrees.

A rotation of 0.5 rad/s with a windspeed of 20 m/s corresponds to a change of 0.888 degrees to the effective angle of attack when the velocity triangle is analyzed. That would change the angle of attack for the maximum lift-to-drag ratio for the airfoil from the tabulated data by almost a degree, but that is not a substantial change.

One of the confounding problems of this simulation is the pronounced impact that wind shade has on the design. The dramatic shifts from large to small values indicate that under these conditions there would be large changes

The most likely explanation for why the MATLAB program was unable to draw a correct conclusion was the low-resolution data approaching 180 degrees. The first twenty-seven degrees are measured per every degree, but from 30 to 180 degrees only every fifth degree was measured. The airfoil is "symmetric" meaning that it is reflected across the top and bottom, but it is not symmetric from the leading edge (which is rounded) to the trailing edge (which is pointed). Overlaying the two sets of data makes it clear how low the resolution was, and how that failure to capture the separation point makes it difficult to apply the data. Because there appears to be very little airfoil lift and drag coefficient data to use to explore other designs with, further development of the MATLAB code ceased, but the equations used in its development, particularly the velocity triangles, remained valuable to exploring the wind turbine. If airfoil data becomes available in the future, the script may become useful as a first-pass estimation for power output and turbine performance.

All future simulations would be run using an ANSYS CFD program, and the MATLAB program was neither confirmed nor denied by the simulations due to the extreme severity of the wakes confounding the estimation of power production. However, without information about airfoils at various angles of attack, it is not practical to continue trying to develop such a program.

CHAPTER 7: PUTTING THE TURBINE IN PLACE

Putting the Turbine in Place: Introduction

Knowing the conditions within the tower and how to analyze a turbine using sliding mesh, some decisions regarding the design of the turbine could be made. The radius of the turbine, the number of airfoils, the chord length of those airfoils, and the shape of the airfoil are all critical factors to the power produced by the turbine. Any turbine designed must be well suited to operating in the extremely low speed, high turbulence, asymmetric flow environment found within the wind tower, and it needs to do so without disrupting the natural ventilation function of the tower.

Putting the Turbine in Place: Methodology

The radius was selected based on the distribution of wind energy within the tower. While a larger radius does produce more power (since the lift and drag on the airfoil have a longer moment arm for generating torque), the power equation scales with velocity cubed, but only linearly with the radius. Recall Equation 3 from the Introduction. Because of the flow pattern visible in Figure 23, the turbine radius was set to 0.45 m (45 cm, or almost 17 ¾ inches).

There is also a question of how far around the blades the flow will travel, and avoiding wall effects from getting too near the wall is another good reason not to make the radius the absolute maximum. If the boundary layer from the wall and the turbine blade were to overlap, the flow in that area might change its behavior to behave more like flow within a pipe, which would restrict the amount of air passing through.

How Many Blades

The questions of how many blades there should be and how long the chord length should be are interrelated. Usually, turbine blades are space equally to provide balance, so that they are located at the vertices of a regular polygon. However, to reduce wind shade, it is important to consider wake behavior behind the windward blades. Therefore, the fewer blades there are, the farther apart they will be, but the longer each blade will be. This concept is commonly referred to as "solidity", and solidity is defined

$$S \equiv \frac{N * c}{r} \tag{28}$$

where S is the solidity, N is the number of blades, c is the chord length, and r is the radius of the turbine.

There were two potential wakes to consider. One was the wake behind the turbine blades coming from relative wind, and the other was the wake from the freestream which would be behind the turbine blade. For the freestream wake, it was already clear from the work in Chapter 6 that six blades resulted in large amounts of wind shade, so there should be fewer than six blades to avoid that problem. Also, knowing that the turbine would be placed in the throat, the amount of blockage in the throat should be minimal to avoid preventing the capture of wind. One of the problems ducted turbines face is that the turbine is itself a blockage in the wind tower that can hinder flow. This reduced the options to 1, 3, or 5 blades. Any 1-blade or 2-blade turbine carried some risk of stopping in the dead zone between flows, leaving it unable to self-start, so that option was eliminated. To consider the wake from relative wind, the distance between the blades would be most important, since the blades all follow the same path around the turbine as they rotate. A spreadsheet was developed to calculate what the distance would

need to be between turbine blades to limit the effect of each turbine blade on the following blades.

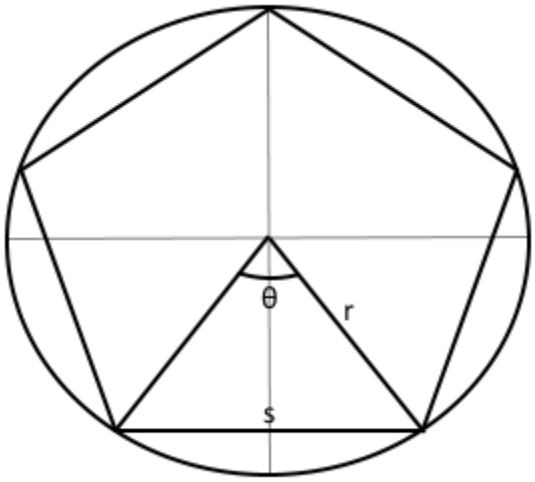

FIGURE 36 – A circumscribed pentagon

The distance between chords was calculated from a geometric analysis. The turbine blades should be spaced evenly to get regular, repeating power generation. For a regular polygon, the length of each side is equal to each other, and the length can be calculated geometrically. Consider a circle circumscribing the regular polygon (see Figure 36). The length from the center of the circle to the vertices is equal to the radius (r) of the circle. The central angle (θ) is equal to 360 degrees (or 2π in radians) divided by the number of sides (N). The length of the side (s) can then be calculated by applying the law of cosines, often written as

$$a^2 + b^2 - 2ab\cos\theta = c^2 \tag{29}$$

and substituting in the variables from Figure 28 obtains

$$r^2 + r^2 - 2r^2\cos\frac{360}{N} = s^2 \tag{30}$$

then combine terms and solve for *s* to get

$$\sqrt{2r^2\left(1 - \cos\frac{360}{N}\right)} = s \tag{31}$$

Equation 23 calculates the distance between regularly spaced turbine blades based on the radius of the circumscribing circle and the number of vertices (equal to the number of sides). The wake resource [24] suggested that the recovery time behind a cube is usually

be six to eight times longer than the length of the cube's side. This estimation was derived from buildings being modeled in urban wind-like conditions. The previous analysis with six blades suggested six chord lengths would not be enough distance to separate the effect of one blade from the next, so two estimations based on chord length were generated, one separated by seven chord lengths, and one separated by eight chord lengths. This data is collected in Table 6 for comparison.

TABLE 6 - Comparison of chord length if determined from a wake estimation of eight chord lengths and a wake estimation of seven chord lengths. Lengths in meters.

Number		Chord length by wake		Solidity		Area
of sides	Side Length	Chord if Eight	Chord if Seven	Solidity (8)	Solidity (7)	safe
2	0.9000	0.1125	0.1286	0.5000	0.5714	0.2025
3	0.7794	0.0974	0.1113	0.6495	0.7423	0.2631
4	0.6364	0.0795	0.0909	0.7071	0.8081	0.2864
5	0.5290	0.0661	0.0756	0.7347	0.8397	0.2976
6	0.4500	0.0563	0.0643	0.7500	0.8571	0.3038
7	0.3905	0.0488	0.0558	0.7593	0.8678	0.3075
8	0.3444	0.0431	0.0492	0.7654	0.8747	0.3100
9	0.3078	0.0385	0.0440	0.7695	0.8795	0.3117
10	0.2781	0.0348	0.0397	0.7725	0.8829	0.3129
11	0.2536	0.0317	0.0362	0.7748	0.8854	0.3138
12	0.2329	0.0291	0.0333	0.7765	0.8874	0.3145
13	0.2154	0.0269	0.0308	0.7778	0.8889	0.3150
14	0.2003	0.0250	0.0286	0.7788	0.8901	0.3154
15	0.1871	0.0234	0.0267	0.7797	0.8911	0.3158
16	0.1756	0.0219	0.0251	0.7804	0.8918	0.3160
17	0.1654	0.0207	0.0236	0.7809	0.8925	0.3163

Larger numbers of blades resulted in a larger surface area, which would give the turbine a larger active surface. It was certain that the design called for more than two blades to prevent the possibility that the turbine would find itself stopped vertically in the "dead zone" of very little velocity in the middle of the tower, unable to generate enough torque to start itself. Increasing the number of blades from six did not seem prudent,

since that would only generate more wind shade at the most critical areas for a drag-based turbine, and the problems from wakes behind the turbine blades was already extreme when investigated previously. Based on this information, there would either three or five turbine blades. Based on the chord length analysis, the five-blade turbine would have a 13% larger collective blade area than the three-blade turbine and a more even moment distribution over time, so the turbine was designed with five blades. A three-blade turbine might be viable, but would not be the first design examined and will be reserved to future work since it did not appear to be the superior option at this time.

What Airfoil Shape

The choice of airfoil shape was also a question to be answered. One of the major questions to answer was whether a turbine should be drag-based or lift-based. By considering the velocity field with the turbine moment potential, it becomes clear that the majority of the velocity is in the region favoring drag-based designs, while the lift-favoring portion of the turbine in the middle has barely any resource at all. There may be some lift from the lifting region of the C_L curve near 45^o, but trying to optimize for both conditions at this point was not feasible. This is the first compelling reason to favor a drag-based turbine and turbine blade.

The second argument to favor a drag-based design comes from the argument in Appendix I, discussing why turbulence changes the velocity triangle too much for the standard high lift-to-drag ratio designs to work well. Based on the turbulent velocity triangle argument, a drag-based approach is favored because it will be more robust in turbulence, since changes to the drag force due to changes in angle of attack will be minimized. If using a lift-based approach, this argument suggests that using the blade

near 45^{o} as opposed to the very good lift/drag ratio found at low angles of attack would be preferable because it is a more robust design.

NACA series airfoils are lift based instead of drag based, and would not be well adapted to this application. All of the airfoils in SAND80-2114 [26] were NACA symmetric lifting airfoils. Several papers were reviewed to explore drag-based turbines and turbine blades, primarily Savonius turbines.

The question was what turbine blade would generate the most thrust for a given flow. A similar question has already been answered for jet engines using a control volume analysis. From that control-volume analysis, it can be demonstrated that thrust can be generated in one of two ways: pressure difference or momentum change. Although derived for jet engine analysis [34], the same basic principle should apply to thrust from turbine blades. The thrust equation as it applies to turbine blades is

$$F = \dot{m}_{out}u_{out} - \dot{m}_{in}u_{in} + (p_{out} - p_{in})A_{control\ volume} \quad 32$$

Considering the shape of turbine blades is informative in light of this premise. Most drag based turbines are primarily pressure-based, meaning that they build up a large pressure difference on two faces to generate thrust. The other option is to generate thrust by changing the momentum of the air. Both designs can work, but the control volume analysis suggests that changing the momentum of the air will generate more thrust than building up pressure.

Also, when considering the small area the turbine blade has for building up pressure along its surface, a pressure-based design did not seem favorable.

Pressure based airfoils can be identified by their cup shape, which allows them to build up stagnation pressure over a large area. Momentum-based airfoils resemble a

heavily cambered airfoil, or less technically the slides that a child might enjoy on a playground. Most drag-based airfoils in literature are pressure based with some kind of cup design, so it was necessary to conceptualize a different blade to be in line with the design principles outlined above.

A turbine blade was located in literature which was defined by a polynomial [23]. One of the turbine blades investigated in that study was defined by a polynomial. That polynomial was

$$\frac{y}{D} = -3.4868\left(\frac{x}{D}\right)^4 + 8.16507\left(\frac{x}{D}\right)^3 - 7.5605\left(\frac{x}{D}\right)^2 + 2.8507\left(\frac{x}{D}\right) + 0.040493 \quad (33)$$

where x was the x-coordinate, y was the y-coordinate, and D was a normalizing term equal to the chord length (in the original paper, also equal to the diameter of the turbine). This turbine blade was modified by changing the first term of the polynomial from negative to positive, which changed the shape of the blade so that it conformed to what seemed desirable in a turbine blade. The blade shape was scaled by a factor of 0.0661 and translated to the appropriate location in the nozzle (3.5 m above the origin). A list of points for the turbine blade as it was modeled is listed in Appendix VI.

Thus, a turbine blade defined by an equation with chord length 0.0661 m (6.61 cm) extending to a maximum of 0.45 m from the turbine center was selected for examination. The turbine blade was defined by a formula but no thickness was prescribed in the source, so the blade was modeled as 0.002 m (2 mm) thick. The turbine would have five turbine blades because this was a good balance between concerns about wind shade, steady torque, and the surface size of the turbine's airfoils.

The question remained how much power the turbine design would produce. Once that value was known and understood, the central research questions could be answered.

Focused on Nozzle

For the investigation of the turbine in the nozzle, a subsection of the major steady state simulation was cut out of the bigger simulation so that the simulation could be run using only the nozzle. This was done primarily for the sake of time; the steady state simulations could take multiple days to converge with 17+ million mesh, and introducing a moving piece into the nozzle that would need to be solved for thousands timesteps would take prohibitively long to complete. Finding the power curve was projected to take 5-10 points for several angular velocities. Knowing that multiple operational conditions were also required to be investigated, this method was investigated as a way to possibly save time. Care must be taken when implementing the turbine that the turbine itself does not substantially change the nozzle throat in order to ensure the simulation remains valid. As is known from wind tunnel design, too much blockage will invalidate results. For wind tunnels, between 5% and 10% blockage is often considered acceptable, and the 0.0661 m chord length conforms to this standard in the nozzle which is 1.27 m wide (5.2% blockage), so the blockage is likely not enough to substantially change the flow upstream. If the turbine blade were larger, it might be necessary to run the full simulation, even at the expense of time.

The windward and leeward inlets to the nozzle were exported as a "profile" of velocities from the steady state simulation of the tower in Fluent, then imported to the "nozzle only" simulation. Even though the leeward surface was defined as an "inlet", the velocity profile caused it to behave as an outlet. The bottom of the nozzle was similarly exported, but as a pressure profile instead. These formed the boundaries of the nozzle simulation (see Figure 37).

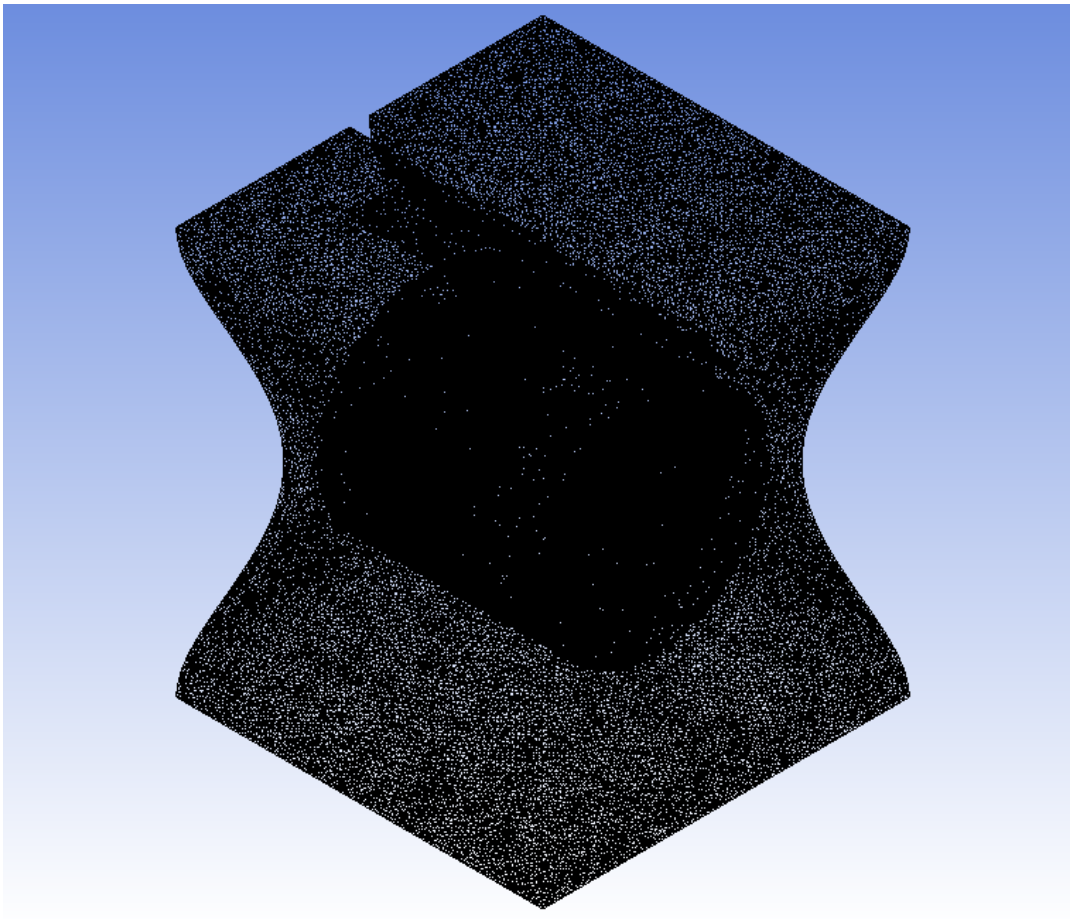

FIGURE 37 - Mesh of nozzle excerpt from tower with rotating section. The windward inlet is on the left and the leeward "inlet" is on the right. The pressure outlet is on the bottom.

The first simulation was initialized using "hybrid initialization" in Fluent. This required several days for the simulated wind to blow out of the system and delayed the collection of useful data. All subsequent simulations were initialized using the result from a steady-state, non-rotating turbine section with the same inlet and outlet profiles as the sliding mesh simulation. While later simulations still took time to settle into normal operation, this resulted in moderately useful data almost immediately for the later simulations and decreased time necessary to check the simulation was set up correctly.

The first simulation was run with a tip speed ratio (TSR) of 1.5, since that is a common starting point for turbine analysis and design. This corresponds to an angular velocity (ω) of 13.33 rad/s for a turbine with a 0.45 m radius. Operating at this condition resulted in another turbine simulation which would have consumed power as it ran instead of generating power, which would not be a practical wind turbine; but the simulation also generated much useful data. Using this simulation, one can clearly see that the wakes behind the quickly-moving turbines do not significantly overlap with the turbine behind them. The negative moment coefficients suggest the turbine is putting energy into the flow, which is consistent with the increase in velocity seen in Figure 38. The value of the power generated was negative, but the characteristic rising and falling pattern as a turbine blade enters or leaves the vertical flow is visible (See Figure 39 in Results section).

To better inform the subsequent simulations, a rough power curve was developed using a rough estimation of power production so that key points such as the power maximum, minimum, and zeroes could be estimated and targeted better in future simulations.

Deriving a Power Expression

Recall that the equation for power produced by torque is

$$P_{turb} = \tau\omega \tag{34}$$

where P_{turb} is power, τ is torque, and ω is angular velocity. Torque is defined as a force acting at some distance, thus

$$\tau \equiv FR_{\tau} \tag{35}$$

where F is the perpendicular force and R_τ is the distance that force is acting at. The magnitude of the force is resolved from lift (L) and drag (D)

$$F = \sqrt{L^2 + D^2} \tag{36}$$

And recall the definitions of lift and drag to get

$$F = \sqrt{(0.5C_L\rho u^2 A)^2 + (0.5C_D\rho u^2 A)^2} \tag{37}$$

$$F = 0.5\rho u^2 A\sqrt{{C_L}^2 + {C_D}^2} \tag{38}$$

Also recall that u (the local velocity) is a combination of velocity and the relative wind due to the rotation of the turbine, so

$$\vec{u} = \vec{u}_{wind} + \vec{u}_{relative} = \vec{u}_w + \vec{u}_{rel} \tag{39}$$

$$\vec{u}_{rel} = -\vec{\omega} \times \vec{R}_{local} \tag{40}$$

thus

$$\vec{u} = \vec{u}_w - \vec{\omega} \times \vec{R}_{local} \tag{41}$$

But the definition of the lift and drag coefficients uses a scalar u^2 to calculate the magnitude of the forces, so expanding the above equation

$$u^2 = \vec{u} \cdot \vec{u} \tag{42}$$

$$u^2 = {u_w}^2 - 2\omega R_{local} + \omega^2 {R_{local}}^2 \tag{43}$$

Substituting into the above equations

$$F = 0.5\left({u_w}^2 - 2\omega R_{local} + \omega^2 {R_{local}}^2\right)\rho A\sqrt{{C_L}^2 + {C_D}^2} \tag{44}$$

And substituting into the original power equation

$$P_{turb} = \omega R_{\tau}\left({u_w}^2 - 2u_w\omega R_{local} + \omega^2 {R_{local}}^2\right)\rho A\sqrt{{C_L}^2 + {C_D}^2} \quad (45)$$

Because the turbine blade is relatively small compared to the radius (between R_{local} values of 0.45 m and 0.38) the R_{local} value was approximated as a constant. This allowed the continued algebraic manipulation without requiring calculus. The force F was assumed to be perpendicular to simplify the analysis and because the magnitude of C_L and C_D could not be known to estimate the correct direction. When the NACA0012 blade was considered, the average lift and drag coefficient magnitude over the entire blade was approximately 1.1. The goal of this brief investigation was not to find the exact value, but to estimate where the investigation should begin looking for key points to generate a power curve, so approximation was acceptable. This expression allows for the consideration of power produced by a single point around rotation. It is documented for those who come behind, if ever one should need it.

Also noting that the center of pressure for a bluff body is usually near the center of that body, one can approximate $R_{\tau} \approx R_{local}$ so those terms can be combined into a single R. Multiplying through,

$$P = \left(\omega {u_w}^2 R - 2u_w\omega^2 R^2 + \omega^3 R^3\right)\rho A\sqrt{{C_L}^2 + {C_D}^2} \quad (46)$$

This expression describes the power provided by one blade at a specific point. However, the power produced will vary depending on whether the turbine blade is in a wind resource or not. Considering the sum of all five blades for a full rotation, about half the time (0.5) the blades were estimated to be active in the primary resource (at 5 m/s), for three tenths (0.3) of the time they were idle (drag only), and for one-fifth (0.2) of the time they were in the secondary resource (wind at 3 m/s).

The lift and drag coefficient curves for the airfoil of interest were not known, but the average value for the NACA 0012 was near one. The radius was 0.45m by design. Substituting in those values provides a power equation

$$P = 0.5\left(\omega {u_1}^2 R - 2u_1\omega^2 R^2 + \omega^3 R^3\right)\rho A\sqrt{{C_L}^2 + {C_D}^2}$$

$$+ 0.2\left(\omega {u_2}^2 R - 2u_2\omega^2 R^2 + \omega^3 R^3\right)\rho A\sqrt{{C_L}^2 + {C_D}^2} - 0.3\rho\omega^3 R^3 A C_D$$

Note the drag in dead zones must necessarily be negative because it opposes the motion of the turbine. Plotting this function (see Figure 38), the graph suggested there should be a zero (and an upper operational limit) somewhere near ω=5, so that was the next value investigated. There was also a local maximum near ω=2.5, which was the third point investigated. From there, the power curve was followed using results from previous simulations to look for minimums and maximums.

This equation would seem to suggest that, at moderately high values of rotation, the turbine would transition from consuming to producing power (again), but that seems like an absurdity, and the turbine would never naturally pass through to those values, so they were disregarded. Again, the goal was not to find an exact power curve, but to make an educated guess for where to run the next simulation so that it might be nearer to a useful value.

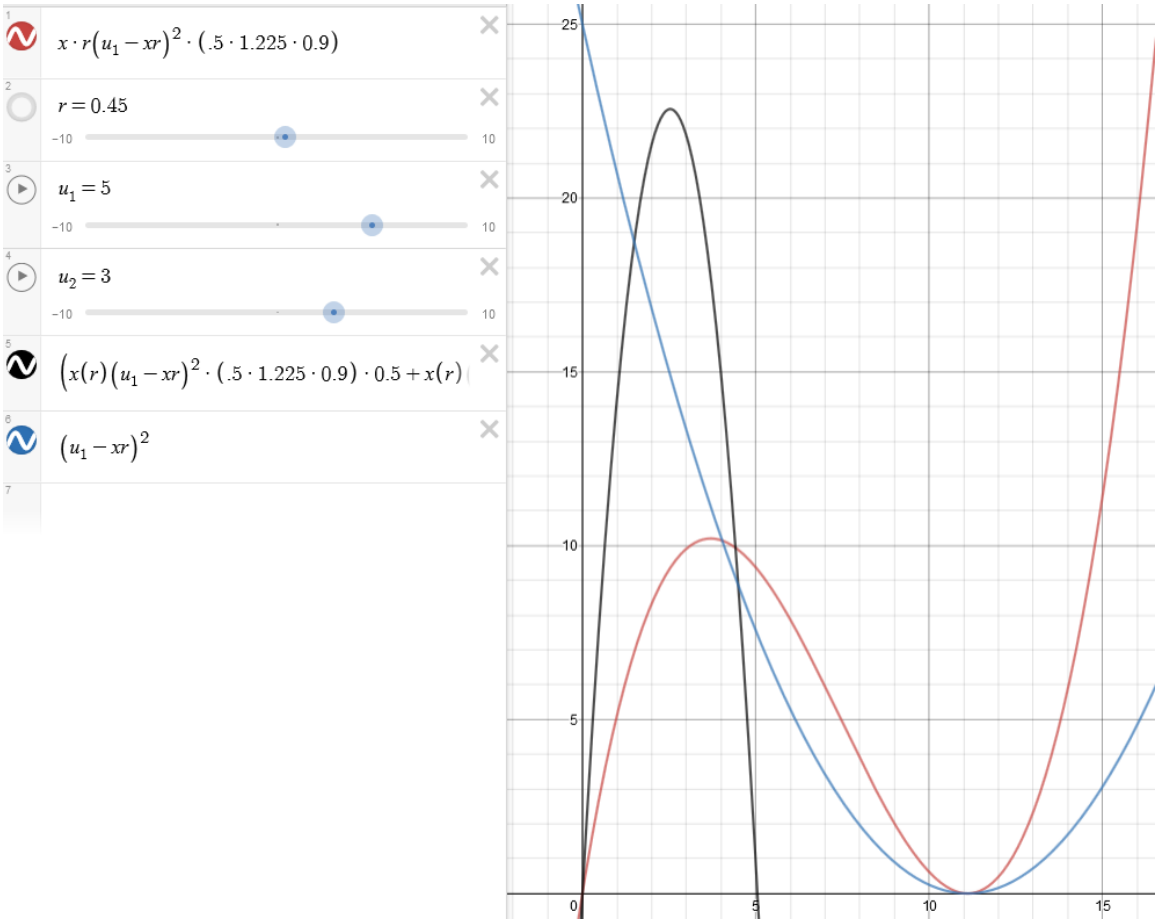

FIGURE 38 - Two power curves and a moment curve plotted using DESMOS. The black curve is the power estimation as described above. The red curve is the idealized power estimation from one blade if it were always in the 5 m/s resource. The blue curve is the moment acting on a drag-based turbine blade, which begins large and declines as the tip speed increases.

Putting the Turbine in Place: Results and Discussion

The output from Fluent were force coefficients acting on the turbine blades and resulting moment coefficients about the center of the turbine, which could then be used to calculate the resulting power.

The first simulation was run at ω=13.33 rad/s, or TSR λ=1.5. This first simulation took around a second of simulated time (about 800 time steps) to reach operational conditions. This part of the simulated time took around four days to compute. This was because the simulation was initialized automatically. All other simulations were improved by using the steady state, non-rotating condition as the initial condition for the simulation. The average moment coefficient, once normal operating conditions were achieved, was -68.24. With C_m=-68.24, the consumed power would be 35.06 W. While this first simulation does not represent a productive turbine, it does show that the power can be calculated. The equation to calculate power from moment coefficient is

$$P = \frac{1}{2} * \rho * {u_w}^2 * r * C_m * \omega \qquad 47$$

A profile view of the first simulation result from post processing can be seen in Figure 39. The graph for this first simulation can be seen in Figure 40.

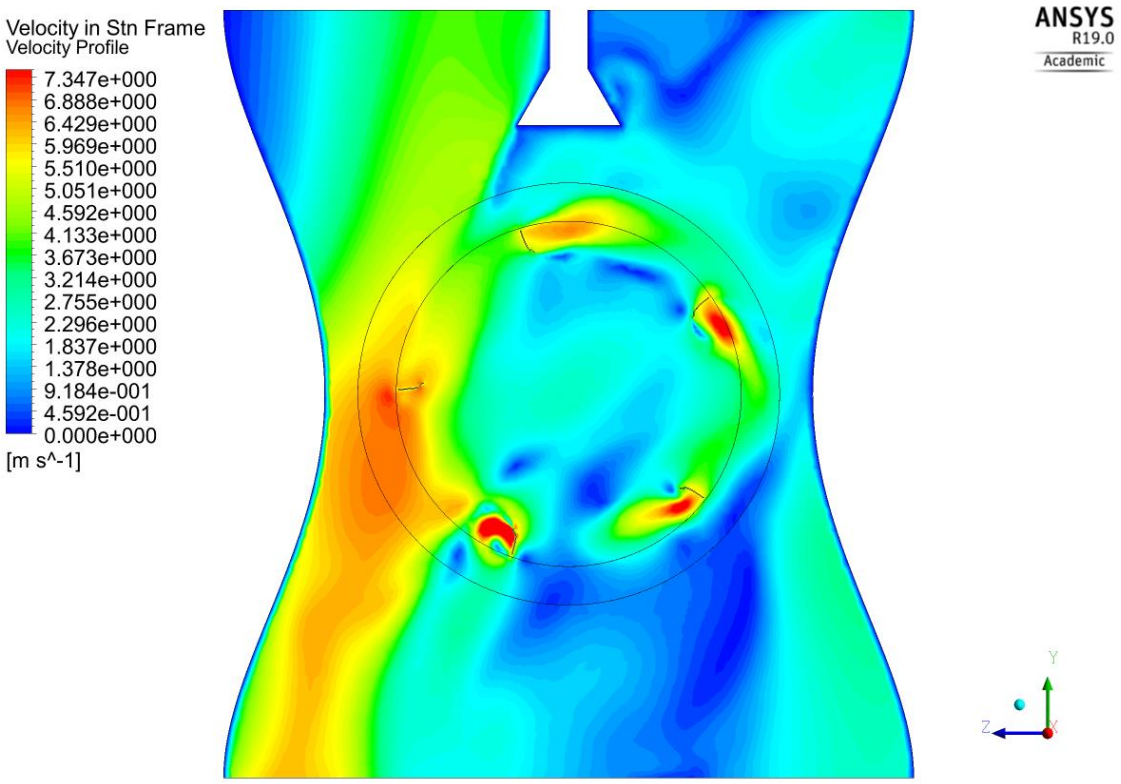

FIGURE 39 - Profile view of first (for TSR λ=1.5, at ω=13.33) simulation with scale set to highlight wake behind each blade. The wind is flowing down on the left (windward) side, and up on the right (leeward) side of this turbine. Note how the blades are putting more energy into the flow because the velocity increases after the turbine.

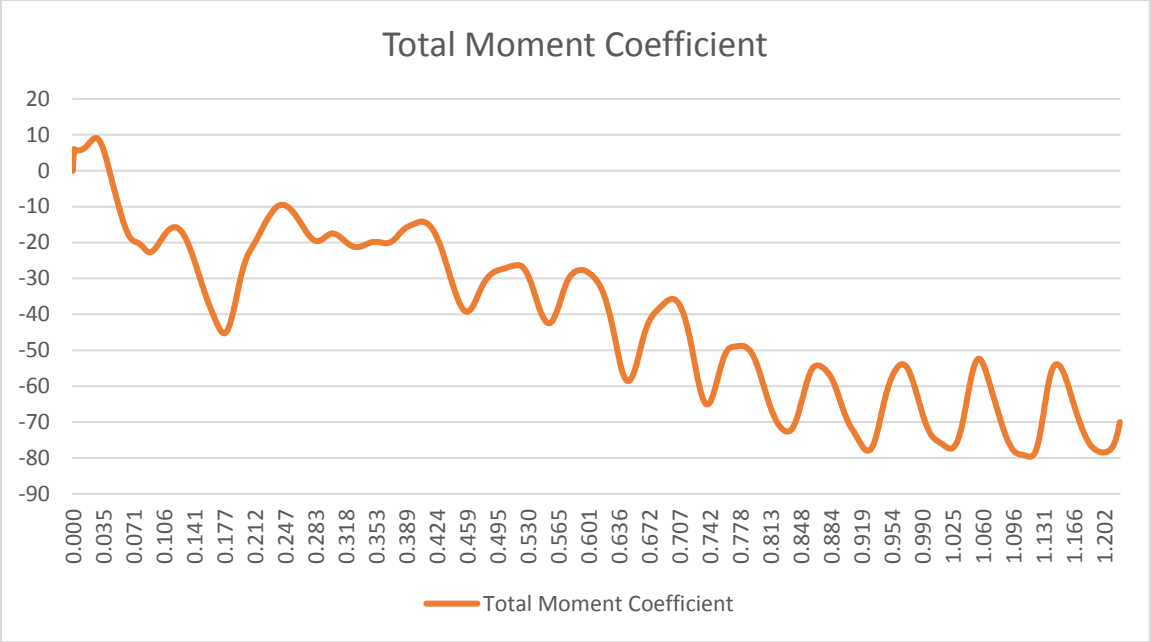

FIGURE 40 - Total Moment Coefficient for TSR λ=1.5, at ω=13.33.

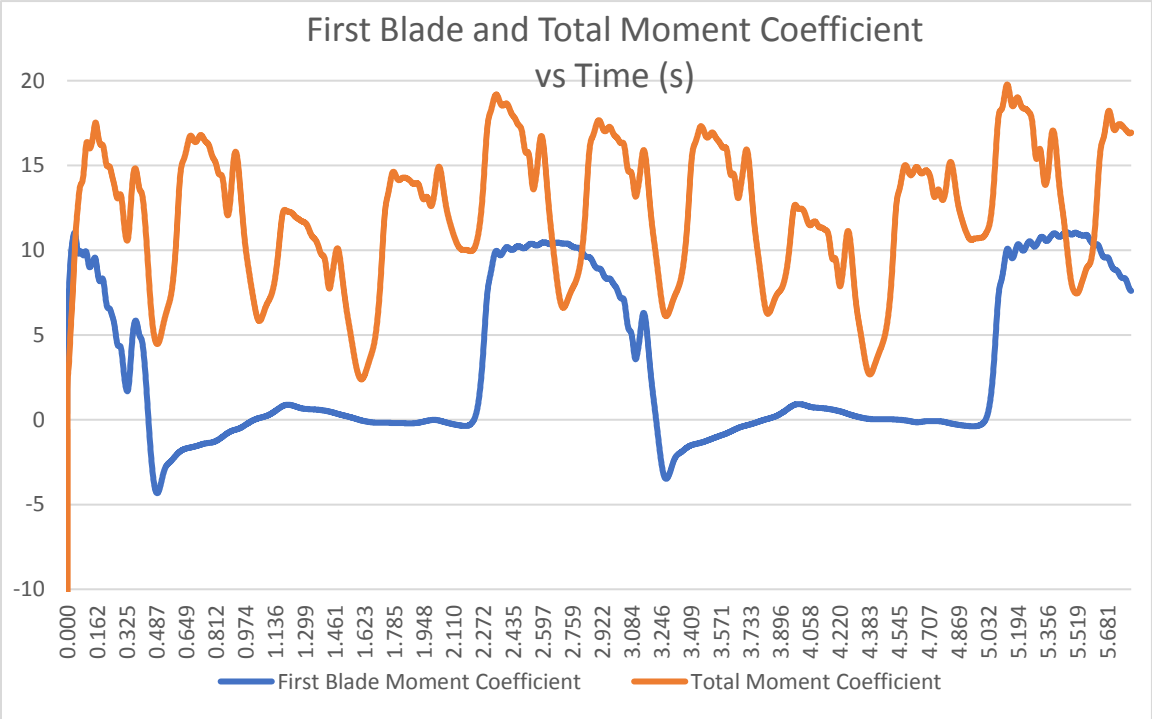

FIGURE 41 - Record of the moment coefficient on the first blade (the blade which began in the flow) and the total moment acting on all five blades of the turbine, for ω=2.25 or TSR λ=0.253

Figure 41 shows a long running simulation which recorded two complete revolutions of the turbine. The orange total moment coefficient line is the sum of all five blades simultaneously, while the blue first blade moment coefficient line is the moment coefficient of a single blade, the one which started in the wind resource (on the left). As discussed in Chapter 6, the moment coefficients are especially large because of the long radius and short chord length.

As can be clearly seen in the middle of the graph (the time between 2.217 and 3.168 seconds), the moment on each blade of the turbine contributes to two of the major peaks of the total moment coefficient. There are also small peaks near 1.21 seconds and 4.00 seconds, where the first blade is in the reversed flow on the opposite side of the tower. The deep troughs between the main total moment peaks seems to come from the moment acting on the turbine becoming negative, so it not only no longer contributes to but actually retards the motion of the turbine. This happens as the turbine passes through the relative dead zone between the two flows. The small drop in moment coefficient comes from a brief moment of wind shade on one of the turbine blades, but the wind-shade phenomenon appears to have been mostly but not entirely eliminated. As angular velocity increases to better operating conditions, the wind shade effect disappears.

The extremely large moment coefficients are not an error in calculation, but a result of the choice to make the chord length small while placing the airfoil at a large radius from the turbine center, as discussed previously. The moment coefficient as calculated in Fluent [35] is

$$M_x = F_z Y - F_y Z$$

48

Where M_x is the moment about the x-axis, F_z is the force in the z-direction, Y is the perpendicular distance in the y-direction, F_y is the force in the y-direction, and Z is the perpendicular distance in the z-direction. The center of pressure is acting with a relatively long moment arm (about 0.4 m) compared to the chord length (0.0661 m).

$$C_m = \frac{M_x}{\frac{1}{2}\rho u^2 c} \tag{49}$$

Where the moment is divided by the dynamic pressure using the reference velocity and a characteristic length; here, the chord.

One of the predictions of the power equation above was that there would be a zero somewhere near angular velocity ω=5. This was investigated, as seen in Figure 42.

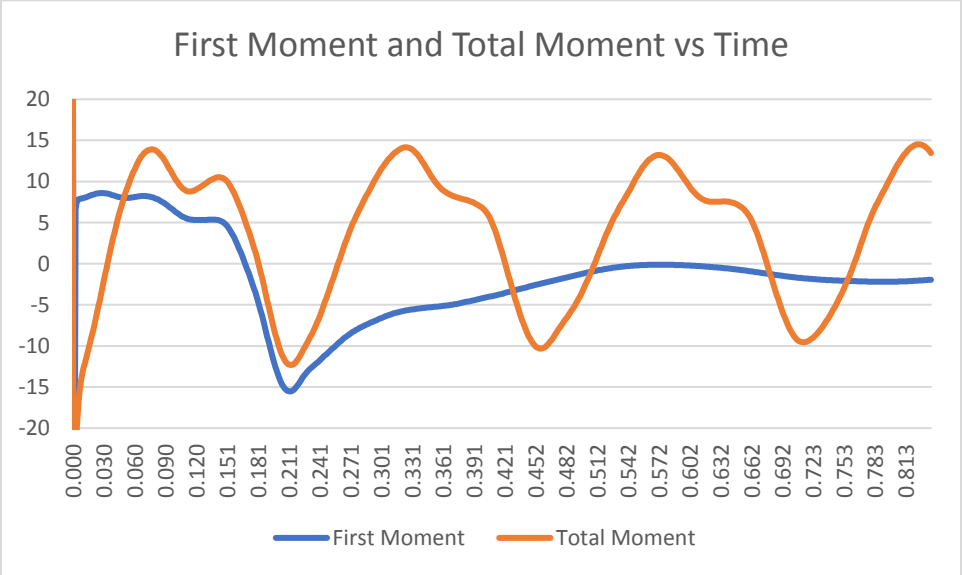

FIGURE 42 - The moment on the first blade and the total moment acting on the turbine over 0.812 seconds at ω=5 (TSR λ=0.5625)

Taking the average total moment coefficient for the second two peaks (between times 0.215 and 0.717 seconds), we find the total moment coefficient to be 3.24. This is

positive, but the moments acting on the turbine blade are fluctuating about zero, and compared to the lower tip speed ratios a moment coefficient of 3.24 is quite low. The moment coefficient is nearing zero, and the deepest troughs in the total moment are much deeper than they were for the lower operational speed, even becoming negative. This suggests that the estimated power equation was not completely correct, but was successful for its intended use of getting near the correct region of interest.

For the nine completed simulations, the results are tabulated in Table 7. The TSR, angular velocity, average moment coefficient, estimated power output, and power coefficient (C_P) are collected there. The data follow a clear trend, and appear to maximize near ω=4, which had a power coefficient of 0.041.

TABLE 7 - Table of Power Generation

TSR	ω	C_M	Moment	Power (W)	C_P
0.17	1.5	20.768	0.800	1.200	0.024
0.25	2.25	12.076	0.465	1.047	0.021
0.28	2.5	17.509	0.675	1.687	0.034
0.34	3	15.509	0.598	1.793	0.036
0.39	3.5	14.680	0.566	1.980	0.040
0.45	4	13.129	0.506	2.024	0.041
0.51	4.5	9.850	0.380	1.708	0.035
0.56	5	3.248	0.125	0.626	0.013
1.50	13.33	-68.245	-2.630	-35.057	-0.710

Realistically, most turbines operate at capacity around 25% of the time, which would reduce power production by a factor of 4, but how much time a turbine could operate would depend on the wind rose for that area and the cut in speed for the final, optimized turbine. A turbine designed with a lower cut in speed would be able to operate in lower wind speeds, which would increase the operational time. Also, when angular velocity was 0 in the steady state initialization case, the moment coefficient was

approximately 24. This suggests the turbine generates large torque at low TSR and decreases as TSR increases. This is consistent with the drag-based design which was intended. For more detailed discussion of drag based turbines, see Appendix II.

This turbine demonstrates that it is capable of operating within the confines of the wind tower. When operational, the turbine has a wake which trails behind it in the wind instead of in a circle, as seen in Figure 43 and unlike the Figure 39. However, the sliding mesh technique applied allows for the investigation of even single problem points, allowing for troubleshooting specific problems with the rotor. There are two prime examples of this from the data.

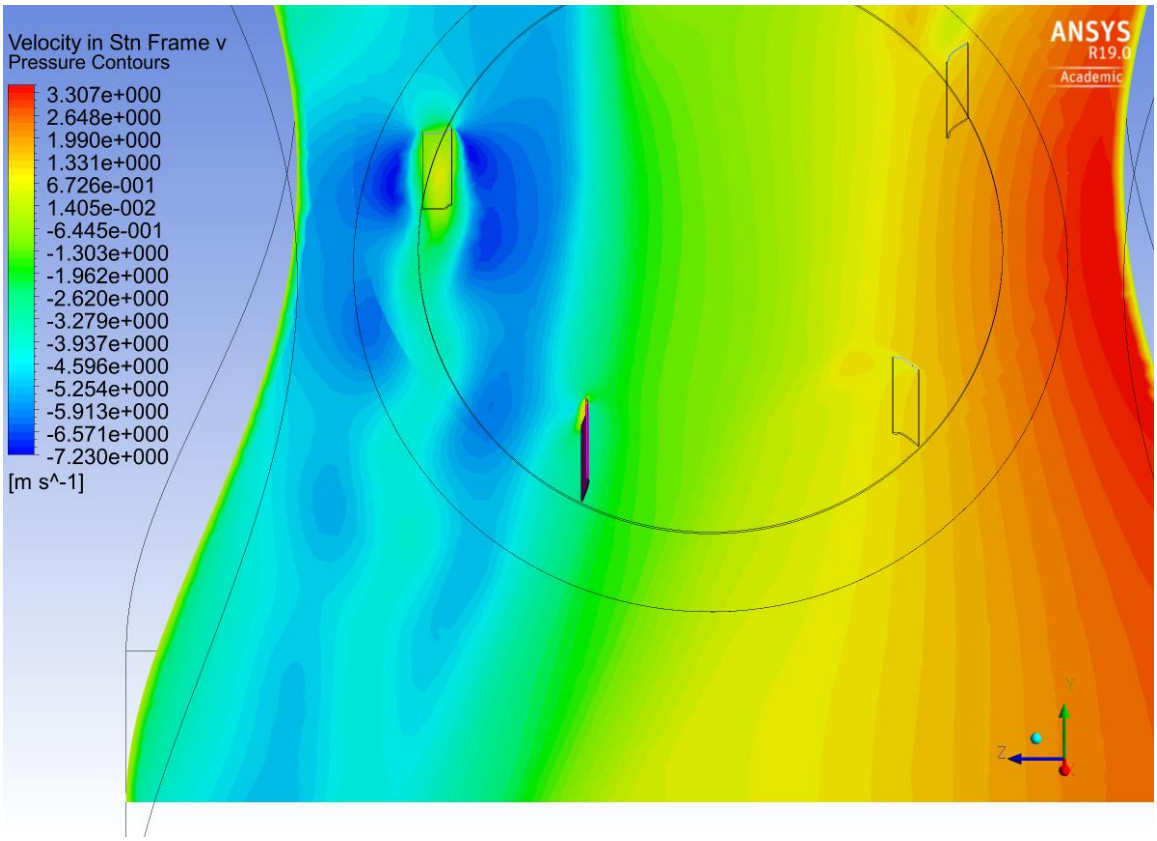

FIGURE 43 - Vortex shedding intensified for the ω=2.25 case.

First, the ω=2.25 case shows an uncharacteristic drop in power production which does not follow other trends (see Table 7). This appears to be the result of vortex shedding which intensifies at this condition (see Figure 43).

Second, the intense drop off that happens immediately after passing out of the wind resource is visible when investigated more closely. Going to the related timestep in the transient simulation, one can clearly see both the low pressure region behind the blade and the development of a small high pressure region on the front of the blade. While this highlights some of the shortcomings of the blade (which still needs to be optimized), it also emphasizes the power of using the sliding mesh technique for analyzing the turbine.

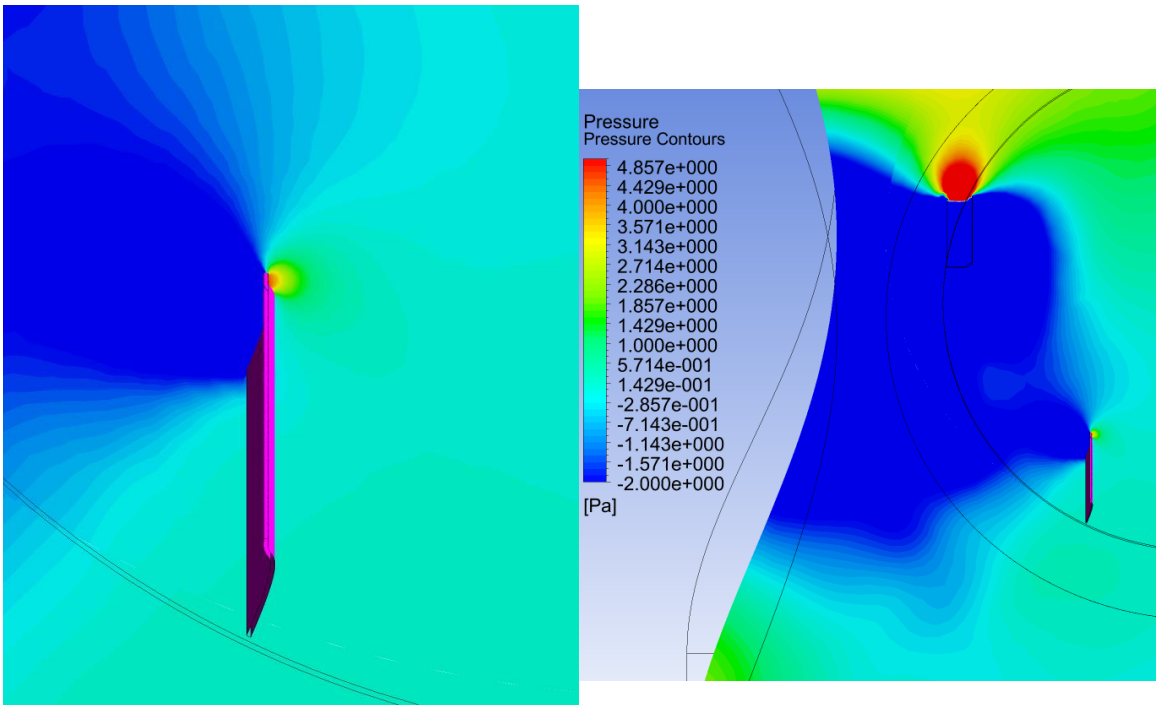

FIGURE 44 - Close up view of airfoil at moment of power decrease (left) and wider view of same moment (right). The pressure values are displayed. The development of a small high pressure region on the advancing blade is also visible. From the same timestep as Figure 43.

CHAPTER 8: CONCLUSIONS

Five main questions were proposed in the introduction, and will be answered explicitly here.

The first question was how to effectively conduct the analysis. For analyzing the tower, it is critical to use an enclosure so that the amount of wind captured by the tower can be properly estimated. Analyses which do not consider spillage will inevitably arrive at an incorrect conclusion. Removing the turbine from the tower does appear to work as a solution, provided that the boundary conditions are determined using a full analysis that does incorporate the mass loss at the inlet and no dramatic changes happen within the excerpted region. This may be an effective method for comparing turbine blades of similar chord length. Energy within a flow can be obtained by exporting the velocities in a plane and then calculating the energy using Microsoft Excel or any similar spreadsheet. Ideally, the turbine and tower would be considered together in an enclosure, and this is how optimized simulations should be run once the design is closer to its ideal. If the turbine blockage within the tower is not too large, the steady state boundary conditions may be used for the transient simulation, but a turbine that small does not produce much power.

Can a tower provide both natural ventilation and power production? Technically, yes, it can. Could existing wind towers be retrofitted for profit? Probably not. The design goals of wind towers and the needs of wind turbines are too different.

The biggest problem is that the needs of natural ventilation and power generation come into conflict at times. A wind tower dedicated to natural ventilation works well for exchanging air in a building. A wind tower dedicated to power generation could

potentially work well if optimized expressly for that purpose. Trying to combine both into one device to provide both natural ventilation and power generation simultaneously requires resolving the conflicting demands. Natural ventilation benefits from the largest mass flow possible, and requires that the flow into the building to be slow and steady. Power generation operates best when the flow speed is maximized, regardless of effect on mass flow. Although a turbine necessarily causes the flow behind it to become unsteady, this does not appear to be much to the detriment of the natural ventilation of the tower if the turbine is small. The wake and disruption to the flow appear to be small and dissipate quickly, so as long as there is an adequately long diffuser behind the turbine there should not be a problem. However, large turbines produce more power.

The turbine developed above is ideally suited for use in a wind tower. Because the wind in the tower is slow, the long moment arm for the turbine allows the smaller lift and drag forces to provide a large moment coefficient. The inability to operate at large tip speed ratios is irrelevant in the context of a low speed turbine. If the large negative spike which follows the major peak can be eliminated through blade design, then the turbine will be able to provide consistent if modest power. The current maximum power coefficient of 0.041 is quite low compared to industry standards, but compared to the many turbines that do not function at all under these conditions in the built environment it shows promise.

The impact of turbulence on turbine blades was discussed in Appendix I. As described in that section, turbines in urban areas should not attempt to design around low angles of attack because turbulence undermines designs around that point. The effect is amplified with low-wind speeds over smaller turbine blades because the small Reynolds

number promotes flow separation. Lift-based designs should plan to operate around 45^{o} angle of attack, while drag-based designs will likely be more robust. The smaller size of turbines within urban areas make the relatively large unwanted forces generated under each of those conditions easier to cope with. The normal method of operating wind turbines cannot reliably work in the built environment.

The behavior of the wind within the tower was more clearly understood. A wind tower develops flow in two opposite directions inside. On the windward side, there is a downward flow of air, while the suction on the leeward side causes an updraft on the opposite side of the tower. The flows seem to mix chaotically with no partition (in the diffuser), but with a partition the flows stay separated, even a short distance beyond the end of the partition. Future tower designs should include a partition below the nozzle and turbine, and may try to incorporate some partition into the center of the turbine if using a turbine that can accommodate it (such as the design suggested above).

One of the limitations of the investigation was that the tower planform was originally optimized for unrealistic flow conditions because the analysis assumed 100% of the flow would pass through the inlet. This would be a realistic condition for a sealed duct, but is not appropriate to the inlet of a wind tower. The associated design limited the amount of mass entering and flowing through the tower, which then reduced the power available at the turbine. Future investigation redesigning the tower itself might improve the performance of both the tower and the turbine. When investigated using an enclosure, the four-sided tower in this paper was only capturing 19% of the mass flow available in the freestream before adjustments, while the two-sided tower captured 34.8%

after adjustments. Literature suggests that 35-45% of the freestream is a reasonable value to expect for a two-sided tower [7].

Fifth, the turbine, which was the primary focus of the investigation, was functional. Because of the bidirectional flow within the tower at the nozzle, a VAWT was implemented. The radius was chosen based on the location of the wind resource within the tower. The benefit of a large radius made one large turbine superior to several smaller turbines, because smaller turbines would need to turn much more quickly to match production from a large turbine. The turbine blade selected was chosen due to higher anticipated thrust from momentum than designs which primarily build up pressure. This was partly because of a control volume analysis and partly because of the small surface area on the turbine blade. The number of turbine blades and the chord length were selected based on an analysis which suggested power produced could be enhanced by increasing solidity without developing wind shade. When implemented, wind shade was a non-issue for most of the turbine operational conditions, including the largest power producing operational conditions. The depth and complexity of wake behavior warrants its own full investigation, but some early simulation was done and the use of sliding mesh allows investigation of wake effects in transient simulations.

There is potential for a power producing wind tower, and research into the device should definitely continue. As described in Future Work, there is enormous room for improvement in the operation of the tower and the turbine. It may operate independently or as part of a renewable suite including solar power, but the potential cannot be ignored. Now that the general form of the device and the methods to analyze it have been completed, the system optimization can now begin.

Future Work

Because this was an exploratory investigation, there are many areas for future work which have been identified. These areas will be discussed in order.

First, the tower needs to be reexamined and redesigned. The inlet design was identified as a critical deficiency in the wind tower. The tower described in [6] does not perform as well as claimed. The inlet should be revamped for better flow capture. Drawing inspiration from jet propulsion intakes would likely improve the percentage of flow and energy capture, in other words reducing spillage. Inlet design has filled multiple papers and is a complex topic, and could easily fill a thesis by itself.

Second, the partition needs to extend down the length of the tower as much as possible without inhibiting the turbine's ability to rotate. The mixing of the downflow and the upflow created large dead zones which were detrimental to power production and also natural ventilation. The mixing which takes place in the diffuser is disruptive to the turbine above, and dividing those flows would address the dead zones.

Third, a more rigorous understanding and application of wake theory will be important. Modeling wake behavior more accurately will be useful to optimizing the number and size of the turbine blades if the turbine radius is increased.

Fourth, the turbine blade airfoil also needs to be optimized. While one turbine blade was modeled to develop the process, there is significant room for improvement. Savonius turbines often generate some lift and some drag to enhance their productivity, and comparisons to more traditional turbine blades would be informative. Turbine blade design and selection are complex topics able to fill a thesis by themselves, and the topic

could not possibly be explored fully in this work. This is a critical area for future development.

The nozzle in the tower could also be reconceptualized. Because the turbine itself represents a blockage in the tower, the turbine might be optimized to fill the role of the nozzle at the throat. This would allow for a larger turbine to improve the small power coefficient. Because of the decision to use a substantial gap between turbine blades, it may be useful to integrate part of the partition into the turbine, perhaps as a cylindrical blockage in the center of the turbine. The primary role of the gap was to increase the distance the lift and drag were applied at, thus increasing the moment. Keeping blockage in the tower low was another benefit, but if the partition and/or nozzle were integrated into the turbine in this way, the turbine could be increased to a larger radius. For power production, wind turbines nearly always benefit from becoming larger.

One of the important practical questions not explored herein was whether introducing the turbine to the wind tower would add additional heat to the system through friction and viscous effects. This aspect of thermal comfort was not investigated in this work, but will be important to fully understanding the effect of the turbine on the tower's primary role providing natural ventilation. Likewise, the acoustic impact of noise was not explored, but will need to be at some point. The impact of stack effect will also need to be explored in the future.

There is a significant amount of future work still to be done, but the problem has been outlined, the major areas of interest identified, and the methods useful to investigating them are now known. Initializing the turbine design was a primary goal of the investigation, and this turbine may now be optimized for maximum performance.

REFERENCES

[1] United Nations "World's Population Increasingly Urban with More Than Half Living in Urban Areas" accessed April 27, 2019 https://www.un.org/en/development/desa/news/population/world-urbanization-prospects-2014.html

[2] US Energy Administration "Electricity in the U.S." accessed April 27, 2019 https://www.eia.gov/energyexplained/index.php?page=electricity_in_the_united_states

[3] Santiago, Leyla and Gallon, Natalie "Puerto Rico Says Power Restoration after Hurricane Maria is Complete, but That's Not Quite Right" https://www.cnn.com/2018/08/14/us/puerto-rico-power-restored/index.html

[4] Calautit, John Kaiser and Hughes, Ben Richard and Shahzad, Sally Salome "CFD and wind tunnel study of the performance of a uni-directional wind catcher with heat transfer devices" Renewable Energy 83, pp 85-99 DOI: http://dx.doi.org/10.1016/j.renene.2015.04.005

[5] Delso, D. (2016, September 21). [Building in Yazd, Iran]. Retrieved July 1, 2018, from https://en.wikipedia.org/wiki/Windcatcher#/media/File:Edificios_en_Yazd,_Irán,_2016-09-21,_DD_17.jpg

[6] Sheikhshahrokhdehkordi, M., Goudarzi, N. (2018) "A Comprehensive Numerical Investigation of Internal Flow Analysis of A Novel Two-Sided Wind Catcher." Manuscript submitted for publication. University of North Carolina at Charlotte, Charlotte, NC.

[7] N. Goudarzi, W.D. Zhu, H. Bahari, (2013) "Wind Energy Conversion: The Potential of a Novel Ducted Turbine for Residential and Commercial Applications", Proceedings of the ASME 2013 International Mechanical Engineering Congress and Exposition, San Diego, California, USA

[8] J. Fields, F. Oteri, R. Preus, and I. Baring-Gould (2017) "Deployment of Wind Turbines in the Built Environment: Risks, Lessons, and Recommended Practices".

[9] H. Montazeri (2011) "Experimental and Numerical Study on Natural Ventilation Performance of Various Multi-Opening Wind Catchers". Building and Environment, Volume 46, Issue 2, Pages 370-378

[10] K. Esfeh, Mohamad and Dehghan, Ali A. and Dehghan Manshadi, Mojtaba and Mohagheghian, Shahrouz and Dehghan Kamaragi, Gholamreza. (2012). Visualized flow structure around and inside of one-sided wind-catchers. Energy and Buildings. 55. 10.1016/j.enbuild.2012.09.015.

[11] Nejat, Payam and Calautit, John Kaiser and Abd Majid, Muhd.Zaimi and Hughes, Ben and Zeynali, Iman and Jomehzadeh, Fatemeh. (2016). Evaluation of a two-sided windcatcher integrated with wing wall (as a new design) and comparison with a conventional windcatcher. Energy and Buildings. 126. 10.1016/j.enbuild.2016.05.025.

[12] P. Nejat, J. K. Calautit, M. Z. A. Majid, B. R. Hughes, F. Jomehzadeh "Anti-short-circuit device: A new solution for short-circuiting in windcatcher and improvement of natural ventilation performance". *Building and Environment* 105 (2016): pp 24-39

[13] Osborn, Liz. "Windiest Cities in the United States". Retrieved April 27, 2019 from URL https://www.currentresults.com/Weather-Extremes/US/windiest-cities.php

[14] Kirk, Stuart and Kolokotroni, Maria (2004) "*Windcatchers in Modern UK Buildings: Experimental Study, International"* Journal of Ventilation Vol 3:1, pp 67-78

[15] P. Gipe (Jan 9, 2018) "Another Ducted Device Dead: SheerWind-Invelox Bankrupt" Retrieved Mar 18, 2019 from URL http://www.wind-works.org/cms/index.php?id=64&tx_ttnews%5Btt_news%5D=4971&cHash=a734f6787ce80e93ff54d44c74842cce

[16] P. Gipe (Feb 23, 2017) "SheerWind-Invelox--Is the End Nigh for Another Ducted Turbine?". Retrieved Mar 18 2019 from URL https://www.linkedin.com/pulse/sheerwind-invelox-is-end-nigh-another-ducted-turbine-paul-gipe/

[17] Wind Turbines Efficiency & Comparison Calculator?". Retrieved April 24, 2019 from URL http://perso.bertrand-blanc.com/Resume/Experience/Energy/index.html

[18] Frank M. White, 2011, Fluid Mechanics 7th Edition, McGraw Hill, New York, New York. Chap. 11

[19] Celis, S. (2005, July 4). [Wind Turbine]. Retrieved January 23, 2018, from URL https://www.flickr.com/photos/scelis/717687465/in/photostream

[20] Clifton, A. (2017, October 4). [The 55-kW Darrieus-type vertical axis wind turbine at Heroldstat]. Retrieved January 23, 2018, from https://www.flickr.com/photos/windfors/36841063103/sizes/l

[21] H. H. Al-Kayiem, B. A. Bhayo, M. Assadi (2016) "Comparative Critique on the Design Parameters and Their Effect on the Performance of S-rotors", Renewable Energy, Volume 99, pp 1306-1317

[22] Roy, Sukanta and Saha, Ujjwal. "Review of experimental investigations into the design, performance and optimization of the Savonius rotor" *Journal of Power and Energy* 227, 4 (2013): pp 528-542

[23] Kumar, Anju and Saini, R.P. "Investigation on Performance of Improved Savonius Rotor: An Overview" *2015 International Conference on Recent Developments in Control, Automation, and Power Engineering (RDCAPE)* pp 151-156. Noida, India, March 12-13 2015 **DOI:** 10.1109/RDCAPE.2015.7281386.

[24] Perfected Flight.com [Lift-Drag 1976x1266]. Retrieved October 17, 2018, from https://www.perfectedflight.com/the-truth-about-induced-drag/ via Google.com at https://www.google.com/imgres?imgurl=http%3A%2F%2Fwww.perfectedflight.com%2Fhome%2Fwp-content%2Fuploads%2F2016%2F09%2FLift-Drag.png&imgrefurl=https%3A%2F%2Fwww.perfectedflight.com%2Fthe-truth-about-induced-drag%2F&docid=qWHOWuNAtWgwEM&tbnid=5KOKZbDXkthNyM%3A&vet=10ahUKEwjq-5TE2cLjAhVCzlkKHXW8CWIQMwhiKA4wDg..i&w=1976&h=1266&safe=off&bih=651&biw=1408&q=lift%20and%20drag%20diagram&ved=0ahUKEwjq-5TE2cLjAhVCzlkKHXW8CWIQMwhiKA4wDg&iact=mrc&uact=8

[25] Anderson, John D. *Introduction to Flight, Fifth Edition.* McGraw-Hill, Boston (2005)

[26] Sheldahl, Robert and Klimas, Paul. "Aerodynamic Characteristics of Seven Symmetrical Airfoil Sections Through 180-Angle of Attack for Use in Aerodynamic Analysis of Vertical Axis Wind Turbines." SAND80-2114. Sandia National Laboratories, Albuquerque, NM. 1981. https://prod-ng.sandia.gov/techlib-noauth/access-control.cgi/1980/802114.pdf.

[27] Simon McBeath, *Competition Car Aerodynamics, A Practical Handbook.* Veloce Publishing, p 231

[28] Argyropoulos, C.D. and Markatos, N.C. "Recent Advances on the Numerical Modeling of Turbulent Flows". *Applied Mathematical Modeling* 39 (2015) pp. 693-732 DOI:http://dx.doi.org/10.1016/j.apm.2014.07.001

[29] Menter, F.R., and Kuntz, M. and R. Langtry. "Ten Years of Industrial Experience with the SST Turbulence Model" *Turbulence, Heat and Mass Transfer* (2003) 4 pp 1-8

[30] Fu, Chen and Uddin, Mesbah and Robinson, A. Clay. "Turbulence Modeling Effects on the CFD Predictions of Flow over a NASCAR Gen 6 Racecar". *Journal of Wind Engineering & Industrial Aerodynamics*. 176 (2018) pp 98-111

[31] Airfoiltools.com, 2018, "NACA0012H for VAWT from Sandia report SAND80-2114 (naca0012h-sa)", retrieved Nov 6, 2018 from http://airfoiltools.com/airfoil/details?airfoil=naca0012h-sa

[32] J.C. Corbett, N. Goudarzi, M. Sheikhshahrokhdehkordi (2019) “WIND CATCHER TECHNOLOGY: THE IMPACT OF TOWER CROSS SECTION AND TURBINE ON WIND POWER HARNESSING”, Proceedings of the ASME 2019 Power Conference and Nuclear Forum, Salt Lake City, Utah, USA

[33] Aynsley, R.M. “A Resistance Approach to Analysis of Natural Ventilation Networks” *Journal of Wind Engineering and Industrial Aerodynamics* 67 & 68 (1997) pp 711-719 DOI: https://doi.org/10.1016/S0167-6105(97)00112-8

[34] Farokhi, Saeed *Aircraft Propulsion.* John Wiley and Sons, Inc., United States (2009) Ch 3, pp 99-101

[35] SAS IP, 2019, “Computing Moments, Forces, and the Center of Pressure” retrieved July 17, 2019 from https://www.sharcnet.ca/Software/Ansys/17.0/en-us/help/flu_th/flu_th_sec_report_force_moment.html

APPENDIX I: WHY TURBULENT FLOWS DEVASTATE TURBINE PRODUCTION

One of the more theoretical aspects of the work being done is an exploration of why turbines underperform so badly when placed into turbulent environments such as those found in cities. This failure happens for several reasons explored herein.

First, it is important to recall the nature of lift and drag production in turbines. Recall that for a HAWT, the most common design approach is to maximize lift while minimizing drag. This position puts the turbine into a low angle of attack (somewhere before stall), where the lift is large but the drag is low. This design point is chosen to limit the total force acting on the turbine blades and to decrease the energy lost to drag from rotation.

However, one must consider the nature of turbulence. During and after transition, there are erratic changes to velocity in the bulk flow direction and the addition of some amount of vorticity. Recall that for a steady fluid flow the energy equation is:

$$H_1 + \frac{1}{2}mu_1{}^2 + mgh_1 + Q - W = H_2 + \frac{1}{2}mu_2{}^2 + mgh_2 \quad (50)$$

However, in turbulent flows at large scales, the energy cascades into smaller vortices before being dissipated at the microscopic scale. For a turbine blade, the smaller scales of motion are irrelevant and can be neglected because they are several orders of magnitude smaller than the turbine blade itself, and will not impact the angle of attack.

With no temperature and no pressure changes from the transition from laminar to turbulent, the enthalpy does not change (*i.e.* $H_1=H_2$). There is no heat transfer and no work being done during transition, so Q and W are both zero. Also, motion in the vertical direction is usually negligible (*i.e.* $mgh_1=mgh_2$). Thus, all the energy of motion in turbulence must go into other motions in the turbulent flow; indeed, large scale

motions at the beginning of the energy cascade are often characterized this way. Thus, when the velocity from the bulk flow decreases, it must increase in the other directions. This necessarily changes the direction of the wind at the scale of the turbine blade.

This is important because when the energy goes into velocity vectors which are not the same direction as the bulk fluid flow, it changes the angle of the velocity for the fluid encountering the turbine blade. Recall that turbines are often designed for the best lift-to-drag ratio, but this happens at low angles of attack where the lift and drag curve undergo dramatic changes with changes to angle of attack. Also recall lift coefficient is maximized near stall, which is the operating condition for most optimized turbines. For changes reducing the angle of attack, the turbine blade will lose lift, so less moment will be generated for rotation and power will be reduced. On the other hand, if the change increases the angle of attack, the blade may enter stall, where lift is substantially reduced or even eliminated completely, and drag is increased. This also reduces power production.

This engenders the question of how much turbulence changes the angle of the flow interacting with the turbine blade, and whether that change is large enough to cause the problems described above and observed in practice. If one considers wind at 10 m/s with 5% turbulence, the change to the bulk fluid motion is as little as ±0.5 m/s, but in the other directions the velocity change for an equivalent amount of energy are as much as 4.47 m/s. This is the magnitude of the velocity vectors in the y and z directions combined.

To calculate this, consider the change to the energy of motion in a single particle of arbitrary mass m. The change to the kinetic energy is the difference between the energy of the two particles. Mathematically, this can be expressed

$$\Delta E = \frac{1}{2} m {u_0}^2 - \frac{1}{2} m {u_1}^2 \tag{51}$$

$$E = \frac{1}{2} m({u_0}^2 - {u_1}^2) = \frac{m}{2}(110.25 - 90.25) = 12.25m \tag{52}$$

This is the energy that then goes into one or more of the other directions of motion. The velocity in that direction then becomes

$$12.25m = \frac{1}{2} m v^2 \rightarrow \ v \approx 4.472 \ \frac{m}{s} \tag{53}$$

Due to the chaotic nature of this part of the velocity vector, this will change the velocity of the wind encountering the turbine blade by an angle somewhere between ±27.48 degrees. Even at lower speeds, the change to the velocity vector is significant. For wind at 4 m/s (the speed analyzed in this thesis), 5% turbulence also corresponds to ±27.48 degrees. The angle does not vary with wind speed, but with turbulence intensity. This analysis describes the maximum range that the wind's angle might change due to turbulence.

Even considering that the turbine is also rotating (which changes the relative wind experienced by the turbine blade as observed in velocity triangle analyses), this represents a substantial change to the angle of attack that increases rapidly with increasing turbulence. For small turbines – such as those found in the built environment– the relative wind from rotation is small because of the small radius of the turbine. When considered in the context of the design point most turbines are optimized about – the low

angle of attack with high lift-to-drag ratio – it becomes obvious why traditionally designed turbines do not successfully operate in urban settings.

If one considered the maximum value the third standard deviation (since 99.7% of values lie within three standard deviations), then one standard deviation would be 1/3 of the maximum. For 5% turbulence intensity, that would be more than ±9 degrees. In the context of low Reynolds number flows such as those applicable to small, built environment turbines, the average lift acting on turbine blades decreases significantly, either because the turbine blade entered stall or because the angle of attack was decreased to an unproductive value. This effectively eliminates the productivity of turbine blades in this region, especially when considering the forces required for starting a turbine from rest.

When considering the lift curve near 45 degrees or the drag curve near 90 degrees, one sees that for the same range of ±9 degrees the change makes substantially less difference to the lift or drag coefficient of interest (see Figure 11). This is why it is possible to design around those maxima, but turbines designed around low angles of attack consistently fail in the built environment.

APPENDIX II: THE LIMIT ON DRAG-BASED TORQUE

One of the limitations when choosing to use a drag-based airfoil design is that the maximum torque that can be produced is directly limited by the speed of the incoming wind. Recall the definition of drag coefficient from equation 6:

$$C_L = \frac{L}{\frac{1}{2}\rho u^2 A} \tag{54}$$

$$C_D = \frac{D}{\frac{1}{2}\rho u^2 A} \tag{55}$$

$$C_M = \frac{M}{\frac{1}{2}\rho u^2 A c} \tag{56}$$

The drag coefficient is nondimensionalized using the velocity squared. Therefore, as the velocity increases, the drag increases. Similarly, if the velocity decreases, the drag produced will decrease. Since the drag is the primary motivator for the moment (M) in the moment coefficient (Eq. 7) for a drag-based design, if velocity decreases, the drag and the subsequent moment will decrease.

The velocity which matters is the total velocity of the wind at the airfoil, which is a combination of the freestream and the relative wind from the motion of the turbine. Recall those equations were

$$\vec{u} = \vec{u}_{wind} + \vec{u}_{relative} = \vec{u}_w + \vec{u}_{rel} \tag{57}$$

$$\vec{u}_{rel} = -\vec{\omega} \times \vec{R}_{local} \tag{58}$$

$$\vec{u} = \vec{u}_w - \vec{\omega} \times \vec{R}_{local} \tag{59}$$

As can be seen from the equations above, as the angular velocity (ω) increases, the relative wind increases. The wind velocity (u_w) is a finite value (whether 4 m/s, 5 m/s, or some other instantaneous value), so when the relative wind from motion exceeds that speed, then there will be no point on the turbine providing any torque to the rotor shaft. This is the reason that the turbine transitions from power producing (at low velocities) to power consuming, because for large angular velocities there is not enough wind to operate the device.

One of the benefits of using the sliding mesh was the ability to examine any operational condition for the turbine, but that also means that it is possible to examine unrealistic operating conditions, such as the turbine rotating faster than the wind will support. If the velocity at the tip of the rotor equals the wind speed, necessarily no power can be generated.

In layperson's terms, it is similar to the reason that sailing ships cannot sail faster than the wind that carries them. As the ship picks up speed, the relative wind decreases, until eventually the drag of the water on the ship balances with the power provided by the sails. In the case of the turbine examined herein, the drag comes from the turbine blades outside the primary wind resource (*e.g.* in dead zones).

This limitation is a direct result of the choice to focus on a drag-based design that draws inspiration from Savonius turbines. There may be some occasional confusion if trying to consider Darrieus turbines using this argument. Darrieus turbine operate by generating lift, so the behavior of those turbines will be significantly different (*i.e.* this argument does not apply to Darrieus turbines because they are different). Darrieus

turbines were not the focus of this investigation, and so will not be examined in the same detail.

APPENDIX III: MESH ANALYSIS OF TOWER AND NOZZLE

A mesh analysis was conducted for the tower. In order to conduct a mesh analysis, the velocities along a line in the center of the tower nozzle from one corner to the opposite corner were exported from ANSYS Fluent (See Figure 42). The velocities measured are graphed in Figure 43.

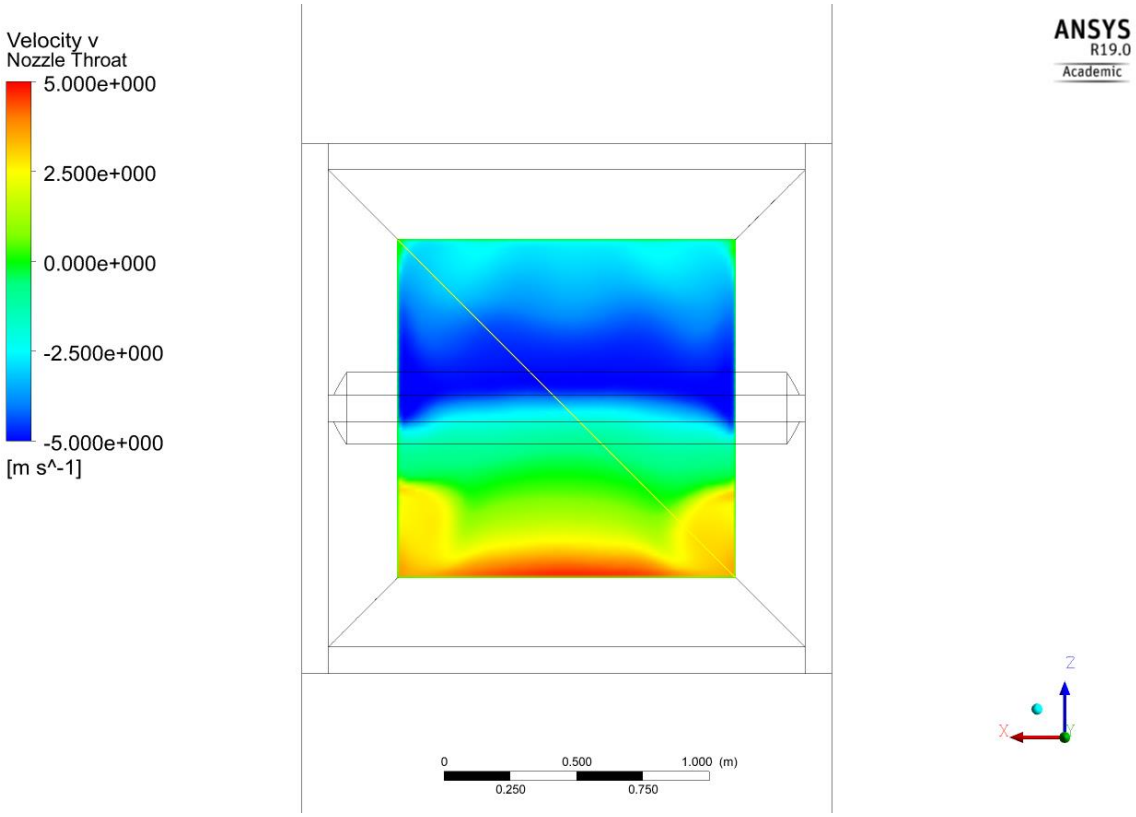

FIGURE 45 - Mesh Analysis line in nozzle throat. The windward side is the top. The mesh analysis line was X points from one corner to the opposite corner.

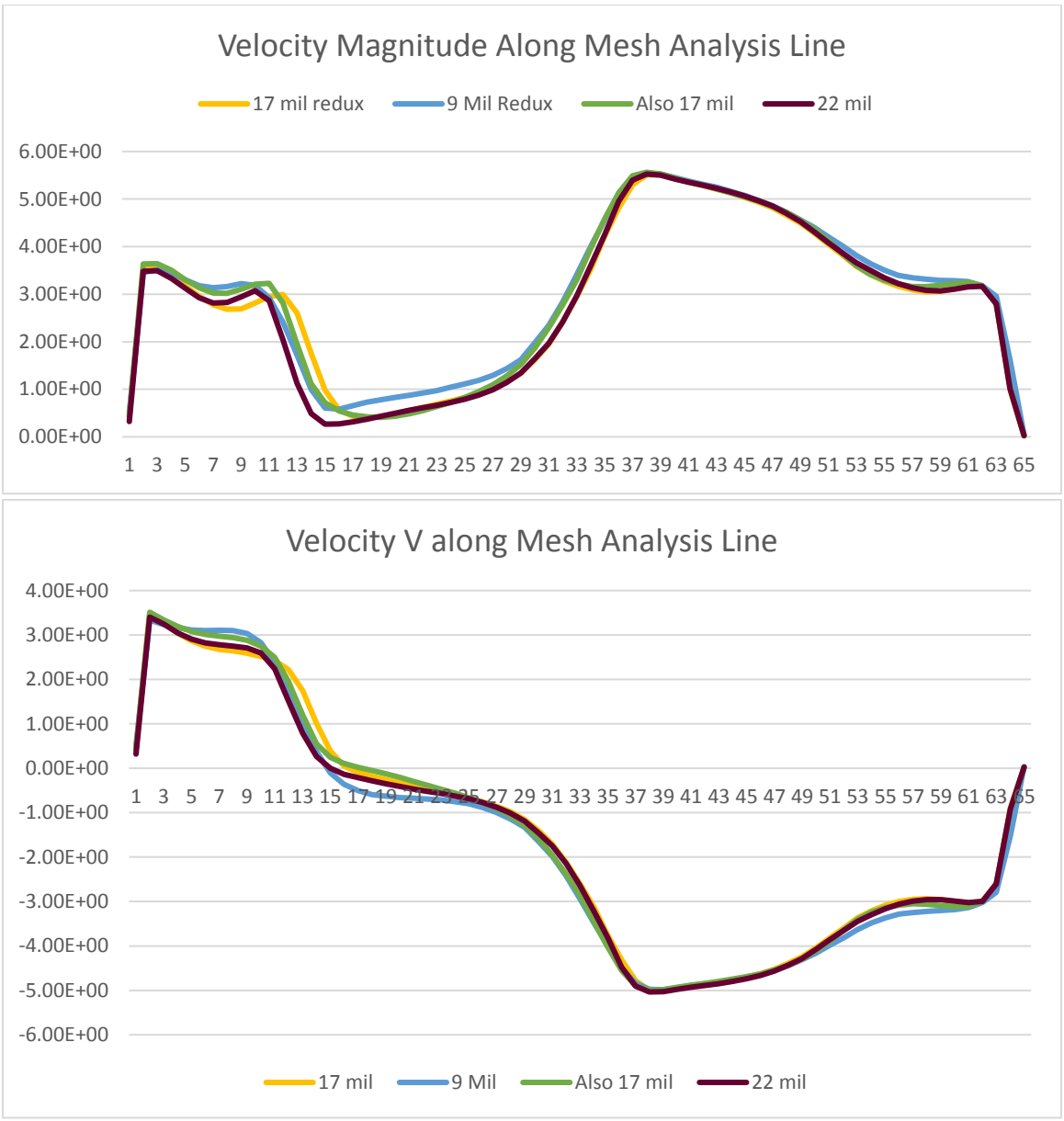

FIGURE 46 - Velocities exported along Mesh Line; velocity magnitude (top) vs. point, and velocity component in the vertical (y) direction (bottom).

As can be seen clearly, the points along the velocity curves are very similar, but do not overlap exactly. This can be attributed to two factors, which are limiting how much the "final" solution will be able to converge.

The first limiting factor on convergence is the inlet condition. Because the inlet is being modeled with 5% turbulence intensity, the inlet velocity varies by 5%. Because of

this, there will always be some variation in "final" steady state solutions, since the tower was modeled in steady state.

The second limiting characteristic comes from the tower. The tower was deliberately designed with strong flow separation on the leeward side (where the leeward inlet is located). This leads to a certain amount of unsteadiness on the rear face of the tower as a result of vortex shedding that happens there, which will propagate into the tower via the desired suction. This effect is expected to be relatively small compared to the effect of 5% turbulence at the inlet, but also exists.

Since the variation between points is less than 5% (the turbulence intensity) when the mesh is increased from 17 million to 22 million, the mesh is converged with 17 million elements in the mesh. This was true for both velocity magnitude and vertical velocity in the tower (v).

TABLE 8 - Resting torque of turbine for mesh analysis.

Elements (million)	Cm First	Cm Second	Cm Third	Cm Fourth	Cm Fifth	Cm Total
1.7	19.252	2.933	0.250	0.603	-1.251	21.788
3.8	23.345	1.916	0.090	0.406	-1.482	24.276
6.2	24.246	1.493	0.101	0.392	-1.478	24.753

The nozzle section which was removed was also analyzed. Using the steady state simulation (*i.e.* the turbine at rest), the moment values for each of the five turbine blades was calculated for the unmoving case. This is essentially finding the starting torque of the rotor, a value of interest since that is the primary motivator for generating power (see in depth explanation in Appendix II for how drag-based turbines generate power). The test cases were 1.7 million, 3.8 million, and 6.2 million elements each. As can be seen in

Table 8, increasing from 3.8 million to 6.2 million altered the starting torque by less than 2%, which was well under the variation within the data alone.

APPENDIX IV: MATLAB ANGLE OF ATTACHMENT OPTIMIZATION CODE

Optimization code is presented as-is. Development was ceased when it was determined there was a paucity of published airfoil information to use for inputs, which limited how much use the code could be. Future work may develop the code further if it becomes possible to quickly obtain lift and drag coefficients for all operational angles.

```
clc
clear all
close all

%Code by Jonathan Conrad Corbett

%List of Variables

%lambda = 5;  %Tip Speed Ratio; removed
omega = 0;    %Angular velocity
theta = 0;    %angular position
rho   = 1.225; %Density of air, 1.225 at STP.
Programmed assuming incompressible.

r= 0.60  %Radius, in meters, of drum turbine

cl = importdata("clNACA0012.txt");      %Lift
Coefficient; valid for angles 0-360
cd = importdata("cdNACA0012.txt");      %Drag
coefficient; probably also needs to be an array with
360 values or something

w = 20;        %freestream velocity, m/s; in update
version hopefully import my values
u = 0 ;       %Local velocity, "x" component m/s
v = 0  ;      %Local velocity, y component m/s

%Airfoil Parameters
c = .20     %Chord length
B = 0;        %"Attachment angle of airfoil", relative
to the radius.  0 is along radius; +/- 90 is in line
with theta
L = 1.2     %width of the wing/airfoil, probably
roughly spanning the throat
```

```
%m = 2700    %Density of material; 2700 kg/m^3 Al, 8050
steel, oak ~6000-9000, 160 Balsa wood (solid)
            %Probably would not be made of a solid
piece of material
            %this variable removed, not used.


tantot=0;    %The total tangent force acting on the
turbine

phi = 0;     %The wind angle
psi = 0;     %The angle the chord line makes at a given
location and time.

alpha = 0;   %The angle of attack - comes from the
chord line and wind angle

%omega=lambda*w/r; %Rate of rotation for estimated
ideal TSR; TSR probably ~5
omegar=-omega*r; %might regret that name; relative
induced wind from rotation

rads = pi()/180; %Conversion factor to convert to
radians.

Power=zeros(181,40);

filename='output.xls';

for omega= 0:100;
    omegar=-omega*r*.1;  %This changes the rotation
from a whole number to a tenth;

    for B= -90:90;
        tantot=0; %reinitialize for each run
        for theta= 0:359;   %Summation of the lift and
drag forces in tangential directions

            u = w+omegar*sin(theta*rads); %Recall
omegar=omega*r
            v = omegar*cos(theta*rads);
            utot = sqrt(u^2+v^2); %Magnitude of
velocity locally
```

```
            phi= atan(v/u); %Wind angle, based on local
velocity vectors, in rads
            psi=B+theta;    %Finding the relative angle
for this B;
            alpha=psi-phi/rads;  %Here, I'm finding the
angle of attack in degrees

            if alpha<0        %Keeping alpha between 0
and 360
                alpha=alpha+360;
            end
            if alpha>360
                alpha=alpha-360;
            end

            lift=cl(round(alpha)+1)*.5*rho*utot^2*c*L;
%cl*(1/2)*density*u^2*chord*wingspan
            drag=cd(round(alpha)+1)*.5*rho*utot^2*c*L;
%Must make sure that the lower half of the values are
negative
            %The +1 is necessary because the angles
start at 0 but the indicies
            %start at 1.

            %Now that we have lift and drag, we need to
find the local
            %tangential force causing rotation of the
system.

tangentforce=lift*sin(phi)*cos(theta*rads)+lift*cos(phi
)*sin(theta*rads)+drag*cos(phi)*sin(theta*rads)+drag*si
n(phi)*cos(theta*rads);
            tantot=tangentforce+tantot;
        end
        %Now that we know the total force acting on the
turbine,
        %we need to calculate the associated
        tantot=tantot/360;
        Power(B+91,omega+1)=tantot*(r-.25*c)*omega*.1;
        %The center of pressure for most airfoils in
low speed flows is at
        %the quarter chord, or .25c.  That means the
aerodynamic forces
        %should be applied at that point.
```

```
    end
    xlswrite(filename, Power);
end
```

0
0.11
0.22
0.3376
0.4464
0.5276
0.6115
-0.0212
-0.0615
-0.016
0.0344
0.0869
0.1406
0.1945
0.2484
0.3024
0.3563
0.4107
0.4644
0.5178
0.5708
0.6232
0.6755
0.7283
0.7809
0.834
0.8873
0.9407
0.932133333
0.923566667
0.915
0.936
0.957
0.978
0.999
1.02
1.031
1.042
1.053
1.064
1.075
1.077
1.079
1.081
1.083
1.085
1.076
1.067
1.058
1.049
1.04
1.025
1.01
0.995
0.98
0.965
0.947
0.929
0.911

0.893
0.875
0.853
0.831
0.809
0.787
0.765
0.742
0.719
0.696
0.673
0.65
0.623
0.596
0.569
0.542
0.515
0.486
0.457
0.428
0.399
0.37
0.34
0.31
0.28
0.25
0.22
0.19
0.16
0.13
0.1
0.07
0.042
0.014
-0.014
-0.042
-0.07
-0.1
-0.13
-0.16
-0.19
-0.22
-0.25
-0.28
-0.31
-0.34
-0.37
-0.398
-0.426
-0.454
-0.482
-0.51
-0.533
-0.556
-0.579
-0.602
-0.625
-0.647
-0.669
-0.691
-0.713
-0.735

-0.756
-0.777
-0.798
-0.819
-0.84
-0.854
-0.868
-0.882
-0.896
-0.91
-0.917
-0.924
-0.931
-0.938
-0.945
-0.945
-0.945
-0.945
-0.945
-0.945
-0.938
-0.931
-0.924
-0.917
-0.91
-0.898
-0.886
-0.874
-0.862
-0.85
-0.828
-0.806
-0.784
-0.762
-0.74
-0.724
-0.708
-0.692
-0.676
-0.66
-0.663
-0.666
-0.669
-0.672
-0.675
-0.71
-0.745
-0.78
-0.815
-0.85
-0.818
-0.786
-0.754
-0.722
-0.69
-0.552
-0.414
-0.276
-0.138
0
0.138
0.276

0.414
0.552
0.69
0.722
0.754
0.786
0.818
0.85
0.815
0.78
0.745
0.71
0.675
0.672
0.669
0.666
0.663
0.66
0.676
0.692
0.708
0.724
0.74
0.762
0.784
0.806
0.828
0.85
0.862
0.874
0.886
0.898
0.91
0.917
0.924
0.931
0.938
0.945
0.945
0.945
0.945
0.945
0.945
0.938
0.931
0.924
0.917
0.91
0.896
0.882
0.868
0.854
0.84
0.819
0.798
0.777
0.756
0.735
0.713
0.691
0.669
0.647

0.625
0.602
0.579
0.556
0.533
0.51
0.482
0.454
0.426
0.398
0.37
0.34
0.31
0.28
0.25
0.22
0.19
0.16
0.13
0.1
0.07
0.042
0.014
-0.014
-0.042
-0.07
-0.1
-0.13
-0.16
-0.19
-0.22
-0.25
-0.28
-0.31
-0.34
-0.37
-0.399
-0.428
-0.457
-0.486
-0.515
-0.542
-0.569
-0.596
-0.623
-0.65
-0.673
-0.696
-0.719
-0.742
-0.765
-0.787
-0.809
-0.831
-0.853
-0.875
-0.893
-0.911
-0.929
-0.947
-0.965
-0.98

-0.995
-1.01
-1.025
-1.04
-1.049
-1.058
-1.067
-1.076
-1.085
-1.083
-1.081
-1.079
-1.077
-1.075
-1.064
-1.053
-1.042
-1.031
-1.02
-0.999
-0.978
-0.957
-0.936
-0.915
-0.923566667
-0.932133333
-0.9407
-0.8873
-0.834
-0.7809
-0.7283
-0.6755
-0.6232
-0.5708
-0.5178
-0.4644
-0.4107
-0.3563
-0.3024
-0.2484
-0.1945
-0.1406
-0.0869
-0.0344
0.016
0.0615
0.0212
-0.6115
-0.5276
-0.4464
-0.3376
-0.22
-0.11
0

0.0175
0.0177
0.0181
0.0189
0.0199
0.0218
0.0232
0.058
0.072
0.086
0.101
0.117
0.134
0.152
0.171
0.19
0.21
0.231
0.252
0.274
0.297
0.32
0.344
0.369
0.394
0.42
0.445
0.473
0.505333333
0.537666667
0.57
0.605
0.64
0.675
0.71
0.745
0.78
0.815
0.85
0.885
0.92
0.951
0.982
1.013
1.044
1.075
1.103
1.131
1.159
1.187
1.215
1.241
1.267
1.293
1.319
1.345
1.37
1.395
1.42

1.445
1.47
1.491
1.512
1.533
1.554
1.575
1.593
1.611
1.629
1.647
1.665
1.679
1.693
1.707
1.721
1.735
1.744
1.753
1.762
1.771
1.78
1.784
1.788
1.792
1.796
1.8
1.8
1.8
1.8
1.8
1.8
1.796
1.792
1.788
1.784
1.78
1.774
1.768
1.762
1.756
1.75
1.74
1.73
1.72
1.71
1.7
1.687
1.674
1.661
1.648
1.635
1.619
1.603
1.587
1.571
1.555
1.537
1.519
1.501
1.483
1.465

1.442
1.419
1.396
1.373
1.35
1.325
1.3
1.275
1.25
1.225
1.197
1.169
1.141
1.113
1.085
1.053
1.021
0.989
0.957
0.925
0.891
0.857
0.823
0.789
0.755
0.719
0.683
0.647
0.611
0.575
0.544
0.513
0.482
0.451
0.42
0.4
0.38
0.36
0.34
0.32
0.302
0.284
0.266
0.248
0.23
0.212
0.194
0.176
0.158
0.14
0.123
0.106
0.089
0.072
0.055
0.049
0.043
0.037
0.031
0.025
0.031
0.037

0.043
0.049
0.055
0.072
0.089
0.106
0.123
0.14
0.158
0.176
0.194
0.212
0.23
0.248
0.266
0.284
0.302
0.32
0.34
0.36
0.38
0.4
0.42
0.451
0.482
0.513
0.544
0.575
0.611
0.647
0.683
0.719
0.755
0.789
0.823
0.857
0.891
0.925
0.957
0.989
1.021
1.053
1.085
1.113
1.141
1.169
1.197
1.225
1.25
1.275
1.3
1.325
1.35
1.373
1.396
1.419
1.442
1.465
1.483
1.501
1.519
1.537

1.555
1.571
1.587
1.603
1.619
1.635
1.648
1.661
1.674
1.687
1.7
1.71
1.72
1.73
1.74
1.75
1.756
1.762
1.768
1.774
1.78
1.784
1.788
1.792
1.796
1.8
1.8
1.8
1.8
1.8
1.8
1.796
1.792
1.788
1.784
1.78
1.771
1.762
1.753
1.744
1.735
1.721
1.707
1.693
1.679
1.665
1.647
1.629
1.611
1.593
1.575
1.554
1.533
1.512
1.491
1.47
1.445
1.42
1.395
1.37
1.345
1.319

1.293
1.267
1.241
1.215
1.187
1.159
1.131
1.103
1.075
1.044
1.013
0.982
0.951
0.92
0.885
0.85
0.815
0.78
0.745
0.71
0.675
0.64
0.605
0.57
0.537666667
0.505333333
0.473
0.445
0.42
0.394
0.369
0.344
0.32
0.297
0.274
0.252
0.231
0.21
0.19
0.171
0.152
0.134
0.117
0.101
0.086
0.072
0.058
0.0232
0.0218
0.0199
0.0189
0.0181
0.0177
0.0175

APPENDIX V: AIRFOIL ROTATOR

What follows is the MATLAB code used to rotate the airfoil (either NACA 0012 or the polynomial). The input is a comma-separated-value (CSV) file containing a set of points in the xy-plane with x and y coordinates, and the output will be a three-column tab-delimited text file (or files) suitable for import to SolidWorks with values in the xy-plane and all zeroes in the z-direction.

All of these operations could be completed in a spreadsheet program (like Excel), but because of the frequency with which airfoils were rotated and translated and the potential for error it was safer to automate the process. This script can produce multiple files if each airfoil needs to be produced, such as when working with a CAD program that does not easily or automatically rotate airfoils.

```
clear all
close all
clc

%Script by Jonathan Conrad Corbett
%Script to rotate an airfoil imported from text

%This script will rotate an airfoil saved as a csv
file.
%The variable below is how many degrees to rotate the
variable.
%Counterclockwise positive
%The script is for degrees.  If one wants to rotate
using a value in radians, change the pi()/180
%converstion factor to 1.

rotation = 0   %Enter degrees; will rotate the airfoil
COUNTERCLOCKWISE that many degrees
conversion=pi()/180 %Keep this expression active when
working in degrees
%conversion=1   %Switch to this conversion factor if
working in radians
rads=rotation*conversion
```

```
%Next is the numeber of airfoils.  They will be equally
spaced, starting at
%zero degrees (along the x-axis) first.

howmany = 1

%By default most airfoil generators do the shape, but
not at the right
%scale.  This allows you multiply to scale the chord
length down.

scaling= 0.0661  %This will scale the airfoil by a
factor; 1 is no change
flipx= 1;  %If set to a negative, the airfoil will be
flipped (mirrored)
flipy= 1;   %If set to 1, it will not be.

centerradius= 0.41  %If 0, the airfoil will be centered
on the origin. (In meters)

%Center radius - how far from the origin to the center
of the airfoil.
%Remember that is not the tip of your airfoil.

%centerradius = 0.6175-.5*scaling*cos(rads)  %Even
though my planned radius is 0.62, I want to leave room
for fillets


airfoil=readtable("airfoil.csv")   %The file name to
import should be in quotation marks
%File format that worked best for me is comma separated
value file (saved in
%Excel).  This command will import the file to MATLAB
as a table.

%The file should have two or three columns, X and Y or
X, Y, and Z.
%The next for-loop finds the center of the airfoil

%Initializing the variables xmax-ymin as empty
variables.
```

```
sz=size(airfoil)
xmax=[]
ymax=[]
xmin=[]
ymin=[]
foilx=[sz(1)]
foily=[sz(1)]
foilz=[sz(1)]
tempx=[sz(1)]
tempy=[sz(1)]
tempz=[sz(1)]
%output=[0,0,0;,0,0,0]


%a special loop just to get output initialized



%This block of code finds the center of the airfoil.
%maybe is the value under consideration, which maybe
larger or smaller than
%the max x file.  Concurrently, the variable is loaded
into an array to make
%it easier to work with.

for x= 1:sz(1)
    maybe=airfoil{x,1}  %Curly braces are used for
extracting value from the table
    if isempty(xmax)    %The isempty command checks the
variable to see if it is empty.  It will return "true"
if it is.
        xmax=maybe
    end
    if maybe>xmax
        xmax=maybe
    end
    if isempty(xmin)
        xmin=maybe
    end
    if maybe<xmin
        xmin=maybe
    end
    foilx(x)=maybe
    tempx(x)=maybe
```

```
    foilz(x)=0
    output(x,1)=0
end
xavg= (xmax+xmin)/2

for y= 1:sz(1)
    maybe=airfoil{y,2}  %As above, curly braces are
used to extract data from table (parenthesis would keep
table format).
    if isempty(ymax)    %Returns true if ymax is empty
        ymax=maybe
    end
    if maybe>ymax
        ymax=maybe
    end
    if isempty(ymin)
        ymin=maybe
    end
    if maybe<ymin
        ymin=maybe
    end
    foily(y)=maybe
    tempy(y)=maybe
    tempz(y)=0
end
yavg= (ymax+ymin)/2

%We now have the center point of the airfoil data, and
have it loaded to foilx and foily.
%Next, we will translate the airfoil points so the
center is at the origin.

for x=1:sz(1);
    foilx(x)=foilx(x)-xavg
end

for y=1:sz(1)
    foily(y)=foily(y)-yavg
end

%If airfoil requires scaling, this is where it happens.
foilx=flipx*scaling*foilx
foily=flipy*scaling*foily
```

```
%Next we will rotate the airfoil by a fixed number of
degrees
%Change that variable at the top of the file for
convenience
%Recall the rotation matrix is c -s 0, s c 0, 0 0 1 for
simple planar
%rotation.



for pt=1: sz(1);    %Using pt for "point" to make this
section more readable
    x=foilx(pt)     %Can't just use foilx and foily
directly because you need both for the reassignment
step
    y=foily(pt)
    foilx(pt)=x*cos(rads)-y*sin(rads)
    foily(pt)=x*sin(rads)+y*cos(rads)
    foilz(pt)=0
end

%Now, we need to start getting the airfoils filled out
around the center.
%First, move the airfoil out to the right distance
pt=0
for pt=1:sz(1)
    foilx(pt)=foilx(pt)+centerradius %Translating
airfoil in x direction; moves to position 0.
    %y values should not need to be updated at this
time
end


i=0 %reinitialize

for t=1: howmany;
    foilspot=(t-1)*2*pi()/howmany
    i=0
    for i=1: sz(1);    %Using pt for "point" to make
this section more readable
        x=foilx(i);     %Can't just use foilx and foily
directly because you need both for the reassignment
step
```

```
        y=foily(i);
        tempx(i)=x*cos(foilspot)-y*sin(foilspot)
        tempy(i)=x*sin(foilspot)+y*cos(foilspot)
        tempz(i)=0;
    end



    for f=1:sz(1);
        output(f,1)=tempx(f);
        output(f,2)=tempy(f);
        output(f,3)=tempz(f);
    end

    numb=int2str(t)
    filename= strcat('airfoiloutput',numb,'.txt')  %The
bracket makes this an array of strings
    %ischar(filename) %Was used for debugging
    %xlswrite(filename,fishnugget);

    %OUTPUT=array2table(output);
    %xlswrite(filename, OUTPUT)  %Always remember the
correct order filename,data
    dlmwrite(filename,output,'  ')

end
```

APPENDIX VI: POINTS OF MODELED AIRFOIL

This is a table of the points which were used to model the airfoil. The airfoil was modeled with these shapes and was 2 mm thick (used 1 mm offset in SolidWorks both up and down from imported curve). The first column was x-values, the second was y-values, and the third column was z-values.

TABLE 9 - Airfoil Definition

0	3.500001	0.58057
0	3.50053	0.58076
0	3.50103	0.58095
0	3.501504	0.58114
0	3.501952	0.58133
0	3.502375	0.58152
0	3.502774	0.58171
0	3.503149	0.5819
0	3.503502	0.5821
0	3.503834	0.58229
0	3.504145	0.58248
0	3.504437	0.58267
0	3.50471	0.58286
0	3.504966	0.58305
0	3.505204	0.58324
0	3.505427	0.58343
0	3.505635	0.58362
0	3.505828	0.58381
0	3.506009	0.584
0	3.506177	0.58419
0	3.506334	0.58438
0	3.50648	0.58457
0	3.506617	0.58476
0	3.506745	0.58495
0	3.506866	0.58514
0	3.506979	0.58533
0	3.507087	0.58552
0	3.507189	0.58571
0	3.507287	0.5859
0	3.507382	0.5861
0	3.507475	0.58629

0	3.507566	0.58648
0	3.507657	0.58667
0	3.507747	0.58686
0	3.507839	0.58705
0	3.507933	0.58724
0	3.508029	0.58743
0	3.50813	0.58762
0	3.508235	0.58781
0	3.508346	0.588
0	3.508462	0.58819
0	3.508587	0.58838
0	3.508719	0.58857
0	3.50886	0.58876
0	3.509011	0.58895
0	3.509173	0.58914
0	3.509347	0.58933
0	3.509533	0.58952
0	3.509732	0.58971
0	3.509945	0.5899
0	3.510173	0.5901
0	3.510418	0.59029
0	3.510679	0.59048
0	3.510957	0.59067
0	3.511254	0.59086
0	3.51157	0.59105
0	3.511906	0.59124
0	3.512264	0.59143
0	3.512643	0.59162
0	3.513044	0.59181
0	3.513469	0.592
0	3.513919	0.59219
0	3.514394	0.59238
0	3.514894	0.59257
0	3.515422	0.59276
0	3.515977	0.59295
0	3.51656	0.59314
0	3.517173	0.59333
0	3.517816	0.59352
0	3.51849	0.59371
0	3.519196	0.5939
0	3.519934	0.5941
0	3.520706	0.59429
0	3.521512	0.59448

0	3.522353	0.59467
0	3.523231	0.59486
0	3.524144	0.59505
0	3.525096	0.59524
0	3.526085	0.59543
0	3.527114	0.59562
0	3.528182	0.59581
0	3.529292	0.596
0	3.530443	0.59619
0	3.531636	0.59638
0	3.532873	0.59657
0	3.534153	0.59676
0	3.535478	0.59695
0	3.536849	0.59714
0	3.538266	0.59733
0	3.53973	0.59752
0	3.541243	0.59771
0	3.542803	0.5979
0	3.544414	0.5981
0	3.546075	0.59829
0	3.547786	0.59848
0	3.54955	0.59867
0	3.551366	0.59886
0	3.553236	0.59905
0	3.55516	0.59924
0	3.557139	0.59943